UCLA
UCLA Electronic Theses and Dissertations

Title
Non-mutated kinases in prostate cancer metastasis: drivers and therapeutic targets

Permalink
https://escholarship.org/uc/item/7615v8xd

Author
Faltermeier, Claire

Publication Date
2016

Peer reviewed|Thesis/dissertation

eScholarship.org Powered by the California Digital Library
University of California

UNIVERSITY OF CALIFORNIA

Los Angeles

Non-mutated kinases in metastatic prostate cancer:

drivers and therapeutic targets

A dissertation submitted in partial satisfaction of the

requirements for the degree Doctor of Philosophy

in Molecular Biology

by

Claire Faltermeier

2016

© Copyright by

Claire Faltermeier

2016

ABSTRACT OF THE DISSERTATION

Non-mutated kinases in prostate cancer:

drivers and therapeutic targets

by

Claire Faltermeier

Doctor of Philosophy in Molecular Biology

University of California, Los Angeles, 2016

Professor Hanna K. A. Mikkola, Chair

Metastatic prostate cancer lacks effective treatments and is a major cause of death in the United States. Targeting mutationally activated protein kinases has improved patient survival in numerous cancers. However, genetic alterations resulting in constitutive kinase activity are rare in metastatic prostate cancer. Evidence suggests that non-mutated, wild-type kinases are involved in advanced prostate cancer, but it remains unknown whether kinases contribute mechanistically to metastasis and should be pursued as therapeutic targets. Using a mass-spectrometry based phosphoproteomics approach, we identified tyrosine, serine, and threonine kinases that are differentially activated in human metastatic prostate cancer tissue specimens compared to localized disease. To investigate the functional role of these kinases in prostate cancer metastasis, we screened over 100 kinases identified from our phosphoproteomic and previously-published transcriptomic studies for their ability to drive metastasis. In a primary

screen using a lung colonization assay, we identified 20 kinases that when overexpressed in murine prostate cancer cells could promote metastasis to the lungs with different latencies. We queried these 20 kinases in a secondary *in vivo* screen using non-malignant human prostate cells. The kinases MERTK, NTRK2 and RAF family members drove the formation of bone and visceral metastasis confirmed by PET/CT imaging and histology. Immunohistochemistry of tissue microarrays indicated these kinases are highly expressed in human metastatic prostate cancer tissues. Lastly, inhibition studies in metastatic prostate cancer cell lines have revealed that one of the RAF family members, CRAF, may block metastasis. These data demonstrate the strong capability of wild-type protein kinases to drive metastatic colonization and implicate select kinases as potential targets for therapeutic intervention.

The dissertation of Claire Faltermeier is approved.

Peter M. Clark

Donald Barry Kohn

Michael Alan Teitell

Owen N. Witte

Hanna K. A. Mikkola, Committee Chair

University of California, Los Angeles

2016

DEDICATION

This dissertation is dedicated to my late father, Joseph E. Faltermeier who is missed more than words can express. I thank my father for always believing in me, and showing by example that with determination, dedication, and compassion, anything is possible. His courageous battle with metastatic ocular melanoma has been a key inspiration to my dissertation research.

TABLE OF CONTENTS

List of Figures

List of Tables

ACKNOWLEDGMENTS

Obtaining a PhD is not an individual experience. It involves the support of many persons, whom I would like to thank sincerely.

First, and most of all, I would like to thank my mentor, Dr. Owen Witte, for his strong commitment to supporting my professional development. When I entered the Witte lab, I aspired to become a scientist but lacked confidence in my abilities. Dr. Witte created a stimulating research environment and taught me how to generate thoughtful scientific questions. He gave me the freedom to design and carryout experiments on my own, but at the same time the guidance to prevent or learn from my mistakes. He is and will always be my role model of an extraordinary scientist- someone who holds themselves to the highest standards, who never stops learning, and is passionate about how science can improve medical conditions. While I know I have still have much more to learn, Dr. Witte has given me the foundation upon which I hope I can make contributions as a scientist during my career.

I would like to thank my committee members, Drs. Mikkola, Kohn, Teitell, Ribas, and Clark for their support, suggestions, and encouragement. I am also grateful for their examples of being excellent scientists and physician-scientists.

I would like to express my gratitude to the current and previous members of the Witte Lab. The engaging discussions and technical advice were critical to the development of my project. I am indebted to those who helped me conduct my experiments, in particular Peter Clark, Yang Zong,

Justin Drake, Donny Johnson, Colleen Mathis, Donghui Cheng, and Carmen Volpe. Without their assistance, I would not have been able carryout the large-scale experiments for this dissertation.

I wish to acknowledge the financial support I have received from multiple sources including: the UCLA-Caltech Medical Scientist Training Program, the Eli and Edythe Broad Center of Regenerative Medicine and Stem Cell Research, and the Tumor Cell Biology Institutional Training Grant. I also appreciate the support from the American Association of Cancer Research which enabled me to travel to multiple conferences.

Chapter 1 contains figures from the review articles, “Targeting metastasis” and “The pathogenesis of cancer metastasis: the ‘seed and soil’ hypothesis revisited” both published in Nature Reviews Cancer, “Metastatic colonization: settlement, adaptation and propagation of tumor cells in foreign tissue environment” published in Seminars in Cancer Biology, and “Clinical targeting of mutated and wild-type protein kinases in cancer” published in Molecular and Cellular Biology. I am thankful for the kind permission offered by these publication sources to include these figures in my dissertation. Chapters 2 and 3 are reproduced with permission from the Proceedings of the National Academy of Sciences.

Last but not least, I am thoroughly grateful for the support of my family and friends. Their encouragement, advice, and consistent care kept me going even during difficult times.

VITA

Education

2006	B.A. Biological Sciences Columbia College, Columbia University, New York, NY
2010-	M.D./Ph.D. Candidate David Geffen School of Medicine, UCLA, Los Angeles, CA

Awards

2007-2009	Award Recipient/Trainee Fred Hutchinson Cancer Research Center (FHCRC)-Safeway Inc., Breast Cancer Research Grant, FHCRC, Seattle, WA
2013-2014	Award Recipient/Trainee California Institute for Regenerative Medicine Training Grant, University of California, Los Angeles, CA
2014-2016	Award Recipient/Trainee USHHS Ruth L. Kirschstein Institutional Research Service Award, University of California, Los Angeles, CA
2015	Award Recipient American Association for Cancer Research (AACR) Scholar in Training Award, AACR Annual Meeting, Philadelphia, PA
2015	Award Recipient Best oral presentation selected by peers and faculty, UCLA Pharmacology Department Retreat, Huntington Beach, CA
2016	Award Recipient AACR Scholar in Training Award, AACR-Japanese Cancer Association (JCA) Joint Conference on Breakthroughs in Cancer Research, Maui, HI

Publications

Ghorbal, M., Scheidig-Benatar, C., Bouizem, S., Thomas, C., Paisley, G., **Faltermeier, C.,** Liu, M., Scherf, A., Lopez-Rubio, J.J., & Gopaul, D.N. Initial characterization of the Pf-Int recombinase from the malaria parasite Plasmodium falciparum. *PLoS One* **7**, e46507 (2012).

Drake, J.M., Graham, N.A., Lee, J.K., Stoyanova, T., **Faltermeier, C.M.,** Sud, S., Titz, B., Huang, J., Pienta, K.J., Graeber, T.G., & Witte, O.N. Metastatic castration-resistant prostate cancer reveals intrapatient similarity and interpatient heterogeneity of therapeutic kinase targets. *Proc Natl Acad Sci USA* **110**, E4762-4769 (2013).

Faltermeier, C.M.*, Zhao, H.*, Mendelsohn, L., Porter, P.L., Clurman, B.E., & Roberts, J.M. Mislocalization of p27 to the cytoplasm of breast cancer cells confers resistance to anti-HER2 targeted therapy. *Oncotarget* **5**, 12704-12714 (2014). *Equal contribution

Faltermeier, C.M., Drake, J.M., Clark, P.M., Smith, B.A., Zong, Y., Volpe, C., Mathis, C., Morrissey, C., Castor, B., Huang, J., & Witte, O.N. Functional screen identifies kinases driving prostate cancer visceral and bone metastasis. *Proc Natl Acad Sci USA* **113**, E172-181 (2016).

Commentaries:

Feng, F.Y., & Kothari, V. Driven to metastasize: Kinases as potential therapeutic targets in prostate cancer. *Proc Natl Acad Sci USA* **113**, 473-475 (2016).

Stone, L. Prostate cancer: A walk on the wild side – wild-type kinases promote metastasis. *Nature reviews. Urology* **13**, 63 (2016).

Stoyanova, T., Riedinger, M., Lin, S., **Faltermeier, C.M.**, Smith, B.A., Zhang, K., Going, C.C., Goldstein, A.S., Lee, J.K., Drake, J.M., Nowroozizadeh, B., Castor, B., Orellana, S.Y., Blum, S., Cheng, D., Pienta, K.J., Reiter, R.E., Pitteri, S.J., Huang, J., & Witte, O.N. Activation of Notch 1 synergizes with multiple pathways in promoting castration-resistant prostate cancer. 2016. In review.

Drake, J.M., Paul, E.O., Graham, N., Lee, J.K., Smith, B.A., Titz, B., Stoyanova, T., **Faltermeier**, C.M., Carlin, D.E., Sudha, S., Vashisht, A.A., Huang, J., Wohlschlegel, J.A., Graeber, T.G., Witte, O.N., & Stuart, J.M. Patient-specific druggable networks in lethal prostate cancer through proteome-guided multi-omic integration. 2016. In review.

Presentations

Oral presentations

2009: AACR Molecular Targets and Cancer Therapeutics Meeting, Boston, MA
2014: UCLA Stem Cell Club, Los Angeles, CA
UCLA-Caltech MSTP Tutorial Series, Los Angeles, CA
UCLA Molecular Biology Institute Student Seminar Series, Los Angeles, CA
2015: UCLA Tumor Cell Biology/Tumor Immunology Seminar Series, Los Angeles, CA
UCLA-Caltech MSTP Annual Symposium, Los Angeles, CA
UCLA Pharmacology Department Retreat, Huntington Beach, CA
2016: UCLA Tumor Cell Biology/Tumor Immunology Seminar Series, Los Angeles, CA
UCLA Molecular Biology Institute Annual Retreat, Lake Arrowhead, CA

Poster Presentations

2014: Broad Stem Cell Research Center Annual Symposium, Los Angeles, CA
USC, UCSF, and UCLA Tri-Institutional Stem Cell Retreat, Asilomar, CA
UCLA-Caltech MSTP Annual Symposium, Los Angeles, CA
Cell Symposia: Hallmarks of Cancer, Beijing, China
2015: AACR Annual Meeting, Philadelphia, PA
2016: Broad Stem Cell Research Center Annual Symposium, Los Angeles, CA
AACR-JCA Joint Conference on Breakthroughs in Cancer Research, Maui HI

Chapter 1:

Introduction to metastasis, kinases, and prostate cancer

Overview of metastasis

The clinical problem of metastasis

In 2016, an estimated 1.7 million individuals in the US will be diagnosed with cancer and approximately 600,000 will die from their disease(*1*). The majority of patients diagnosed with localized cancer have 5-year survival rates of ~ 90%(*2*). However, once cancer has metastasized survival is poor. For patients with metastatic bladder, lung, and pancreas cancers, the 5-year survival is less than 10%. Equally alarming is the decrease in survival of patients with metastatic ovarian, prostate, and uterine cancers that has occurred over the past 10 years (Figure 1)(*2, 3*). Surprisingly, in spite of the clinical importance, metastasis remains one of the most poorly understood processes in cancer biology. In order to improve our understanding of metastasis biology and identify new therapeutic targets, there is an urgent need to identify the genes and pathways responsible for driving metastasis.

What is metastasis?

Metastasis occurs when cancer cells depart from the primary tumor and resume growth at a distant site. The process is complex and proceeds in a step-wise manner often referred to as the "metastatic-cascade" (Figure 2)(*4*). The cascade begins with tumor cells losing adherence to other cells, then migrating and invading through tissue surrounding the primary tumor. To enter circulation, tumor cells penetrate through the walls of blood vessels in a process called intravasation. Survival in circulation is another requirement for cells to reach sites anatomically distinct from the primary tumor. Once at the target organ, cells invade through vascular walls (extravasation) and enter the organ parenchyma. In order to successfully complete the last step of the cascade, metastatic colonization, tumor cells must survive and proliferate in a new and often hostile microenvironment(*5*).

Given these steps, a critical question is: which step of the metastatic cascade should be considered for therapeutic targeting? Since the early steps of metastasis have been extensively studied, targeting genes or pathways which regulate loss of adhesion, migration, and invasion may block metastasis. For instance, activation of the developmental program epithelial-to-mesenchymal transition (EMT) promotes loss of adhesion and migration in numerous cancers(*4*). The EMT-associated transcription factors, snail, slug, and twist, downregulate the cell-to-cell adhesion molecule E-cadherin and upregulate pro-migratory genes(*6, 7*). Tumor cell secretion of extracellular matrix-degrading enzymes such as cathepsins and metalloproteinases (MMPs) are key contributors to invasion through the stroma and basement membrane(*8*). Hence, targeting EMT-associated transcription factors or MMPs could be an approach to block the early steps of the metastatic cascade.

An alterative hypothesis is that the greatest clinical benefit may be observed by blocking the rate-limiting step of the metastatic cascade. Various lines of evidence suggest that the early steps of the cascade may not be the rate-limiting steps. Systemic dissemination of tumor cells is thought to occur early in tumor development and does not correlate with metastatic potential. Indeed, the number of circulating tumor cells found in the blood from patients with cancer, far exceeds the number of overt metastases that develop(*9*). Clinical studies have shown that tumor cells can arrest in distant organs for years without developing into metastases(*10*). Data from a murine model is also consistent with the clinical evidence; after intravenous injection, untransformed mammary epithelial cells could travel to, survive, and remain dormant in the lungs for >4 months(*11*). These data suggest that the ability to lose adherence, migrate, invade, and survive in circulation may not be characteristics specific to metastatic cells. Tumor cells and

even some normal cells may have these characteristics. Thus, the molecular drivers of the early steps of the metastatic cascade are unlikely to be the Achilles' heel of metastasis.

Experimental models suggest that metastatic colonization is highly inefficient and the rate-limiting step of metastasis. To model the inefficiency of metastatic colonization, Fidler and Nicolson injected highly metastatic melanoma cells labeled with a radioactive thymidine analogue into mice(*12*). By measuring radioactivity levels in different organs they were able to follow the metastatic cells. The majority of cells arrested in the lungs hours after injection, but by 24 hours >90% of the cells were lost. Only 0.01% of injected cells formed macrometastases within the lungs. Similarly, using *in vivo* video-microscopy and injection of metastatic cells into the portal vein supplying the liver, Luzzi and colleagues observed that only 2% of cells formed micrometastases, and 0.02% formed macrometastases in the liver(*13*). Since many cells are able to survive in circulation and extravasate, factors that influence cancer cell survival and growth at a secondary site are probably the primary determinants of metastasis. Research on the molecular drivers of metastatic colonization may identify more effective therapeutic targets.

Metastatic colonization

The complexity of metastatic colonization and lack of experimental model systems have hindered research on the process. Upon reaching a secondary site, tumor cells encounter multiple barriers requiring alteration of cell-intrinsic pathways, cell-microenvironment interactions, and cell-immune system interactions (Figure 3)(*14*). Tumor cells must maintain or enhance cell-signaling pathways that promote survival and proliferation. They have to adapt to organ-specific cells and extracellular matrix components. Due to increased susceptibility of immune surveillance in a new microenvironment, tumor cells must also employ mechanisms to escape immune-mediated destruction.

Experimental models and mechanisms driving metastatic colonization

Experimental models used to identify key contributors of metastatic colonization are imperfect. There are no *in vitro* models that can closely recapitulate the complex conditions of the *in vivo* microenvironment. Hence, transgenic murine models, or injection of cells intravenously into mice are best for modeling the conditions of secondary colonization. However, there are drawbacks. Injection of human tumor cells into mice requires use of immune compromised mice, which have a lack of and/or dysfunctional innate and adaptive immune cells. As a result, tumor-immune cell interactions occurring during secondary colonization cannot be faithfully recapitulated. Injection of murine cells, or use of transgenic mice leaves the immune system intact, however these models often do not reflect human disease. For instance, 90% of patients with metastatic prostate cancer will develop metastasis to the bone(*15*). Mouse models that develop prostate cancer metastasis to the bone are rare, making it difficult to identify the molecular determinants of bone metastasis(*16*). These issues encountered with experimental model systems contribute to our incomplete understanding of metastatic colonization.

Despite these challenges, some key pathways in metastatic colonization have been uncovered. Murine models that lack NK and T cells exhibit a dramatic increase in metastasis, suggesting that these immune cells are key players in restraining metastatic colonization(*17-19*). Factors contributing to metastatic cell evasion of NK and T cell killing include: downregulation of innate immune sensors(*20*), or expression of T cell inhibitory molecules such as CTLA4 or PDL1(*14*).

Activation of tumor cell survival pathways is also important for secondary colonization. For example, breast cancer cells rely on activation of the PI3K-AKT signaling pathway for survival(*21*). Cells of the bone marrow and lung microenvironments help activate this signaling

pathway through multiple mechanisms. Bone marrow stromal cells secrete the cytokine CXCL12 which binds to the CXCR4 receptor on breast cancer cells. This ligand-receptor interaction leads to Src kinase activation followed by PI3K-AKT pathway activation(*22*). Alveolar macrophages in the lung express αIVβI integrin which upon binding to VCAM1 also activates PI3K-AKT signaling in breast cancer cells (*23, 24*). Similarly, melanoma cells rely on the RAS-MAPK pathway for survival. This pathway is activated by the keratinocyte secreted ligand, CCL12, binding to the CCR10 receptor on melanoma cells(*25*). These interactions emphasize the importance of microenvironmental factors and activation of kinase signaling pathways in secondary colonization.

How can we therapeutically target metastatic colonization?

Based on the involvement of T and NK cells, immunotherapy which can block tumor-immune cell suppression may be effective in reducing colonization(*14*). Blocking cytokine-receptor interactions is another approach. Small molecules and antibodies inhibiting the CXCL12-CXCR4 interaction have reduced metastatic burden in pre-clinical models(*14*). Since metastatic cells seem to rely on kinase signaling pathways for survival at secondary sites, kinase inhibition may also be a reasonable therapeutic strategy. Kinases are easily druggable and have been excellent therapeutic targets for multiple cancers. Rationale for kinase targeting will be discussed in the following section.

Overview of kinases

Introduction to protein kinases

Over 500 protein kinases have been identified so far in the human genome, enough to have kinases involved in almost every cellular process(*26*). The general schema of how kinases

regulate these processes is by responding to an extracellular signal, activating an intracellular cascade, leading to a transcriptional response, and ultimately inducing a biological outcome(*27*). For instance, cell division starts by extracellular growth factors or hormones binding to and activating receptor tyrosine kinases (RTKs). Phosphorylated tyrosine residues on RTKs serve as docking sites for signaling molecules such as Grb2 and SoS, which recruit and contribute to the activation of intracellular kinases. Activation of cyclin-dependent kinases initiate the G1 to S phase transition by phosphorylating the transcription factors E2F and Rb(*28*). Activation of the polo, aurora and NIMA (never in mitosis A) family kinases are also essential to cellular division by promoting DNA replication and centrosome duplication(*29*). Protein synthesis is activated by phosphorylation of ribosomal protein S6(*30*) and several protein translation initiation factors(*31*). Since kinase activity is critical to regulating key cellular processes, they are well-poised to have important roles in tumorigenesis.

How are kinases activated in tumors?

In normal cells kinase activity is under tight regulation to prevent aberrant cellular activity. At the resting/unstimulated state kinases maintain an "auto-inhibited" conformation. Once kinases are stimulated, their activity is quickly downregulated by multiple mechanisms including negative feedback, dephosphorylation by phosphatases, and receptor-mediated ubiquitylation and degradation(*27*). For instance, EGFR phosphorylates and activates the kinase PKC. Negative feedback then occurs by PKC phosphorylating EGFR in the juxtamembrane domain to prevent further EGF stimulated EGFR activation(*32*). Due to the reliance of kinase pathways in tumorigenesis, cancer cells have devised methods to bypass regulatory mechanisms and promote constitutive signals from either mutated or wild-type kinases (Figure 4).

Activation of kinases in tumors by genetic alterations

Genetic alterations of kinases by chromosomal translocations, point mutations and amplifications are the most studied mechanisms of kinase dysregulation in cancer. Chromosomal translocations result in constitutive kinase activity by causing loss of the kinase's autoinhibitory domain and/or fusion to a gene that drives high levels of kinase expression. For instance, 90% of patients with chronic myelogenous leukemia (CML) have a translocation of the long arms of chromosomes 9 and 22(*33*). This translocation fuses the tyrosine kinase c-ABL to the breakpoint cluster region (BCR)(*34*). The resultant fusion protein, BCR-ABL has lost the auto-inhibitory domains of c-ABL, causing constitutive kinase activity and CML(*35*). Somatic activating mutations usually occur within the kinase activation loop to help stabilize the kinase in its' active conformation(*36*). Over 50% of melanomas harbor a BRAF 1799T>A transversion encoding BRAFV600E, which relieves BRAF of normal autoinhibition(*37*). BRAFV600E drives melanoma pathogenesis by constitutive activation of the pro-survival/proliferation MAPK-ERK pathway(*38*). DNA amplifications resulting in high levels of kinase expression promote ligand-independent kinase dimerization at the cell surface. ERBB2 (Her2) amplification in breast cancers(*39*) and MET amplifications in lung(*40*) and colon cancer(*41*) are the most commonly observed kinase amplifications.

Activation of wild-type kinases in cancer

In contrast to genetically modified kinases which are easily identified by genomic studies, the contribution of wild-type kinases to tumorigenesis is less clear. Proposed mechanisms of wild-type kinase activation in tumors include: altered phosphatase activity, increased ligand production, or involvement in an activated signaling pathway. Phosphatases can both activate and inactivate kinases depending on which residues they dephosphorylate. SHP1 is

a tyrosine phosphatase which dephosphorylates activating residues on the kinase JAK3. Since the JAK3/STAT3 pathway is advantageous to cell survival, some T-cell lymphomas, leukemias, and multiple myelomas use epigenetic mechanisms to silence SHP1 expression(*42*). Autocrine or paracrine production of a ligand can lead to kinase hyperstimulation in cancer. Stromal cell secretion of FGF10 contributes to prostate adenocarcinoma by activation of the kinase FGFR1(*43*). Involvement in a hyperactivated signaling pathway can also increase kinase activity. Bruton's tyrosine kinase (BTK) is downstream of the B-cell receptor (BCR). In multiple B cell malignancies, BCR signaling is hyperactivated leading to downstream activation of BTK(*44, 45*). BTK activates PI3K and MAPK signaling which promotes cell survival and proliferation(*46*). Hence, protein kinase activity can be dysregulated through non-genetic mechanisms to evade normal physiological constraints on growth and survival.

Kinases as therapeutic targets for cancer

The rationale for targeting kinases in cancer is based on their role in important cellular functions vital to tumorigenesis and the fact that they are "druggable." Unlike G-proteins and transcription factors, kinases have a well-defined active site that is amenable to inhibition by small molecules or biologics(*47, 48*). The most common small molecule inhibitors are ATP-competitive inhibitors which recognize the kinase in its active conformation. They present hydrogen bonds to the amino acids near the kinase active site to mimic the hydrogen bond normally formed by ATP. Other small molecules stabilize kinases in their inactive conformation, or bind to allosteric sites. Monoclonal antibodies selectively disrupt kinase-ligand binding. Most antibodies bind the extracellular kinase domain or the kinase-specific ligand.

In addition to being targetable from a drug-design perspective, kinases have been clinically proven to be excellent targets for the treatment of cancer (Table 1). The small molecule

ATP-competitive inhibitor, Imatinib mesylate inhibits BCR-ABL(*49*). Use of imatinib in the treatment of CML has dramatically increased survival for patients. The 8-year survival rate of chronic phase patients has risen from 6% in 1975 (before the use of imatinib) to 81% in 2001(*50-52*). Metastatic melanoma is treated with vemurafenib, an ATP-competitive inhibitor specific to BRAFV600E. In phase III clinical trials, vemurafenib treatment was shown to contribute to both remission rates >80% and >60% relative reduction in the risk of death(*53*). These dramatic clinical responses prove the effectiveness of targeting genetically altered kinases in cancer.

In contrast to targeting genetically altered kinases, clinical trials targeting wild-type kinases have yielded mixed responses. Targeting tumor angiogenesis by blocking the kinase VEGFR or its ligand VEGF, promotes tumor regression in multiple cancers(*54*). However, in breast and pancreatic cancers these therapies failed to extend patient survival and paradoxically caused an increase in metastasis(*55, 56*). In contrast, there has been clinical success in the targeting BTK and MEK1/2. Ibrutinib is a small molecule that covalently binds to BTK resulting in kinase inactivation(*57*). In a phase III trial for patients with CLL, 63% of patients responded to ibrutinib leading to a 57% reduction in mortality(*58*). Similar responses to ibrutinib have also been observed in other B-cell malignancies including: Mantel cell lymphoma(*59*), Waldenstrom's macroglobulinemia(*60*), and B-cell lymphoma(*61*). As mentioned above, vemurafenib has improved survival for patients with BRAF mutant melanoma. Yet, multiple mechanisms of resistance to vemurfenib have been identified, with most converging on BRAF independent MEK1/2 activation(*62, 63*). Clinical trials have demonstrated that addition of the MEK1/2 inhibitor trametinib can prevent resistance to vemurafenib(*64*). The examples of BTK and MEK1/2 suggest that targeting wild-type kinases in the appropriate context can lead to clinical success.

Overview of kinases in prostate cancer

Kinases in prostate cancer

Although numerous oncogenic alterations have been identified in prostate cancer, DNA amplifications, translocations or other mutations resulting in constitutive kinase activity are rare(*36, 65, 66*). Genome sequencing of metastatic prostate cancer tissues from >150 patients identified translocations involving BRAF and CRAF in <1% of patients(*67, 68*). Although uncommon, these genomic aberrations cause enhanced kinase activity and suggest that kinase-driven pathways can be crucial to prostate cancer pathogenesis. Multiple lines of evidence indicate that wild-type kinases may contribute to prostate cancer progression, castration resistance, and metastasis (Table 2).

Clinical samples and functional models demonstrate that wild-type kinases can drive the progression of prostate cancer. Low-grade lesions are usually defined as prostatic intraepithelial neoplasia (PIN), while high-grade tumors are often referred to as aggressive-adenocarcinomas (Figure 5)(*69*). Evaluation of 75 prostatectomy specimens showed that an indirect measure of kinase activity, phosphotyrosine, increased with prostate cancer stage(*70*). 44% of the advanced prostate cancer lesions stained strongly for phosphotyrosine, while only 2% of PIN lesions stained at a similar intensity (Figure 5). In accordance with these observations murine models provide functional evidence that kinases can drive progression. Neither expression of the androgen receptor (AR) nor wild-type Src kinase in murine prostate cells are transforming alone. However, combined expression of Src and AR results in an invasive prostate adenocarcinoma(*71*). Likewise, transgenic mice with prostate-specific PTEN loss develop PIN lesions. Some lesions will develop into adenocarcinoma, but the latency is long. However,

crossing PTEN-/- mice with mice having upregulation of the kinase HER2 results in the development of prostate adenocarcinoma with complete penetrance and a shorter latency(*72*).

Prostate cancer cells require androgens for growth, and first-line treatments for advanced disease block androgen synthesis or signaling through AR. Prostate cancer cells inevitability become resistant to androgen blockade, known as castration resistance prostate cancer (CRPC). Wild-type kinases have been implicated in the development of CRPC. Immunohistochemical and RNAseq analyses of tissue samples from CRPC patients have found frequent high expression and/or transcriptional upregulation of multiple kinases(*73, 74*). Mechanistic studies on the kinases ETK/BMX and Src suggest they contribute to androgen independent growth by directly phosphorylating AR. This phosphorylation enables AR dependent transcription in the absence of a ligand(*75-77*). PI3K and AKT kinases have also been implicated in CRPC. Normally, AR signaling provides negative feedback on the PI3K/AKT pathway. Inhibition of AR relieves this negative feedback, and the PI3K/AKT pathway supports the development of CRPC(*78*). Currently, multiple clinical trials are underway to investigate if combined PI3K and AR inhibition can delay the development of castration resistance(*79*).

The metastatic potential of prostate cancer cells has also been correlated with kinase activation. Overexpression of the kinase PTK6 promotes loss of adherence and migration by downregulating E-cadherin expression and activating RhoGTPases (*80*). Activation of FGFR1 kinase via cancer cell-stroma interaction has been implicated in prostate cancer metastasis to the bone. Osteoblasts secrete FGF2 which activates FGFR1 pro-survival pathways in prostate cells(*81*). Targeting this cross-talk has clinical significance. Treatment of 23 patients with the FGFR1 inhibitor, dovitinib, resulted in one complete and five partial responses(*81*). Results from

this trial provides support that inhibiting kinases may be a rational therapeutic approach to block metastatic colonization.

Overview of dissertation

In this dissertation, we identify and investigate the role of non-mutated kinases in metastatic prostate cancer. The following chapters will provide evidence that kinase signaling pathways are activated in metastatic prostate cancer tissues, and kinases functionally contribute to metastatic colonization. In chapter 2 we describe a phosphoproteomic approach that identified activated tyrosine kinases in human metastatic prostate cancer tissues obtained at rapid autopsy. The functional contribution of kinases to prostate cancer metastasis is evaluated in chapter 3. We find that overexpression of individual wild-type kinases can drive metastatic colonization to visceral and skeletal sites *in vivo*. In chapter 4 we consider future directions and potential implications of this work. Ongoing studies to investigate the mechanism by which kinases drive metastasis and the therapeutic potential of targeting kinases in metastatic prostate cancer are discussed.

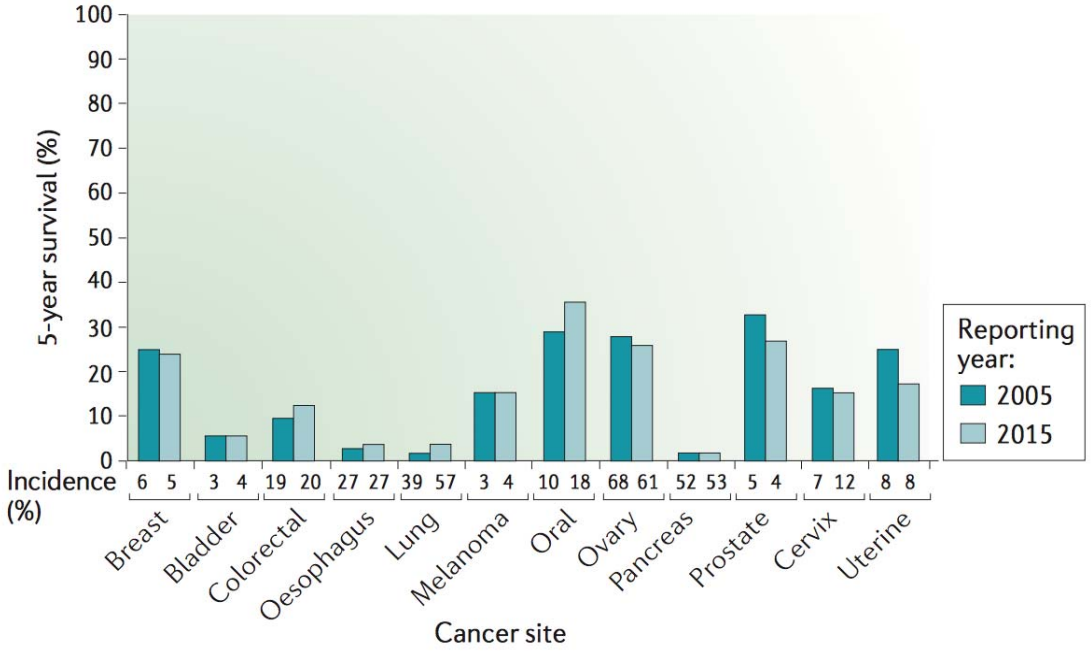

Figure 1. Survival of patients with metastatic cancer. 5-year survival rates of patients with metastatic cancer originating from different organ sites are shown. (Reprinted from Steeg P., 2016, with kind permission from Nature Publishing Group).

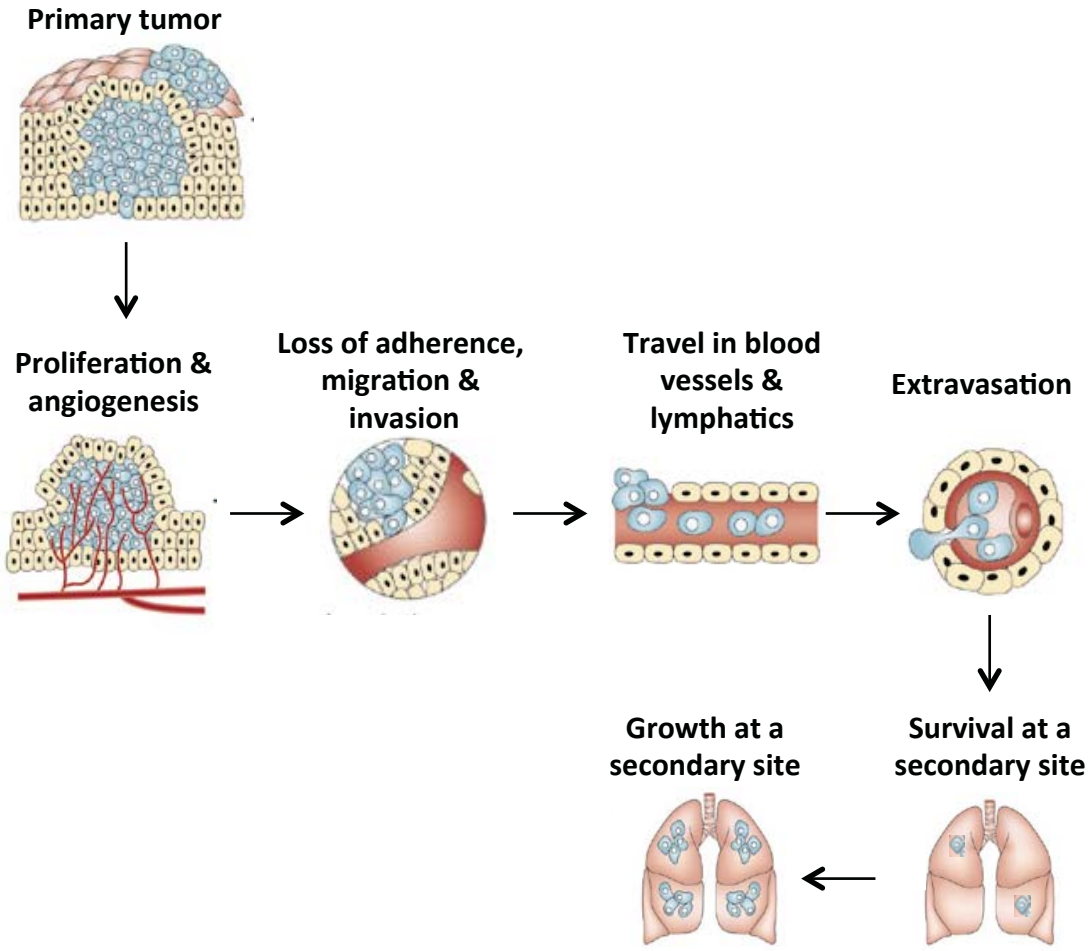

Figure 2. Steps in the metastatic cascade. The metastatic cascade involves multiple steps including: 1) proliferation and angiogenesis, 2) loss of adherence from the primary tumor, 3) migration and invasion through surrounding stroma and basement membrane, 4) intravasation and survival in circulation/lymphatics, 5) extravasation, and 6) growth and survival at a secondary site. (Adapted from Fidler I., 2003, with kind permission from Nature Publishing Group).

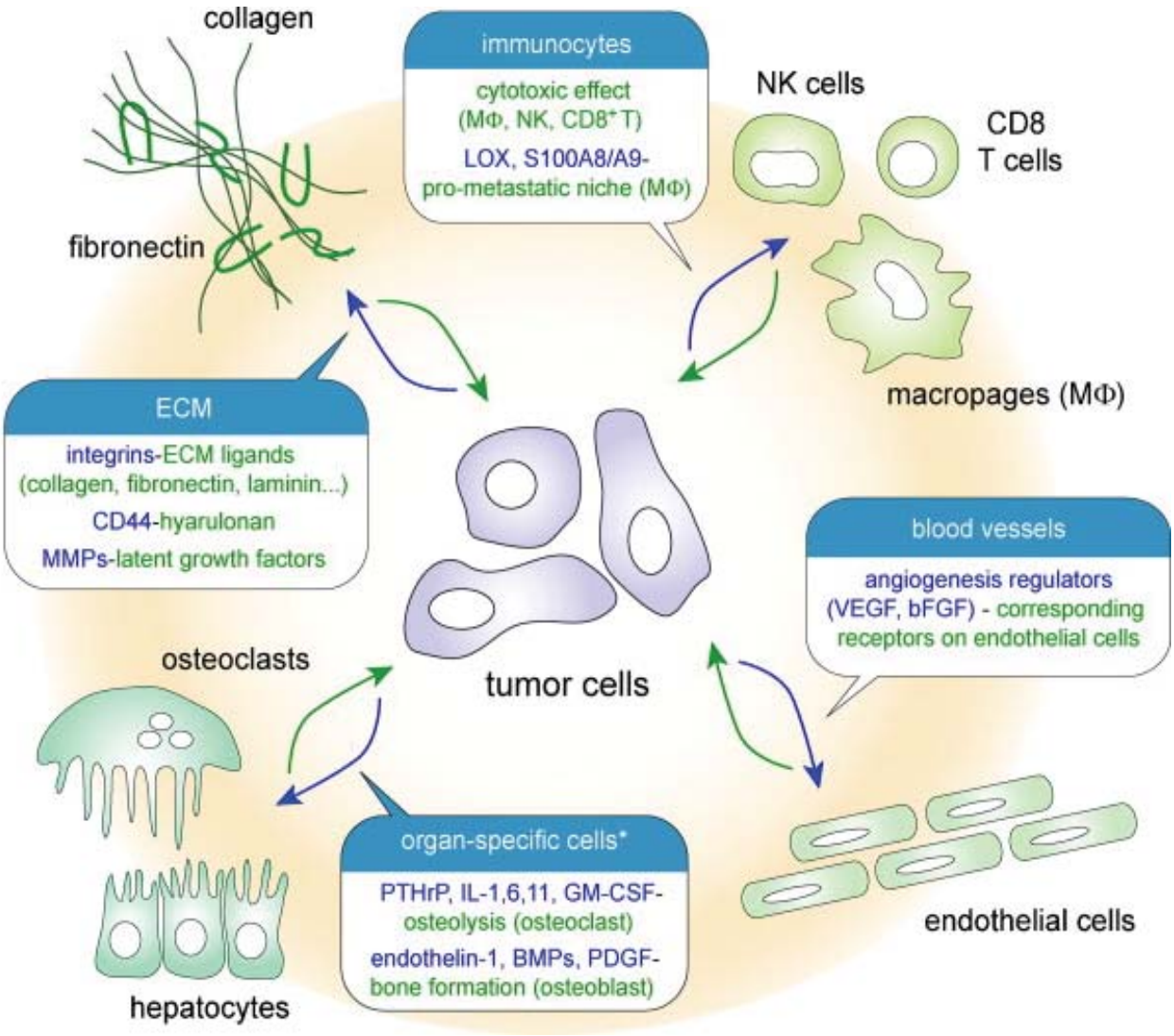

Figure 3. Tumor-microenvironment interactions are required for metastatic colonization. Tumor cells encounter multiple barriers upon colonization of a secondary site. In order to successfully colonize tumor cells must alter cell-intrinsic pathways, cell-microenvironment (ECM, organ specific cells, blood vessels) interactions and cell-immune system (macrophages, T cells and NK cells) interactions. ECM, extracellular matrix. (Adapted from Shibue T., and Weinberg R., 2011, with kind permission from Seminars in Cancer Biology).

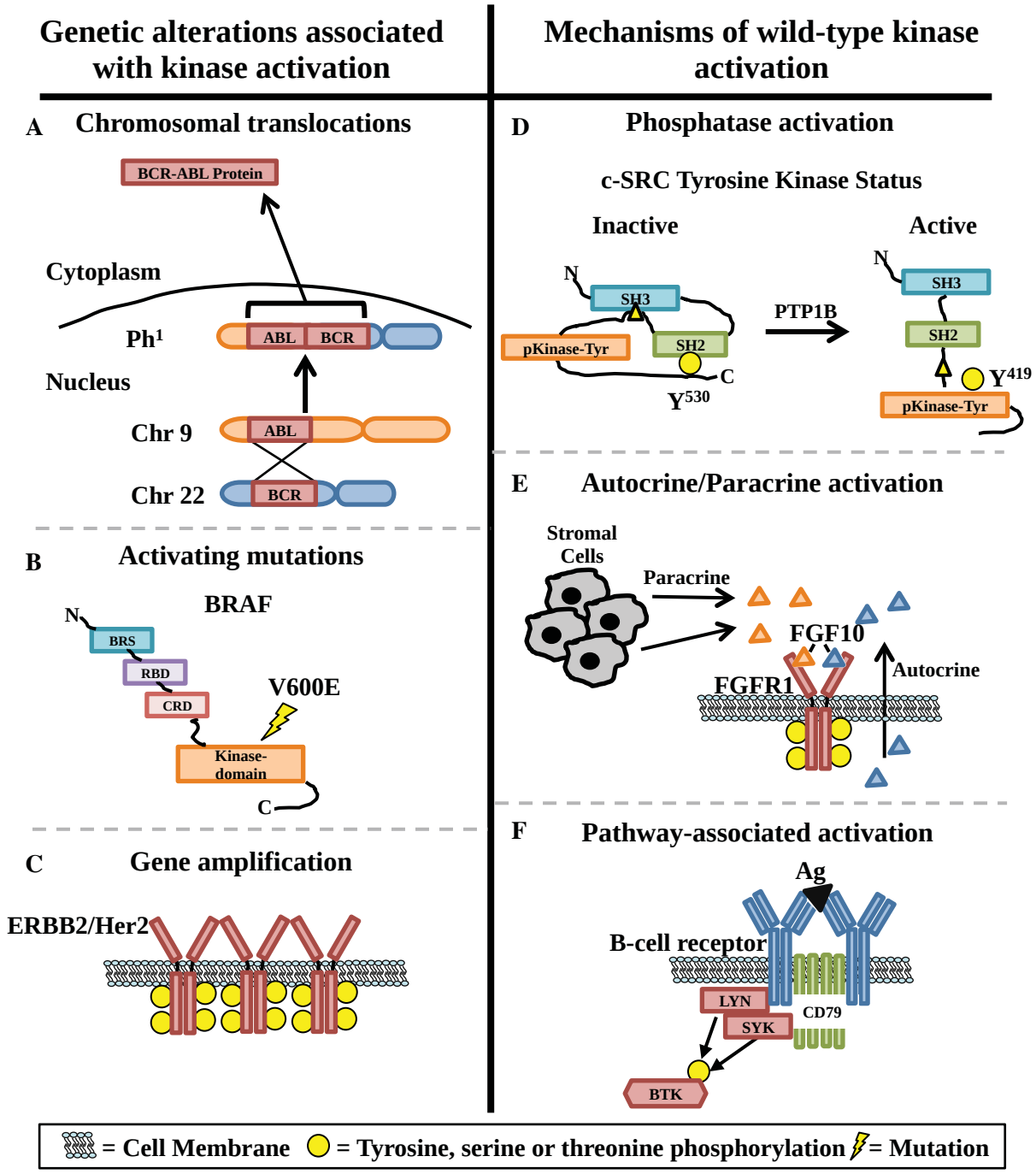

Figure 4. Mechanisms of genetically altered and wild-type kinase activation in cancer. Genetic alterations are the most well-studied mechanisms of kinase activation. Shown are examples of A) chromosomal translocation, B) activating mutations, and C) gene amplification. However, evidence supports that genetic alterations are not essential for kinase activation in cancer. Common mechanisms of wild-type kinase activation include: D) phosphatase activation, E) autocrine or paracrine ligand production, and F) involvement in a hyperactivated signaling pathway. Chr, chromosome; Ph1, Philadelphia chromosome; BCR, breakpoint cluster region; BRS, BRAF-specific region; RBD, Ras-binding domain; CRD, Cys-rich domain; SH2/SH3, Src homology domain 2/3; Ag, antigen. (Adapted from Drake et al., 2014, with kind permission from the American Society for Microbiology).

Kinase	Mutation(s)	Disease(s)	FDA-approved inhibitor(s)
EGFR	Exon 19 and 21	NSCLC	Erlotinib, afatinib
c-KIT	Exon 8, 9, 11, 13 and 17	GIST	Imatinib, sunitinib
PDGFRα	Exon 12, 14 and 18	GIST	Imatinib, sunitinib
RET	Exon 10, 11, 13 and 14	Medullary thyroid carcinoma	Vandetinib, cabozantinib
JAK2	V617F	Myeloproliferative neoplasms	Ruxolitinib
Kinase	**Translocation(s)**	**Disease(s)**	**FDA-approved inhibitor(s)**
ABL1	BCR-ABL1 fusion	CML	Imatinib, dasatinib, nilotinib, bosutinib, ponatinib
RET	RET/PTC family fusions	PTC	Vandetinib
ALK	EML4-ALK fusion	NSCLC	Crizotinib
Kinase	**Amplification(s)**	**Disease(s)**	**FDA-approved inhibitor(s)**
ERBB2	Increased copy number and/or overexpression	Breast cancer Gastric cancer	Trastuzumab Lapatinib Ado-trastuzumab Emtansine Pertuzumab
Kinase	**Pathway Activation**	**Disease(s)**	**FDA-approved inhibitor(s)**
BTK	B-cell receptor signaling	CLL B cell non-Hodgkin's lymphoma	Ibrutinib
VEGFR	Angiogenesis	CCRCC Soft-tissue sarcomas	Sorafenib, sunitinib, pazopanib, axitinib

NSCLC: non-small cell lung cancer, GIST: gastrointestinal stromal tumor, CML: chronic myelogenous leukemia, PTC: papillary thyroid carcinoma, CCRCC: clear cell renal cell carcinoma, CLL: chronic lymphocytic leukemia

Table 1. Genetically altered and wild-type kinases are targets for cancer. Table describes kinases for which there are FDA-approved inhibitors. Kinases in the pathway activation section are non-mutated. (Adapted from Drake et al., 2013, with kind permission from the American Society for Microbiology).

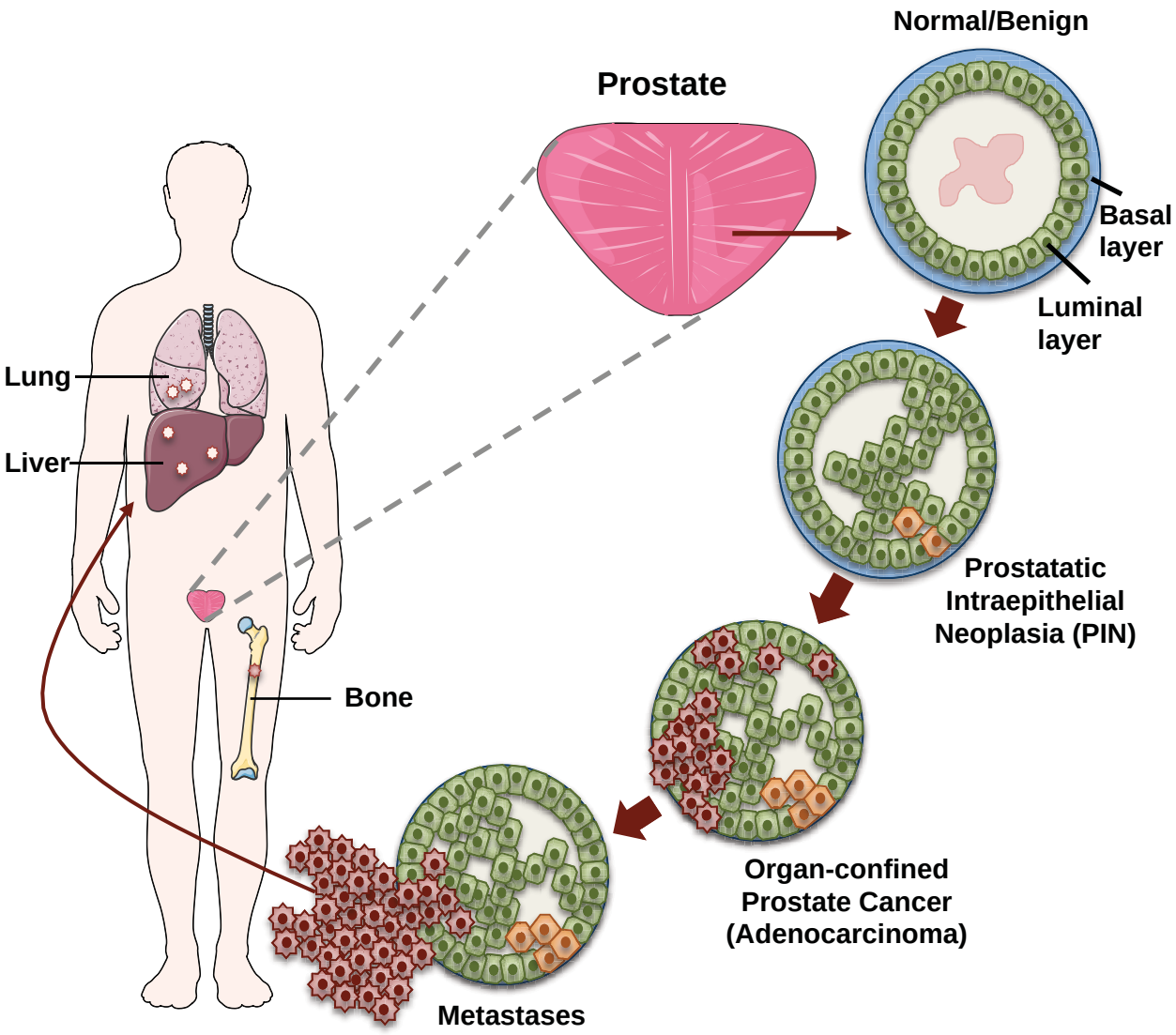

Figure 5. Prostate cancer evolution.
Schematic representation of the development of prostate cancer from a normal gland to metastasis. Most common sites of prostate cancer metastasis (bone, lung, and liver) are illustrated in the figure.

Kinase	Genomic alteration	Stage involvement	Function	Ref
CRAF	Translocation ESRP1-, GOLGA4-RAF1	Metastasis	Unknown	Palanisamy et al., 2010 Robinson et al. 2015
BRAF	Translocation SLC45A3-, KIAA1549-UBN2-BRAF	Metastasis	Unknown	Palanisamy et al., 2010 Robinson et al. 2015
PIK3CA/ PIK3CB	Amplification, mutation	Metastasis	Unknown	Robinson et al. 2015
GRK3	None	Metastasis	Promotes angiogenesis	Li et al. 2014
SRC	None	Adenocarcinoma, CRPC	Proliferation, synergizes with AR	Cai et al. 2010
ERBB2/HER2	None	Adenocarcinoma	Synergizes with PTEN loss to promote progression	Li et al. 2006
PIM1	None	Adenocarcinoma	Enhances transforming potential of myc	Ellwood-Yen et al. 2003
ETK/BMX	None	CRPC	Stabilizes AR	Dai et al. 2010
FGFR1	None	Adenocarcinoma, Metastasis	Promotes proliferation, EMT, angiogenesis, bone colonization	Acevedo et al. 2007, Winter et al. 2007, Wan et al. 2015
MERTK	None	Adenocarcinoma	Promotes cytokine production	Wu et al. 2004
AKT	None	Adenocarcinoma, CRPC	Cell growth, mTOR activation	Majumder et al. 2005
IGFR	None	Adenocarcinoma, metastasis	Proliferation, resistance to apoptosis, invasion	Meinbach et al. 2006
C-MET	None	CRPC, metastasis	Androgen resistance, bone colonization	Varkaris et al. 2011
PDGFR	None	Metastasis	EMT, angiogenesis	Kong et al. 2010

Table 2. Kinases are implicated in advanced prostate cancer.
Table of kinases reported to be involved in advanced prostate cancer. CRPC, castration-resistant prostate cancer; AR, androgen receptor; EMT, epithelial-to-mesenchymal transition.

References

1. E. a. E. R. P. National Cancer Institute: Surveillance, in *SEER Cancer Statistics Review*. (National Cancer Institute, http://seer.cancer.gov/statfacts/html/all.html, 2016), vol. 2016.

2. R. L. Siegel, K. D. Miller, A. Jemal, Cancer statistics, 2015. *CA Cancer J Clin* **65**, 5-29 (2015).

3. A. Jemal *et al*., Cancer statistics, 2005. *CA Cancer J Clin* **55**, 10-30 (2005).

4. S. Valastyan, R. A. Weinberg, Tumor metastasis: molecular insights and evolving paradigms. *Cell* **147**, 275-292 (2011).

5. G. P. Gupta, J. Massague, Cancer metastasis: building a framework. *Cell* **127**, 679-695 (2006).

6. J. Yang *et al*., Twist, a master regulator of morphogenesis, plays an essential role in tumor metastasis. *Cell* **117**, 927-939 (2004).

7. U. Cavallaro, G. Christofori, Cell adhesion and signalling by cadherins and Ig-CAMs in cancer. *Nat Rev Cancer* **4**, 118-132 (2004).

8. M. Egeblad, Z. Werb, New functions for the matrix metalloproteinases in cancer progression. *Nat Rev Cancer* **2**, 161-174 (2002).

9. J. Massague, A. C. Obenauf, Metastatic colonization by circulating tumour cells. *Nature* **529**, 298-306 (2016).

10. S. Braun *et al*., A pooled analysis of bone marrow micrometastasis in breast cancer. *N Engl J Med* **353**, 793-802 (2005).

11. K. Podsypanina *et al*., Seeding and propagation of untransformed mouse mammary cells in the lung. *Science* **321**, 1841-1844 (2008).

12. I. J. Fidler, Metastasis: quantitative analysis of distribution and fate of tumor emboli labeled with 125 I-5-iodo-2'-deoxyuridine. *J Natl Cancer Inst* **45**, 773-782 (1970).

13. K. J. Luzzi *et al*., Multistep nature of metastatic inefficiency: dormancy of solitary cells after successful extravasation and limited survival of early micrometastases. *Am J Pathol* **153**, 865-873 (1998).

14. P. S. Steeg, Targeting metastasis. *Nat Rev Cancer* **16**, 201-218 (2016).

15. L. Bubendorf *et al*., Metastatic patterns of prostate cancer: an autopsy study of 1,589 patients. *Hum Pathol* **31**, 578-583 (2000).

16. M. Ittmann *et al*., Animal models of human prostate cancer: the consensus report of the New York meeting of the Mouse Models of Human Cancers Consortium Prostate Pathology Committee. *Cancer Res* **73**, 2718-2736 (2013).

17. J. Eyles *et al*., Tumor cells disseminate early, but immunosurveillance limits metastatic outgrowth, in a mouse model of melanoma. *J Clin Invest* **120**, 2030-2039 (2010).

18. M. Paolino *et al*., The E3 ligase Cbl-b and TAM receptors regulate cancer metastasis via natural killer cells. *Nature* **507**, 508-512 (2014).

19. M. J. Smyth *et al*., Perforin is a major contributor to NK cell control of tumor metastasis. *J Immunol* **162**, 6658-6662 (1999).

20. S. Malladi *et al*., Metastatic Latency and Immune Evasion through Autocrine Inhibition of WNT. *Cell* **165**, 45-60 (2016).

21. I. Vivanco, C. L. Sawyers, The phosphatidylinositol 3-Kinase AKT pathway in human cancer. *Nat Rev Cancer* **2**, 489-501 (2002).

22. X. H. Zhang *et al*., Latent bone metastasis in breast cancer tied to Src-dependent survival signals. *Cancer Cell* **16**, 67-78 (2009).

23. X. Lu *et al*., VCAM-1 promotes osteolytic expansion of indolent bone micrometastasis of breast cancer by engaging alpha4beta1-positive osteoclast progenitors. *Cancer Cell* **20**, 701-714 (2011).

24. Q. Chen, X. H. Zhang, J. Massague, Macrophage binding to receptor VCAM-1 transmits survival signals in breast cancer cells that invade the lungs. *Cancer Cell* **20**, 538-549 (2011).

25. A. F. Chambers, A. C. Groom, I. C. MacDonald, Dissemination and growth of cancer cells in metastatic sites. *Nat Rev Cancer* **2**, 563-572 (2002).

26. T. Hunter, A thousand and one protein kinases. *Cell* **50**, 823-829 (1987).

27. M. A. Lemmon, J. Schlessinger, Cell signaling by receptor tyrosine kinases. *Cell* **141**, 1117-1134 (2010).

28. J. Pines, Protein kinases and cell cycle control. *Seminars in cell biology* **5**, 399-408 (1994).

29. E. A. Nigg, Mitotic kinases as regulators of cell division and its checkpoints. *Nat Rev Mol Cell Biol* **2**, 21-32 (2001).

30. I. Ruvinsky, O. Meyuhas, Ribosomal protein S6 phosphorylation: from protein synthesis to cell size. *Trends in biochemical sciences* **31**, 342-348 (2006).

31. C. de Haro, R. Mendez, J. Santoyo, The eIF-2alpha kinases and the control of protein synthesis. *FASEB journal : official publication of the Federation of American Societies for Experimental Biology* **10**, 1378-1387 (1996).

32. R. J. Davis, Independent mechanisms account for the regulation by protein kinase C of the epidermal growth factor receptor affinity and tyrosine-protein kinase activity. *J Biol Chem* **263**, 9462-9469 (1988).

33. M. W. Deininger, J. M. Goldman, J. V. Melo, The molecular biology of chronic myeloid leukemia. *Blood* **96**, 3343-3356 (2000).

34. A. de Klein *et al*., A cellular oncogene is translocated to the Philadelphia chromosome in chronic myelocytic leukaemia. *Nature* **300**, 765-767 (1982).

35. J. B. Konopka, S. M. Watanabe, O. N. Witte, An alteration of the human c-abl protein in K562 leukemia cells unmasks associated tyrosine kinase activity. *Cell* **37**, 1035-1042 (1984).

36. J. M. Drake, J. K. Lee, O. N. Witte, Clinical targeting of mutated and wild-type protein tyrosine kinases in cancer. *Mol Cell Biol* **34**, 1722-1732 (2014).

37. H. Davies *et al*., Mutations of the BRAF gene in human cancer. *Nature* **417**, 949-954 (2002).

38. E. R. Cantwell-Dorris, J. J. O'Leary, O. M. Sheils, BRAFV600E: implications for carcinogenesis and molecular therapy. *Mol Cancer Ther* **10**, 385-394 (2011).

39. D. J. Slamon *et al*., Human breast cancer: correlation of relapse and survival with amplification of the HER-2/neu oncogene. *Science* **235**, 177-182 (1987).

40. J. A. Engelman *et al*., MET amplification leads to gefitinib resistance in lung cancer by activating ERBB3 signaling. *Science* **316**, 1039-1043 (2007).

41. A. Bardelli *et al*., Amplification of the MET receptor drives resistance to anti-EGFR therapies in colorectal cancer. *Cancer Discov* **3**, 658-673 (2013).

42. Y. Han *et al*., Loss of SHP1 enhances JAK3/STAT3 signaling and decreases proteosome degradation of JAK3 and NPM-ALK in ALK+ anaplastic large-cell lymphoma. *Blood* **108**, 2796-2803 (2006).

43. S. Memarzadeh *et al*., Enhanced paracrine FGF10 expression promotes formation of multifocal prostate adenocarcinoma and an increase in epithelial androgen receptor. *Cancer Cell* **12**, 572-585 (2007).

44. R. E. Davis *et al*., Chronic active B-cell-receptor signalling in diffuse large B-cell lymphoma. *Nature* **463**, 88-92 (2010).

45. T. Li *et al*., Constitutive membrane association potentiates activation of Bruton tyrosine kinase. *Oncogene* **15**, 1375-1383 (1997).

46. A. J. Mohamed *et al*., Bruton's tyrosine kinase (Btk): function, regulation, and transformation with special emphasis on the PH domain. *Immunological reviews* **228**, 58-73 (2009).

47. J. Zhang, P. L. Yang, N. S. Gray, Targeting cancer with small molecule kinase inhibitors. *Nat Rev Cancer* **9**, 28-39 (2009).

48. K. Imai, A. Takaoka, Comparing antibody and small-molecule therapies for cancer. *Nat Rev Cancer* **6**, 714-727 (2006).

49. M. Carroll *et al*., CGP 57148, a tyrosine kinase inhibitor, inhibits the growth of cells expressing BCR-ABL, TEL-ABL, and TEL-PDGFR fusion proteins. *Blood* **90**, 4947-4952 (1997).

50. H. Kantarjian *et al*., Improved survival in chronic myeloid leukemia since the introduction of imatinib therapy: a single-institution historical experience. *Blood* **119**, 1981-1987 (2012).

51. C. Gambacorti-Passerini *et al*., Multicenter independent assessment of outcomes in chronic myeloid leukemia patients treated with imatinib. *J Natl Cancer Inst* **103**, 553-561 (2011).

52. B. J. Druker *et al*., Five-year follow-up of patients receiving imatinib for chronic myeloid leukemia. *N Engl J Med* **355**, 2408-2417 (2006).

53. P. B. Chapman *et al*., Improved survival with vemurafenib in melanoma with BRAF V600E mutation. *N Engl J Med* **364**, 2507-2516 (2011).

54. L. M. Ellis, D. J. Hicklin, VEGF-targeted therapy: mechanisms of anti-tumour activity. *Nat Rev Cancer* **8**, 579-591 (2008).

55. J. M. Ebos *et al*., Accelerated metastasis after short-term treatment with a potent inhibitor of tumor angiogenesis. *Cancer Cell* **15**, 232-239 (2009).

56. M. Paez-Ribes *et al*., Antiangiogenic therapy elicits malignant progression of tumors to increased local invasion and distant metastasis. *Cancer Cell* **15**, 220-231 (2009).

57. L. A. Honigberg *et al*., The Bruton tyrosine kinase inhibitor PCI-32765 blocks B-cell activation and is efficacious in models of autoimmune disease and B-cell malignancy. *Proc Natl Acad Sci U S A* **107**, 13075-13080 (2010).

58. J. C. Byrd *et al*., Targeting BTK with ibrutinib in relapsed chronic lymphocytic leukemia. *N Engl J Med* **369**, 32-42 (2013).

59. M. L. Wang *et al*., Targeting BTK with ibrutinib in relapsed or refractory mantle-cell lymphoma. *N Engl J Med* **369**, 507-516 (2013).

60. S. P. Treon *et al*., Ibrutinib in previously treated Waldenstrom's macroglobulinemia. *N Engl J Med* **372**, 1430-1440 (2015).

61. A. Wiestner, Targeting B-Cell receptor signaling for anticancer therapy: the Bruton's tyrosine kinase inhibitor ibrutinib induces impressive responses in B-cell malignancies. *J Clin Oncol* **31**, 128-130 (2013).

62. C. M. Johannessen *et al*., COT drives resistance to RAF inhibition through MAP kinase pathway reactivation. *Nature* **468**, 968-972 (2010).

63. J. Villanueva *et al*., Acquired resistance to BRAF inhibitors mediated by a RAF kinase switch in melanoma can be overcome by cotargeting MEK and IGF-1R/PI3K. *Cancer Cell* **18**, 683-695 (2010).

64. C. Robert *et al*., Improved overall survival in melanoma with combined dabrafenib and trametinib. *N Engl J Med* **372**, 30-39 (2015).

65. C. S. Grasso *et al*., The mutational landscape of lethal castration-resistant prostate cancer. *Nature* **487**, 239-243 (2012).

66. B. S. Taylor *et al*., Integrative genomic profiling of human prostate cancer. *Cancer Cell* **18**, 11-22 (2010).

67. D. Robinson *et al*., Integrative clinical genomics of advanced prostate cancer. *Cell* **161**, 1215-1228 (2015).

68. N. Palanisamy *et al*., Rearrangements of the RAF kinase pathway in prostate cancer, gastric cancer and melanoma. *Nat Med* **16**, 793-798 (2010).

69. P. A. Humphrey, Gleason grading and prognostic factors in carcinoma of the prostate. *Mod Pathol* **17**, 292-306 (2004).

70. J. M. Drake *et al*., Oncogene-specific activation of tyrosine kinase networks during prostate cancer progression. *Proc Natl Acad Sci U S A* **109**, 1643-1648 (2012).

71. H. Cai, I. Babic, X. Wei, J. Huang, O. N. Witte, Invasive prostate carcinoma driven by c-Src and androgen receptor synergy. *Cancer Res* **71**, 862-872 (2011).

72. I. Ahmad *et al*., HER2 overcomes PTEN (loss)-induced senescence to cause aggressive prostate cancer. *Proc Natl Acad Sci U S A* **108**, 16392-16397 (2011).

73. J. Edwards, N. S. Krishna, C. J. Witton, J. M. Bartlett, Gene amplifications associated with the development of hormone-resistant prostate cancer. *Clin Cancer Res* **9**, 5271-5281 (2003).

74. G. Di Lorenzo *et al*., Expression of epidermal growth factor receptor correlates with disease relapse and progression to androgen-independence in human prostate cancer. *Clin Cancer Res* **8**, 3438-3444 (2002).

75. Z. Guo *et al*., Regulation of androgen receptor activity by tyrosine phosphorylation. *Cancer Cell* **10**, 309-319 (2006).

76. S. Kraus, D. Gioeli, T. Vomastek, V. Gordon, M. J. Weber, Receptor for activated C kinase 1 (RACK1) and Src regulate the tyrosine phosphorylation and function of the androgen receptor. *Cancer Res* **66**, 11047-11054 (2006).

77. B. Dai *et al*., Compensatory upregulation of tyrosine kinase Etk/BMX in response to androgen deprivation promotes castration-resistant growth of prostate cancer cells. *Cancer Res* **70**, 5587-5596 (2010).

78. B. S. Carver *et al*., Reciprocal feedback regulation of PI3K and androgen receptor signaling in PTEN-deficient prostate cancer. *Cancer Cell* **19**, 575-586 (2011).

79. D. Sarker, A. H. Reid, T. A. Yap, J. S. de Bono, Targeting the PI3K/AKT pathway for the treatment of prostate cancer. *Clin Cancer Res* **15**, 4799-4805 (2009).

80. Y. Zheng *et al*., PTK6 activation at the membrane regulates epithelial-mesenchymal transition in prostate cancer. *Cancer Res* **73**, 5426-5437 (2013).

81. X. Wan *et al*., Prostate cancer cell-stromal cell crosstalk via FGFR1 mediates antitumor activity of dovitinib in bone metastases. *Science translational medicine* **6**, 252ra122 (2014).

82. I. J. Fidler, The pathogenesis of cancer metastasis: the 'seed and soil' hypothesis revisited. *Nat Rev Cancer* **3**, 453-458 (2003).

83. T. Shibue, R. A. Weinberg, Metastatic colonization: settlement, adaptation and propagation of tumor cells in a foreign tissue environment. *Seminars in cancer biology* **21**, 99-106 (2011).

84. W. Li *et al*., GRK3 is essential for metastatic cells and promotes prostate tumor progression. *Proc Natl Acad Sci U S A* **111**, 1521-1526 (2014).

85. K. Ellwood-Yen *et al*., Myc-driven murine prostate cancer shares molecular features with human prostate tumors. *Cancer Cell* **4**, 223-238 (2003).

86. V. D. Acevedo *et al*., Inducible FGFR-1 activation leads to irreversible prostate adenocarcinoma and an epithelial-to-mesenchymal transition. *Cancer Cell* **12**, 559-571 (2007).

87. S. F. Winter *et al*., Conditional activation of FGFR1 in the prostate epithelium induces angiogenesis with concomitant differential regulation of Ang-1 and Ang-2. *Oncogene* **26**, 4897-4907 (2007).

88. Y. M. Wu, D. R. Robinson, H. J. Kung, Signal pathways in up-regulation of chemokines by tyrosine kinase MER/NYK in prostate cancer cells. *Cancer Res* **64**, 7311-7320 (2004).

89. P. K. Majumder, W. R. Sellers, Akt-regulated pathways in prostate cancer. *Oncogene* **24**, 7465-7474 (2005).

90. D. S. Meinbach, B. L. Lokeshwar, Insulin-like growth factors and their binding proteins in prostate cancer: cause or consequence? *Urologic oncology* **24**, 294-306 (2006).

91. A. Varkaris *et al*., The role of HGF/c-Met signaling in prostate cancer progression and c-Met inhibitors in clinical trials. *Expert opinion on investigational drugs* **20**, 1677-1684 (2011).

92. D. Kong *et al*., Epithelial to mesenchymal transition is mechanistically linked with stem cell signatures in prostate cancer cells. *PLoS One* **5**, e12445 (2010).

References used in figures

Figure 1: *(14)*

Figure 2: (*82*)

Figure 3: (*83*)

Figure 4: *(36)*

Table 1: *(36)*

Table 2: (67), (68), (71), (77), (81), (*84*), (*85*), (*86*), (*87*), (*88, 89*), (*90*), (*91*), (*92*)

Chapter 2:

Metastatic castration-resistant prostate cancer reveals intrapatient similarity and interpatient heterogeneity of therapeutic kinase targets

Metastatic castration-resistant prostate cancer reveals intrapatient similarity and interpatient heterogeneity of therapeutic kinase targets

Justin M. Drake[a], Nicholas A. Graham[b,c], John K. Lee[d,e], Tanya Stoyanova[a], Claire M. Faltermeier[e], Sudha Sud[f], Björn Titz[b,c], Jiaoti Huang[g,h,i], Kenneth J. Pienta[f,j], Thomas G. Graeber[b,c,g,k,l], and Owen N. Witte[a,c,l,m,1]

[a]Department of Microbiology, Immunology, and Molecular Genetics, [b]Crump Institute for Molecular Imaging, [c]Department of Molecular and Medical Pharmacology, [d]Division of Hematology and Oncology, Department of Medicine, [e]Molecular Biology Institute, [g]Jonsson Comprehensive Cancer Center, [h]Department of Pathology and Laboratory Medicine, [i]Eli and Edythe Broad Center of Regenerative Medicine and Stem Cell Research, [k]Institute for Molecular Medicine, [l]California NanoSystems Institute, and [m]Howard Hughes Medical Institute, David Geffen School of Medicine, University of California, Los Angeles, CA 90095; [j]The Brady Urological Institute, Johns Hopkins School of Medicine, Baltimore, MD 21231; and [f]Department of Internal Medicine, University of Michigan Medical School, Ann Arbor, MI 48109

Contributed by Owen N. Witte, October 23, 2013 (sent for review September 5, 2013)

In prostate cancer, multiple metastases from the same patient share similar copy number, mutational status, erythroblast transformation specific (ETS) rearrangements, and methylation patterns supporting their clonal origins. Whether actionable targets such as tyrosine kinases are also similarly expressed and activated in anatomically distinct metastatic lesions of the same patient is not known. We evaluated active kinases using phosphotyrosine peptide enrichment and quantitative mass spectrometry to identify druggable targets in metastatic castration-resistant prostate cancer obtained at rapid autopsy. We identified distinct phosphopeptide patterns in metastatic tissues compared with treatment-naive primary prostate tissue and prostate cancer cell line-derived xenografts. Evaluation of metastatic castration-resistant prostate cancer samples for tyrosine phosphorylation and upstream kinase targets revealed SRC, epidermal growth factor receptor (EGFR), rearranged during transfection (RET), anaplastic lymphoma kinase (ALK), and MAPK1/3 and other activities while exhibiting intrapatient similarity and interpatient heterogeneity. Phosphoproteomic analyses and identification of kinase activation states in metastatic castration-resistant prostate cancer patients have allowed for the prioritization of kinases for further clinical evaluation.

metastasis | resistance | personalized medicine | combination therapy | phosphotyrosine

Mutational and copy number analyses from epithelial tumors have identified several activating tyrosine kinase mutations and amplifications, such as epidermal growth factor receptor (EGFR) mutations in lung adenocarcinoma and erythroblastic leukemia viral oncogene homolog 2 (*ERBB2 or HER2/neu*) gene amplification in breast cancer (1). The dependence on these tyrosine kinases for tumor growth and survival has led to successful clinical treatment with tyrosine kinase inhibitors (TKIs) (2, 3). However, recent genomic analyses of prostate adenocarcinoma revealed that activating tyrosine kinase mutations or amplifications are very rare (1, 4–6).

Despite the scarcity of tyrosine kinase amplifications or activating mutations in prostate cancer, tyrosine kinase expression and activity has been shown to play an important role in disease progression. For example, coexpression of wild-type SRC tyrosine kinase and androgen receptor (AR) can synergistically drive the formation of mouse prostate adenocarcinoma (7). Evaluation of nontyrosine-kinase–initiated mouse models of prostate cancer further identified activation of the nonreceptor tyrosine kinases SRC, ABL1, and Janus kinase 2 (JAK2) (8). We also observed increased tyrosine phosphorylation in nearly 50% of castration-resistant prostate cancer (CRPC) tissues examined compared with hormone-naïve prostate cancer (8). These studies suggest that comprehensive evaluation of metastatic CRPC samples for tyrosine kinase activity may lead to the identification of new drug targets.

Studies in melanoma and breast cancer have revealed that despite heterogeneity in primary, localized disease, metastases seem to arise from a single precursor cell (9, 10). The multifocal nature of organ-confined prostate cancer poses a question as to the clonality of metastatic disease (11). Investigation into clonality in metastatic CRPC has found that tumors isolated from anatomically different lesions in the same patient bear similar copy number, mutational status, erythroblast transformation specific (ETS) rearrangements, and methylation patterns from multiple metastatic lesions supporting their clonal origins (6, 12–14). In addition, these studies found a remarkable amount of interpatient heterogeneity, suggesting that personalized medicine approaches may be necessary to efficiently target metastatic lesions. Previous observations of intrapatient similarity hold promise with regard to treatment strategies for metastatic CRPC patients by means of systematically attacking the cancer cell clone contributing to disease.

This led us to investigate whether actionable targets such as tyrosine kinases also maintain similar activation patterns across anatomically distinct metastases from the same patient. With

Significance

Metastatic castration-resistant prostate cancer (CRPC) remains incurable due to the lack of effective therapies. The need to identify new actionable targets in CRPC is crucial as we begin to examine the resistance mechanisms related to androgen withdrawal. Here, we report an unbiased quantitative phosphoproteomic approach to identify druggable kinases in metastatic CRPC. These kinase activation patterns revealed intrapatient similarity and interpatient heterogeneity across a large panel of targets. Interestingly, these kinase activities are not a result of mutation but rather pathway activation within the tumors themselves. The observation that similar kinase activities are present in most if not all anatomically disparate metastatic lesions from the same patient suggests that CRPC patients may benefit from individualized, targeted combination therapies.

Author contributions: J.M.D., N.A.G., K.J.P., T.G.G., and O.N.W. designed research; J.M.D., N.A.G., J.K.L., T.S., C.M.F., and S.S. performed research; J.M.D., N.A.G., J.K.L., C.M.F., B.T., and J.H. analyzed data; and J.M.D., N.A.G., J.K.L., and O.N.W. wrote the paper.

The authors declare no conflict of interest.

Freely available online through the PNAS open access option.

Data deposition: The MS proteomics data have been deposited in ProteomeXchange, www.proteomexchange.org (accession no. PXD000238).

[1]To whom correspondence should be addressed. E-mail: owenwitte@mednet.ucla.edu.

This article contains supporting information online at www.pnas.org/lookup/suppl/doi:10.1073/pnas.1319948110/-/DCSupplemental.

access to rare metastatic CRPC tissue from the University of Michigan's Rapid Autopsy Program (15), we evaluated global tyrosine phosphorylation patterns in lethal metastatic CRPC patients. Phosphotyrosine peptide enrichment and quantitative mass spectrometry (MS) identified diverse phosphorylation events in the metastatic tissues compared with naive primary prostate tissue and prostate cancer cell line-derived xenografts. Validation of activated kinases that were identified via either MS or kinase–substrate relationships revealed intrapatient similarity and interpatient heterogeneity across a large panel of targets. Interestingly, these kinase activities are a result not of mutation (6) but rather of pathway activation within the tumors themselves. In summary, the observation that similar tyrosine kinase activities are present in most if not all anatomically disparate metastatic lesions from the same patient reveals that (*i*) CRPC lesions may be clonal in origin and (*ii*) kinase activation patterns observed in these lesions should be prioritized for further evaluation as new targeted therapeutic strategies.

Results

Phosphotyrosine Peptide Signatures Are Dramatically Different Between Prostate Cancer Cell Line-Derived Xenografts and Treatment-Naïve or Metastatic CRPC Tissues. To identify and discover unique kinase targets in metastatic CRPC, we analyzed 16 metastatic CRPC samples from 13 different patients obtained at rapid autopsy (15) by quantitative label-free phosphotyrosine MS (Fig. 1). These included eight anatomically unique sites as well as two or three distinct sites from three separate patients. Each sample contained greater than 50% tumor content as determined by histological analyses. We also analyzed one benign prostatic hyperplasia (BPH), six treatment-naïve matched benign and cancerous prostates, and metastatic or s.c. xenograft tumors derived from the androgen-insensitive 22Rv1 and androgen-sensitive LNCaP cell lines (Dataset S1) (8). From three separate phosphotyrosine enrichment preparations and MS analyses, we identified 297 unique phosphopeptides corresponding to 185 unique proteins (Dataset S2).

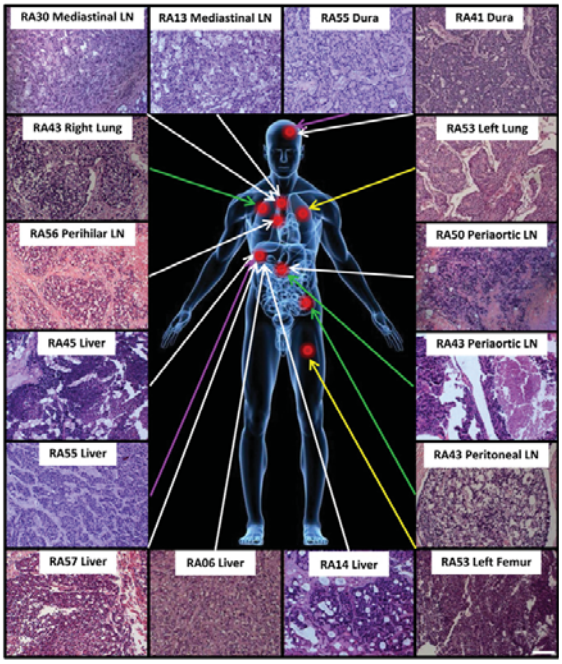

Fig. 1. Anatomical location and histological characterization of metastatic CRPC samples used for phosphoproteomics. Metastatic CRPC tissues were obtained from the Rapid Autopsy Program at the University of Michigan. Sixteen samples from 12 different patients are represented and prepared as previously described for phosphoproteomics (8). Red dots indicate the approximate location of the metastatic lesions analyzed. Same-colored lines represent tissues from the same patient. Patient RA53 left lung and left femur were combined due to limiting material (yellow lines). Only tissues with greater than 350 mg and 50% tumor content were evaluated. (Scale bar, 50 μm.)

To compare different models and stages of prostate cancer, we included cell line-derived xenografts, treatment-naïve primary prostate benign and cancerous tissues, and metastatic CRPC in a single phosphotyrosine enrichment preparation. Unsupervised hierarchical clustering revealed three separate clusters. In particular, the cell line-derived xenografts formed a distinct group compared to the primary tissues, indicating that these xenografts are poor representations of primary patient tissue (Fig. 2*A*). In addition, unsupervised hierarchical clustering also did not distinguish between the patient-matched benign or cancerous prostates, indicating that tyrosine phosphorylation remains relatively unchanged in treatment-naïve benign or cancerous prostates (Fig. 2*A* and Figs. S1 and S2). This suggests that evaluation of phosphotyrosine activity in metastatic CRPC tissues is crucial to testing potential new therapeutic treatments.

Phosphoproteomic Profiling and Kinase/Substrate Enrichment Analyses Identifies Several Druggable Nonmutated Kinase Targets and Pathways in Metastatic CRPC Lesions. Most patients with metastatic CRPC present with metastases at multiple sites, creating a therapeutic dilemma (15). We set out to examine heterogeneity in a cohort of metastatic CRPC patients including those with multiple, anatomically distinct metastatic sites for activated kinase targets. Several metastatic CRPC patients that we evaluated contained similar anatomic sites of involvement including tumors in the liver, lung, dura, and distant lymph nodes. Unsupervised hierarchical clustering of the tyrosine phosphorylation patterns of 10 metastatic lesions, including two patients for which we had two independent metastatic lesions, grouped samples by both patient and metastatic site (Fig. 2*B* and Fig. S3).

Phosphotyrosine peptide identification directly identified several activated kinases and phosphatases [tyrosine kinase 2 (TYK2) Y^{292}, protein tyrosine kinase 2 beta (PTK2B) Y^{579}, MAPK1/3 $Y^{187/204}$, discoidin domain receptor tyrosine kinase 1 (DDR1) Y^{796}, the JAK2/SRC kinase target STAT3 Y^{705}, and protein tyrosine phosphatase, non-receptor type 11 (PTPN11) $Y^{62/63}$]. Kinase–substrate relationship analyses, which predict kinase activity based on phosphopeptide motifs (8), have also identified putative upstream kinases and phosphatases [anaplastic lymphoma kinase (ALK), EGFR, PTK6, SRC, and PTPN2] that were active in individual metastatic CRPC samples (Figs. S1–S3 and Datasets S3–S5). These identifications were notable because of the US Food and Drug Administration–approved late-stage clinical trial of available kinase inhibitors targeting SRC (dasatinib/bosutinib/ponatinib) (16–18), EGFR (erlotinib) (19), ALK (crizotinib) (20), the MAPK1/3 upstream pathway kinases mitogen-activated protein kinase kinase 1/2 (MEK1/2) (trametinib) (21), or the STAT3 upstream kinase JAK2 (ruxolitinib) (22). Western blot analyses from five different patients confirmed the activation states of some of these kinases and also revealed interpatient heterogeneity as each patient evaluated displayed a unique phosphopattern (Fig. 2*C*). As expected, when evaluating prospectively the mutational status of a subset of our samples, we observed little to no activating mutations in these kinases. We did find one patient, RA57 Liver, to have two mutations [one in ephrin type-A receptor 4 (EPHA4) and one in mast/stem cell growth factor receptor (SCFR or KIT)] (6). However, our kinase/substrate enrichment scores did not predict kinase activity of either EPHA4 or KIT, again suggesting

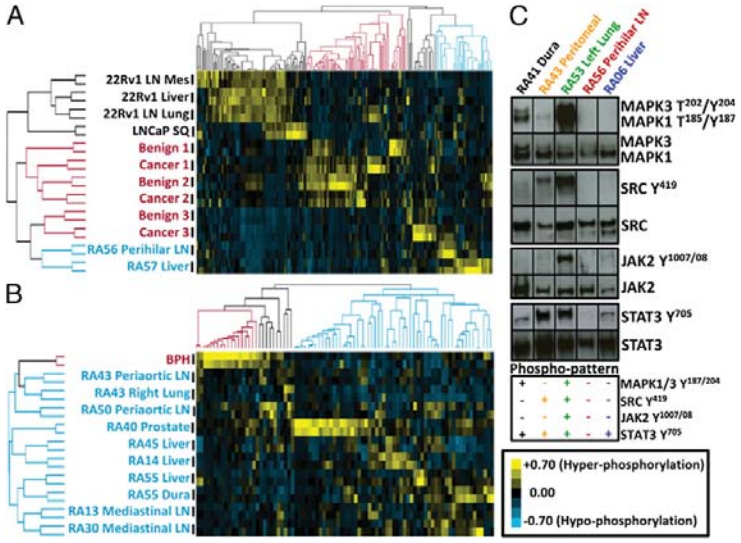

Fig. 2. Phosphoproteomic analyses of cell line-derived xenografts, treatment-naïve prostate cancer, and metastatic CRPC reveal distinct phosphopatterns. (*A*) Unsupervised hierarchical clustering of phosphotyrosine-enriched peptides separates cell line-derived xenograft tumors from primary prostate or metastatic tissue. (*B*) Further evaluation of a separate run of 10 metastatic CRPC lesions reveals patient-specific and metastatic site similarity of phosphotyrosine peptide patterns. (*C*) Western blot validation of four different activated kinases identified from both phosphoproteomics and inferred kinase activities confirms the heterogeneity observed across five different patients, as each patient exhibited a unique phosphopattern. Western blot data were separated to highlight each individual patient but were performed on the same western blot. Yellow, hyperphosphorylation; blue, hypophosphorylation. Intensity bar in Fig. 2*B* is applicable to Fig. 2*A*.

that these mutations did not lead to any detectable levels of activation of these kinases in this tissue sample.

Correlation analysis of the phosphotyrosine signaling patterns revealed a significant level of similarity in the phosphotyrosine profiles from lesions derived from a single patient, despite the fact that these lesions were derived from distinct anatomical sites (Fig. S4). Comparing three liver metastases, we also observed high levels of similarity between two of three lesions (Fig. S4). These MS–based phosphoproteomic data suggest that metastatic CRPC lesions isolated from the same patient may exhibit highly similar tyrosine kinase activation patterns but do not exclude the possibility that anatomical location may also drive similar phosphotyrosine signaling patterns in CRPC. This aspect is further analyzed below.

Large-Scale Analyses of Kinase Activation Patterns Reveals Intrapatient Similarity Across Multiple, Anatomically Distinct Metastases. To determine if signaling patterns were more similar within anatomically distinct metastatic lesions from the same CRPC patient or within sites of metastasis, we examined a larger, independent set of patients that included 28 distinct metastatic lesions from seven different CRPC patients (Fig. S5). Western blot analysis of phosphoproteins identified by MS and kinase/substrate enrichment analysis or the activated states of receptor tyrosine kinase (RTK) targets [EGFR Y^{1173}, ERBB2 Y^{1221}, and hepatocyte growth factor receptor (HGFR or MET) Y^{1234}] for which there are clinical inhibitors available confirmed our initial observation of intrapatient similarities (Fig. 3 and Fig. S6 *A*–*C*). Comparison of different patients revealed dramatically different kinase activation patterns. This ranged from SRC Y^{419}, STAT3 Y^{705}, MAPK1/3 $T^{185/202}/Y^{187/204}$, and AKT S^{473}, activated upon phosphatase and tensin homolog (*PTEN*) loss in the majority of prostate cancers, for patient RA43 to only STAT3 Y^{705} for patient RA55 (Fig. 3). These unique phosphopatterns suggest that shared kinase activities exist in metastatic CRPC lesions isolated from the same patient.

To determine if this pattern of intrapatient similarity across metastases remains consistent with a larger set of other RTK and intracellular kinases, we evaluated five previously analyzed sets of patient metastases using RTK and phosphokinase arrays from R&D Systems. Analysis of three or four anatomically distinct metastatic lesions from each patient revealed signaling patterns that were qualitatively similar within a patient's set of metastatic lesions (Fig. 4*A*). Patient-specific patterns included (*i*) tyrosine phosphorylation of ALK, RYK, and the activation site of AKT T^{308} in patient RA37; (*ii*) hemopoietic cell kinase (HCK) pY^{411} from patient RA56; and (*iii*) cellular RET (c-RET) phosphorylation in RA33 (Fig. 4*A*). Quantitation of these arrays revealed intrapatient similarities for nine phospho- and total proteins (Fig. 4*B*). Principal component analysis (PCA) of the kinases and proteins with detectable phosphorylation or expression ($n = 11$) demonstrated highly similar intrapatient grouping (Fig. 4*C* and Fig. S7). Surprisingly, the signaling patterns found in these metastatic lesions appear to be substantially cell autonomous as lesions from similar anatomical sites did not group together (Fig. 4*D*). Statistical analysis of pairwise correlation coefficients confirmed that metastatic CRPC lesions isolated from the same patient have strongly similar signaling patterns, more so than lesions from similar anatomical sites in different patients (Fig. S8).

Phosphorylation of Neuronal RTK RET in Metastatic CRPC Lesions with a Small Cell Neuroendocrine Carcinoma Phenotype. Further evaluation of the phospho-RTK arrays revealed tyrosine phosphorylation of RET in patient RA33 (Fig. 3*A*). RET is expressed in neuronal cell types, suggesting this patient may have suffered from a rare small cell neuroendocrine carcinoma (SCNC) phenotype (23). Indeed histological analyses of patient RA33 confirmed SCNC as evidenced by a diffuse, solid growth pattern with darkly stained nucleus, a homogeneous chromatin pattern, high nuclear/cytoplasmic (N/C) ratio, lack of nucleoli, and frequent mitotic figures (Fig. S9 *A* and *B*, arrows). These are in sharp contrast

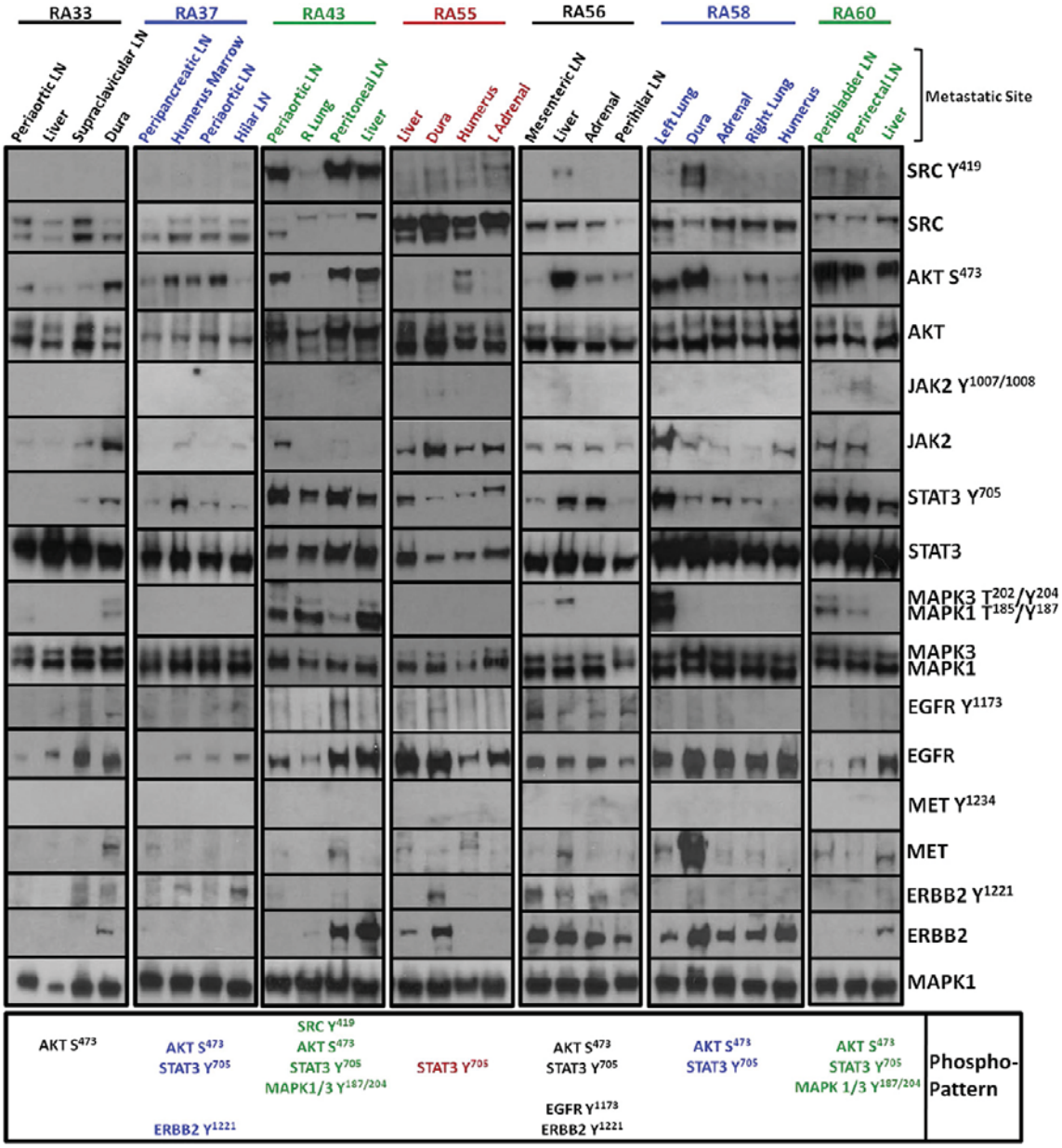

Fig. 3. Related phosphokinase and substrate expression patterns are observed within distinct anatomical metastatic lesions of the same patient. Western blot analyses from seven different sets of patients with three or four distinct metastatic lesions were evaluated for kinase activation patterns that were identified in the phosphoproteomic datasets and kinase–substrate relationships or RTKs that have been previously targeted clinically. Each patient expressed similar activated kinase patterns independent of the anatomical location of the metastatic lesions. The unique phosphopatterns are also depicted schematically below the Western blot data.

to the conventional prostatic adenocarcinoma that shows glandular formation (Fig. S9*C*, dashed circle), nuclear morphology consisting of open and vesicular chromatin patterns, and prominent nuclei (Fig. S9*C*, arrow). These data suggest that the molecular phenotyping of SCNC, as indicated by phospho-RET activity, may drive novel therapeutic strategies for this rarer subtype of prostate cancer.

Stratification of Metastatic CRPC Patients' Kinase Activation Patterns Suggests That Simultaneous Targeting of SRC and MEK Kinases May Be of Potential Therapeutic Value. To predict potential kinase inhibitor combination therapies for metastatic CRPC patients, we evaluated all 16 individual metastatic CRPC lesions that had been analyzed by phosphoproteomics. We pooled kinases that were

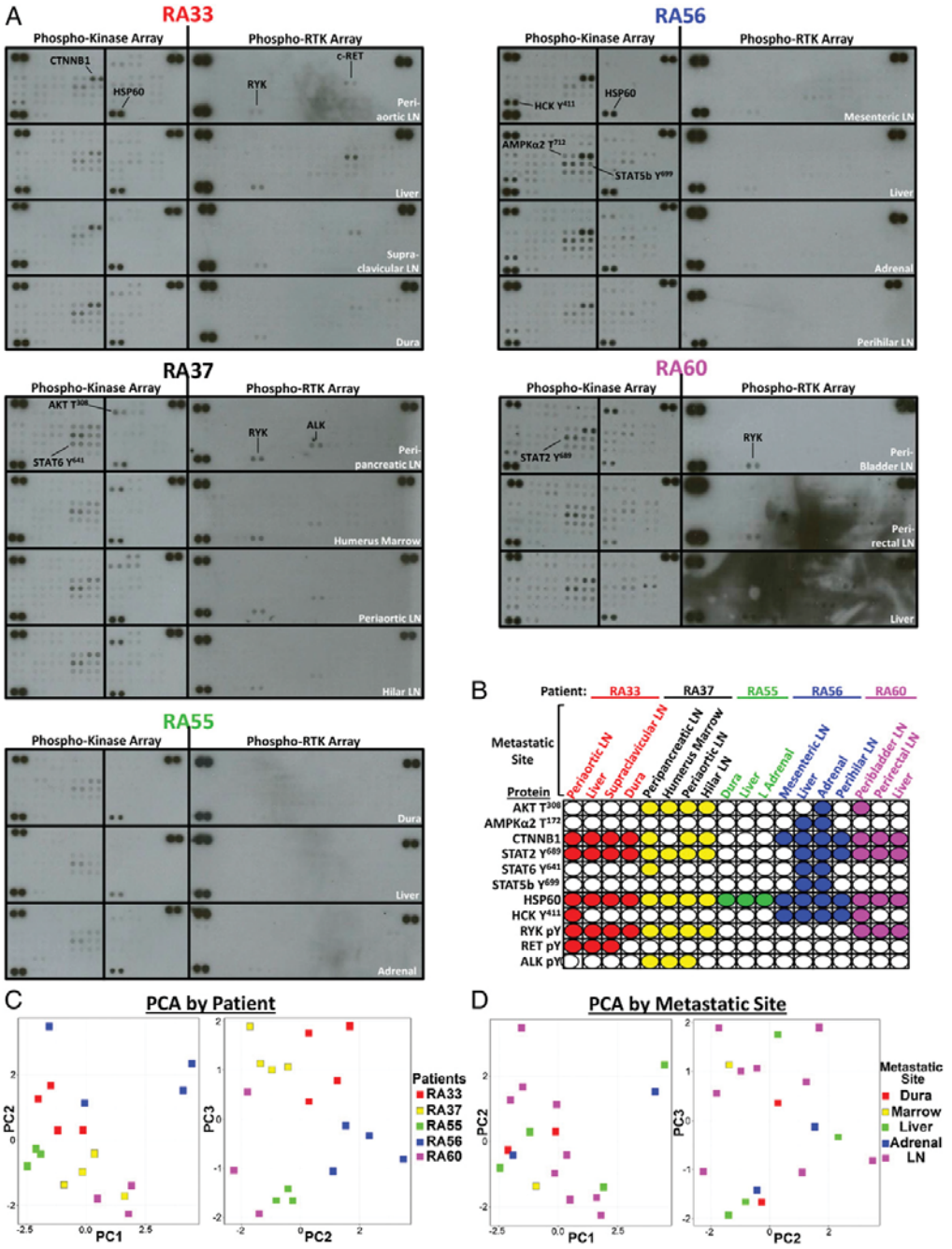

Fig. 4. Large-scale analyses of kinase activation patterns confirm intrapatient similarity across multiple, anatomically distinct metastases. (*A*) Phosphokinase and phospho-RTK arrays were used to analyze metastatic lesions from five different patients from anatomically distinct metastatic lesions. (*B*) Unique phosphopatterns were observed for each patient, and similar patterns were observed within the same patient, as shown with like-colored circles. Each observable phospho- or total protein spot from the phosphokinase and RTK arrays were used for PCA. LN, lymph node. (*C*) PCA analysis of all five patients confirms intrapatient kinase expression similarity and interpatient dissimilarity. (*D*) Grouping metastatic lesions by similar anatomical site shows no significant grouping of samples. Each phosphokinase and phospho-RTK array are spotted in duplicate, and positive control spots are located in the top left, right, and bottom left of each array. The first three principal components represent 77% of the total variance. Adrenal, adrenal gland lesions; LN, distant lymph node lesions; marrow, bone marrow lesion.

Table 1. Kinase and inhibitor stratification of metastatic CRPC patients

Patient number and metastatic location	Identified kinases via MS and western blot plus inferred kinases via kinase–substrate relationships*	Potential clinical inhibitors				
		Dasatinib†	Erlotinib‡	Crizotinib§	Ruxolitinib¶	Trametinib‖
RA06 Liver	EPHA3-7, SRC, PDGFR	X				
RA13 Mediastinal LN	ALK, FLT3/CSF1R/KIT, INSR, MAPK1, MAP3K2, PTK6, SRC	X		X		X
RA14 Liver	EGFR, MAPK1, MAP3K2, PTK6	X	X			X
RA30 Mediastinal LN	ALK, FLT3/CSF1R/KIT, MAP3K2, PTK6, SRC	X		X		X
RA40 Prostate	EGFR, MAPK1/3, MAP2K2, MAP3K2, PTK6, SRC	X	X			X
RA41 Dura	FLT3/CSF1R/KIT, MAPK1/3, SRC	X				X
RA43 Peritoneal and Right Lung	ALK, EGFR, EPHA3-7, MAPK1/3, PTK6, SRC	X	X	X		X
RA43 Periaortic LN	MAPK1/3, SRC	X				X
RA43 Right Lung	EGFR, FLT3/CSF1R/KIT, MAPK1/3, MAP2K2	X	X			X
RA45 Liver	ALK, MAP3K2			X		X
RA50 Periaortic LN	MAPK1/3, MAP3K2					X
RA53 Left Femur and Left Lung	ALK, EPHA3-7, JAK2, MAPK1/3, PDGFR, PTK6, SRC	X		X	X	X
RA55 Liver	ALK, EGFR, EPHA3, MAPK1/3, MAP2K2, MAP3K2, PTK6	X	X	X		X
RA55 Dura	EGFR, PTK6	X	X			
RA56 Perihilar LN	EGFR, HCK, TYK2	X	X		X	
RA57 Liver	EPHA7, MAP3K2, TYK2	X			X	X

*Kinases corresponding to identified phosphopeptides observed as >twofold over benign tissues, via western blotting, or kinase–substrate relationships ($P < 0.1$) as shown in Dataset S4.
†SRC family kinase, KIT, PDGFR, and EPHA receptor inhibitor.
‡EGFR inhibitor.
§ALK inhibitor.
¶JAK2 inhibitor.
‖MEK inhibitor.

identified from MS, western blot, and predicted kinase–substrate relationships to reveal a wide range of predicted kinase activities across the patient samples (Table 1). Mapping clinically available inhibitors to these kinases revealed 11 different TKI combinations with overlap between four sets of inhibitor combinations (Table 1). Notably, the SRC inhibitor dasatinib and the MEK inhibitor trametinib were predicted therapeutic strategies in 14 of 16 (87.5%) or 13 of 16 (81.2%) patients, respectively. If we consider combination therapy, 11 of 16 (68.8%) patients would be predicted to benefit from both SRC and MEK inhibitors, whereas 5 of 16 (31.2%) patients would not. There are no current clinical trials in prostate cancer evaluating the efficacy of SRC and MEK combination therapy in metastatic CRPC, but if initiated, stratification of patients based on activation of these two kinases would be necessary. Overall, the kinases identified in metastatic CRPC patients using phosphoproteomic analyses (*i*) may guide the molecular stratification of patients to direct the proper course of treatment with kinase inhibitor combinations, (*ii*) confirm the complexity observed across patients, and (*iii*) suggest that individualized therapy needs to be considered before clinical treatment decisions.

Discussion

From our study, we were able to measure protein phosphorylation in 41 metastatic CRPC samples from 17 patients including 16 samples by quantitative phosphotyrosine MS. Our phosphokinase profiling and evaluation of active kinases suggests that kinase activity patterns are patient-specific and are maintained across multiple metastatic lesions within the same patient. These data support previous studies suggesting that metastatic disease arises from a single precursor cancer cell or focal mass located at the primary tumor site (6, 12–14). Our findings add actionable information to this perspective. Kinase inhibitor treatment regimens guided by the biopsy of a single accessible metastatic lesion may be sufficient to predict the responses of multiple sites, leading to a more efficacious use of single agents or multidrug combinations, although this concept is still untested.

The development of new targeted therapies for metastatic CRPC presents a number of clinical questions. Major challenges include effective stratification of patients who will benefit from selected treatments and recognition of context-specific molecular targets. One approach to address these issues is the serial sampling and molecular characterization of malignant tissue from patients during the course of their disease. The increasing availability of high-throughput tools has enabled the genomic and transcriptomic profiling of large numbers of clinical carcinoma samples of different subtypes (4, 24, 25). Phosphoproteomic technology, particularly mass spectroscopy–based proteomics, is also rapidly advancing and has recently been applied to the elucidation of tyrosine-kinase–driven pathways in cell lines (26–29) or the discovery of activated kinases that may be useful for therapy in human cancers (30, 31).

Our analysis of phosphotyrosine signaling patterns in primary tumors and xenografts indicates that the prostate cell line-derived xenografts evaluated have different phosphorylation patterns compared with primary tissues. Supporting this notion, gene expression studies in small-cell lung cancer (SCLC) also identified primary tumor-specific signatures that were lost upon transitioning to cell culture (32), and proteomic analyses in colorectal cancer suggest that xenograft tumors are dramatically different from their cell line counterparts (33). This suggests that the stratification and prioritization of therapeutic targets for CRPC will require analysis of primary tissue, rather than cell lines or cell line-derived xenografts.

Interestingly, very few patient sets were positive for the activated states of EGFR, ERBB2, or MET, although they were detected in prostate cancer cell lines. Drugs targeting EGFR and ERBB2 did not produce significant results in CRPC patients (34,

35), however the MET inhibitor cabozantinib has shown promise in the clinic (36). This is in contrast to our observation that MET activity is not detected in our analyzed metastatic CRPC tissues. One explanation is that our sampling of metastatic CRPC tissues is too small or that MET activity was lost before tissue collection and we were not able to detect it. Two other possibilities are that cabozantinib activity in metastatic CRPC is not targeted toward epithelial MET but rather to MET expressed in osteoblasts or other mesenchymal cells in the bone microenvironment (36) and that cabozantinib is inhibiting another tyrosine kinase such as VEGFR2 or RET (37). Although we did not evaluate VEGFR2 activity, we did observe RET activity in SCNC, suggesting this kinase may be potentially targeted by cabozantinib in metastatic CRPC patients.

Rapid autopsy programs have paved the way for studies in genomic mutations, copy number alterations, and splicing variants from metastatic tissues that are otherwise difficult to obtain (4, 6, 15, 38, 39). Although we evaluated many soft tissue metastatic lesions, we were only able to evaluate five bone metastases. Although bone metastases are evident in over 90% of metastatic CRPC patients (15), metastatic bone tumors are hard to study because tumor material is lodged into hard, calcified bone, preventing the procurement of quality material for analysis. This is also especially difficult considering the large amount of tissue (>350 mg) required for phosphoproteomic preparations. A potential outcome could be that kinase patterns are principally determined by site of metastasis due to signals initiated by the surrounding local microenvironment creating a premetastatic niche (40). Tissue-specific kinase activation patterns were not observed in our study, but further evaluation of bone metastases in patients also harboring soft tissue metastases will be necessary to extend these findings.

Materials and Methods

Tissue Culture of Prostate Cancer Cell Lines and Derivation of Xenograft Tumors. 22Rv1 cells were grown in RPMI medium supplemented with L-glutamine, FBS, and nonessential amino acids (NEAAs). LNCaP, DU145, and C4-2 cells were grown in DMEM supplemented with L-glutamine, FBS, and NEAA. Thirty 15-cm plates were collected from each cell line and treated with 2 mM Vanadate for 30 min. Cells were subsequently lysed in 9 M Urea lysis buffer and used for phosphoproteomic analysis.

To generate metastatic tumors, 1×10^5 22Rv1 cells were injected intracardially as previously described, and dissemination was monitored using bioluminescence imaging (41). After 8 wks, tumors were extracted from the metastatic locations including the liver and lymph nodes in the mesenteric and lung regions. Also, to evaluate primary tumor growth, 1×10^6 LNCaP cells were injected s.c. and excised once they reached Division of Laboratory Animal Medicine (DLAM) limits.

Acquisition of Clinically Matched Benign and Cancerous Primary Prostate Tissues and Metastatic CRPC Samples. Patient samples were obtained from the University of California–Los Angeles (UCLA) Translational Pathology Core Laboratory, which is authorized by the UCLA Institutional Review Board to distribute anonymized tissues to researchers as described previously (42–44). Cancer and benign areas were clearly marked on the frozen section slides, and prostate tissue containing the cancer region was separated from the benign area before collecting for phosphoproteomic analyses.

The Rapid Autopsy program at the University of Michigan has been previously described (11, 39). Frozen tissues from the Rapid Autopsy program were sent overnight on dry ice for phosphotyrosine peptide analysis. Sections were stained with hematoxylin and eosin for representative histology.

Quantitative Analysis of Phosphotyrosine Peptides by MS. Tissue lysis was performed as previously described (8). Briefly, greater than 350 mg of frozen tumor mass was homogenized and sonicated in urea lysis buffer (20 mM Hepes pH 8.0, 9 M urea, 2.5 mM sodium pyrophosphate, 1.0 mM beta-glycerophosphate, 1% *N*-octyl glycoside, 2 mM sodium orthovanadate). Total protein was measured using the bicinchoninic acid (BCA) Protein Assay Kit (Thermo Scientific/Pierce), and 25 mg of total protein was used for phosphoproteomic analysis. The remaining protein lysate was frozen for subsequent western blot analyses.

Phosphotyrosine peptide enrichment and liquid chromatography tandem MS (LC-MS/MS) analysis was performed as previously described (8, 26, 45). Phosphopeptides were identified using the Proteome Discoverer software (version 1.4.0.88, Thermo Fisher Scientific). MS/MS fragmentation spectra were searched using SEQUEST against the Uniprot human reference proteome database with canonical and isoform sequences (downloaded January 2012 from uniprot.org). Search parameters included carbamidomethyl cysteine (*C) as a static modification. Dynamic modifications included phosphorylated tyrosine, serine, or threonine (pY, pS, and pT, respectively) and oxidized methionine (*M). The Percolator node of Protein Discoverer was used to calculate false discovery rate (FDR) thresholds, and the FDR for the datasets was adjusted to 1% (version 1.17, Thermo Scientific). The Percolator algorithm uses a target-decoy database search strategy and discriminates true and false identifications with a support vector machine (46). The PhosphoRS 2.0 node was used to more accurately localize the phosphate on the peptide (47). Only phosphopeptides with at least one phosphotyrosine assignment with a reported probability above 20% were considered. MS2 spectra for all reported phosphopeptides are deposited to the ProteomeXchange Consortium with the dataset identifier PXD000238 (48).

Data Analysis. Data analysis was performed as previously described (8). For clustering, we removed any peptides that had an ANOVA score greater than 0.2. Hierarchical clustering of phosphotyrosine data was performed using the Cluster program with the Pearson correlation and pairwise complete linkage analysis (49) and visualized using Java TreeView (50). Quantitative data for each phosphopeptide can be found in Dataset S5, *Batch 1–3*. To evaluate the significance of intrapatient and anatomical site similarity, the Pearson correlation coefficient was calculated for each pair of phosphotyrosine samples, and the resulting correlation matrix was clustered using the pHeatmap package in R. Statistical significance was assessed against the null hypothesis that the correlation was not different from zero.

Prediction of Kinase–Substrate Relationships and Enrichment Analysis of Kinase Activity. Predictions, enrichment, and permutation analyses have been previously described (8). Phosphotyrosine peptides were ranked by the signal-to-noise ratio observed for a given perturbation (e.g., metastatic CRPC compared with benign prostate or BPH). The enrichment scores for all putative upstream kinases are shown in Dataset S4, *Batch 1–3*.

Western Blot. For western blots, equal protein amounts of metastatic CRPC tissue urea lysates (20 or 30 μg) were used from tissues prepared as described previously (8). Antibodies were diluted as follows: AKT (1:1,000, Santa Cruz), pAKT S^{473} (1:2,000, Cell Signaling), EGFR (1:1,000, Cell Signaling), pEGFR Y^{1173} (1:1,000, Cell Signaling), STAT3 (1:1,000, Cell Signaling), pSTAT3 Y^{705} (1:2,000, Cell Signaling), JAK2 (1:1,000, Cell Signaling), pJAK2 $Y^{1007/1008}$ (1:500, Cell Signaling), MAPK1/3 (1:1,000, Cell Signaling), MAPK1/3 $T^{185/202}$/$Y^{187/204}$ (1:2,000, Cell Signaling), SRC (1:1,000, Millipore), pSRC Y^{419} (1:1,000, Cell Signaling), ERBB2 (1:1,000, Cell Signaling), pERBB2 $Y^{1221/1222}$ (1:1,000, Cell Signaling), MET (1:1,000, Cell Signaling), and pMET Y^{1234} (1:1,000, Cell Signaling). ECL substrate (Millipore) was used for detection and development on GE/Amersham film.

Phospho-RTK and Phosphokinase Arrays. Human Phospho-RTK (R&D Sytems) and phosphokinase (R&D Systems) arrays were used according to the manufacturer's instructions. Briefly, 300 μg of 9 M urea lysate for each metastatic sample was diluted in the kit-specific dilution buffer to a final concentration of 0.85 M urea and incubated with blocked membranes overnight. The membranes were washed and exposed to chemiluminescent reagent and developed on GE/Amersham film. Quantitation of each array was performed using Image J. To evaluate the significance of intrapatient and anatomical site similarity, the Pearson correlation coefficient was calculated for each pair of samples using only the kinases and proteins with detectable phosphorylation or expression (n = 11), and the correlation coefficients were clustered using the pHeatmap package in R. Statistical similarity of intrapatient lesions was assessed against the null hypothesis that the correlation was not different from zero. P values from multiple comparisons were combined using Fisher's Method where appropriate.

PCA. Each antibody-related spot on the Phospho-RTK and phosphokinase arrays was quantified using Image J. After background subtraction, the duplicate spots for each antibody were averaged, and antibodies with negligible signal were removed. The data were unit normalized, and principal components were calculated in R.

ACKNOWLEDGMENTS. We thank members of the O.N.W. laboratory for helpful comments and discussion on the manuscript. We thank Mireille Riedinger for purifying the 4G10 antibody used in mass spectrometry studies. We thank the Tissue Procurement Core Laboratory at UCLA for assistance on tissue processing and H&E staining. J.M.D. and T.S. are supported by the Department of Defense Prostate Cancer Research Program (W81XWH-11-1-0504 and W81XWH-12-1-0100, respectively). N.A.G. is supported by UCLA Scholars in Oncologic Molecular Imaging (SOMI) program, National Institutes of Health (NIH) Grant R25T CA098010. J.K.L. is supported by NIH Training Grant 5T32CA009297-28 and the UCLA Specialty Training and Advanced Research (STAR) Program. C.M.F. is supported by the UCLA Medical Scientist Training Program. J.H. is supported by the Department of Defense Prostate Cancer Research Program W81XWH-11-1-0227 and W81XWH-12-1-0206, UCLA Specialized Program in Research Excellence (SPORE) in prostate cancer, National Cancer Institute (NCI) 1R01CA158627, Stand Up to Cancer/AACR Dream Team Award, and Prostate Cancer Foundation Honorable A. David Mazzone Special Challenge Award. K.J.P. is supported by NIH U54 CA163124, NIH 1 U01CA143055-01A1, NIH 2 P50 CA69568, and NIH 1 PO1 CA093900 and receives support from the Prostate Cancer Foundation, the Taubman Research Institute as a Taubman Scholar, and the American Cancer Society as a Clinical Research Professor. T.G.G. is supported by NCI/NIH P01 CA168585 and R21 CA169993, American Cancer Society Research Scholar Award RSG-12-257-01-TBE, the CalTech–UCLA Joint Center for Translational Medicine, the UCLA Jonsson Cancer Center Foundation, the UCLA Institute for Molecular Medicine, the National Center for Advancing Translational Sciences UCLA Clinical and Translational Science Institute (CTSI) Grant UL1TR000124, and a Concern Fondation CONquer CanCER Now Award. J.H. and O.N.W. are supported by a Prostate Cancer Foundation Challenge Award. O.N.W. is an Investigator of the Howard Hughes Medical Institute and co–principal investigator of the West Coast Prostate Cancer Dream Team supported by Stand Up to Cancer/American Association for Cancer Research (AACR)/Prostate Cancer Foundation.

1. Kan Z, et al. (2010) Diverse somatic mutation patterns and pathway alterations in human cancers. *Nature* 466(7308):869–873.
2. Kim KS, et al. (2005) Predictors of the response to gefitinib in refractory non-small cell lung cancer. *Clin Cancer Res* 11(6):2244–2251.
3. Mass RD, et al. (2005) Evaluation of clinical outcomes according to HER2 detection by fluorescence in situ hybridization in women with metastatic breast cancer treated with trastuzumab. *Clin Breast Cancer* 6(3):240–246.
4. Taylor BS, et al. (2010) Integrative genomic profiling of human prostate cancer. *Cancer Cell* 18(1):11–22.
5. Kumar A, et al. (2011) Exome sequencing identifies a spectrum of mutation frequencies in advanced and lethal prostate cancers. *Proc Natl Acad Sci USA* 108(41): 17087–17092.
6. Grasso CS, et al. (2012) The mutational landscape of lethal castration-resistant prostate cancer. *Nature* 487(7406):239–243.
7. Cai H, Babic I, Wei X, Huang J, Witte ON (2011) Invasive prostate carcinoma driven by c-Src and androgen receptor synergy. *Cancer Res* 71(3):862–872.
8. Drake JM, et al. (2012) Oncogene-specific activation of tyrosine kinase networks during prostate cancer progression. *Proc Natl Acad Sci USA* 109(5):1643–1648.
9. Kuukasjärvi T, et al. (1997) Genetic heterogeneity and clonal evolution underlying development of asynchronous metastasis in human breast cancer. *Cancer Res* 57(8): 1597–1604.
10. Fidler IJ, Talmadge JE (1986) Evidence that intravenously derived murine pulmonary melanoma metastases can originate from the expansion of a single tumor cell. *Cancer Res* 46(10):5167–5171.
11. Shah RB, et al. (2004) Androgen-independent prostate cancer is a heterogeneous group of diseases: Lessons from a rapid autopsy program. *Cancer Res* 64(24):9209–9216.
12. Liu W, et al. (2009) Copy number analysis indicates monoclonal origin of lethal metastatic prostate cancer. *Nat Med* 15(5):559–565.
13. Aryee MJ, et al. (2013) DNA methylation alterations exhibit intraindividual stability and interindividual heterogeneity in prostate cancer metastases. *Sci Transl Med* 5(169):69ra10.
14. Mehra R, et al. (2008) Characterization of TMPRSS2-ETS gene aberrations in androgen-independent metastatic prostate cancer. *Cancer Res* 68(10):3584–3590.
15. Rubin MA, et al. (2000) Rapid ("warm") autopsy study for procurement of metastatic prostate cancer. *Clin Cancer Res* 6(3):1038–1045.
16. Cortes JE, et al. (2012) Bosutinib versus imatinib in newly diagnosed chronic-phase chronic myeloid leukemia: Results from the BELA trial. *J Clin Oncol* 30(28):3486–3492.
17. Cortes JE, et al. (2012) Ponatinib in refractory Philadelphia chromosome-positive leukemias. *N Engl J Med* 367(22):2075–2088.
18. Kantarjian H, et al. (2010) Dasatinib versus imatinib in newly diagnosed chronic-phase chronic myeloid leukemia. *N Engl J Med* 362(24):2260–2270.
19. Cohen MH, et al. (2010) Approval summary: Erlotinib maintenance therapy of advanced/metastatic non-small cell lung cancer (NSCLC). *Oncologist* 15(12):1344–1351.
20. O'Bryant CL, Wenger SD, Kim M, Thompson LA (2013) Crizotinib: A new treatment option for ALK-positive non-small cell lung cancer. *Ann Pharmacother* 47(2):189–197.
21. Flaherty KT, et al.; METRIC Study Group (2012) Improved survival with MEK inhibition in BRAF-mutated melanoma. *N Engl J Med* 367(2):107–114.
22. Mascarenhas J, Hoffman R (2012) Ruxolitinib: The first FDA approved therapy for the treatment of myelofibrosis. *Clin Cancer Res* 18(11):3008–3014.
23. Tai S, et al. (2011) PC3 is a cell line characteristic of prostatic small cell carcinoma. *Prostate* 71(15):1668–1679.
24. Anonymous; Cancer Genome Atlas Network (2012) Comprehensive molecular characterization of human colon and rectal cancer. *Nature* 487(7407):330–337.
25. Anonymous; Cancer Genome Atlas Network (2012) Comprehensive molecular portraits of human breast tumours. *Nature* 490(7418):61–70.
26. Rubbi L, et al. (2011) Global phosphoproteomics reveals crosstalk between Bcr-Abl and negative feedback mechanisms controlling Src signaling. *Sci Signal* 4(166):ra18.
27. Wolf-Yadlin A, et al. (2006) Effects of HER2 overexpression on cell signaling networks governing proliferation and migration. *Mol Syst Biol* 2:54.
28. Bai Y, et al. (2012) Phosphoproteomics identifies driver tyrosine kinases in sarcoma cell lines and tumors. *Cancer Res* 72(10):2501–2511.
29. Guha U, et al. (2008) Comparisons of tyrosine phosphorylated proteins in cells expressing lung cancer-specific alleles of EGFR and KRAS. *Proc Natl Acad Sci USA* 105(37):14112–14117.
30. Walters DK, et al. (2006) Activating alleles of JAK3 in acute megakaryoblastic leukemia. *Cancer Cell* 10(1):65–75.
31. Rikova K, et al. (2007) Global survey of phosphotyrosine signaling identifies oncogenic kinases in lung cancer. *Cell* 131(6):1190–1203.
32. Daniel VC, et al. (2009) A primary xenograft model of small-cell lung cancer reveals irreversible changes in gene expression imposed by culture in vitro. *Cancer Res* 69(8): 3364–3373.
33. Sirvent A, Vigy O, Orsetti B, Urbach S, Roche S (2012) Analysis of SRC oncogenic signaling in colorectal cancer by stable isotope labeling with heavy amino acids in mouse xenografts. *Mol Cell Proteomics* 11(12):1937–1950.
34. Nabhan C, et al. (2009) Erlotinib has moderate single-agent activity in chemotherapy-naïve castration-resistant prostate cancer: Final results of a phase II trial. *Urology* 74(3):665–671.
35. Ziada A, et al. (2004) The use of trastuzumab in the treatment of hormone refractory prostate cancer; phase II trial. *Prostate* 60(4):332–337.
36. Smith DC, et al. (2013) Cabozantinib in patients with advanced prostate cancer: Results of a phase II randomized discontinuation trial. *J Clin Oncol* 31(4):412–419.
37. Yakes FM, et al. (2011) Cabozantinib (XL184), a novel MET and VEGFR2 inhibitor, simultaneously suppresses metastasis, angiogenesis, and tumor growth. *Mol Cancer Ther* 10(12):2298–2308.
38. Friedlander TW, et al. (2012) Common structural and epigenetic changes in the genome of castration-resistant prostate cancer. *Cancer Res* 72(3):616–625.
39. Mehra R, et al. (2011) Characterization of bone metastases from rapid autopsies of prostate cancer patients. *Clin Cancer Res* 17(12):3924–3932.
40. Psaila B, Lyden D (2009) The metastatic niche: Adapting the foreign soil. *Nat Rev Cancer* 9(4):285–293.
41. Drake JM, Gabriel CL, Henry MD (2005) Assessing tumor growth and distribution in a model of prostate cancer metastasis using bioluminescence imaging. *Clin Exp Metastasis* 22(8):674–684.
42. Goldstein AS, et al. (2011) Purification and direct transformation of epithelial progenitor cells from primary human prostate. *Nat Protoc* 6(5):656–667.
43. Stoyanova T, et al. (2012) Regulated proteolysis of Trop2 drives epithelial hyperplasia and stem cell self-renewal via β-catenin signaling. *Genes Dev* 26(20):2271–2285.
44. Goldstein AS, Huang J, Guo C, Garraway IP, Witte ON (2010) Identification of a cell of origin for human prostate cancer. *Science* 329(5991):568–571.
45. Graham NA, et al. (2012) Glucose deprivation activates a metabolic and signaling amplification loop leading to cell death. *Mol Syst Biol* 8:589.
46. Spivak M, Weston J, Bottou L, Käll L, Noble WS (2009) Improvements to the percolator algorithm for Peptide identification from shotgun proteomics data sets. *J Proteome Res* 8(7):3737–3745.
47. Taus T, et al. (2011) Universal and confident phosphorylation site localization using phosphoRS. *J Proteome Res* 10(12):5354–5362.
48. Vizcaíno JA, et al. (2013) The PRoteomics IDEntifications (PRIDE) database and associated tools: Status in 2013. *Nucleic Acids Res* 41(Database issue):D1063–D1069.
49. Eisen MB, Spellman PT, Brown PO, Botstein D (1998) Cluster analysis and display of genome-wide expression patterns. *Proc Natl Acad Sci USA* 95(25):14863–14868.
50. Saldanha AJ (2004) Java Treeview—Extensible visualization of microarray data. *Bioinformatics* 20(17):3246–3248.

Supporting Information

Drake et al. 10.1073/pnas.1319948110

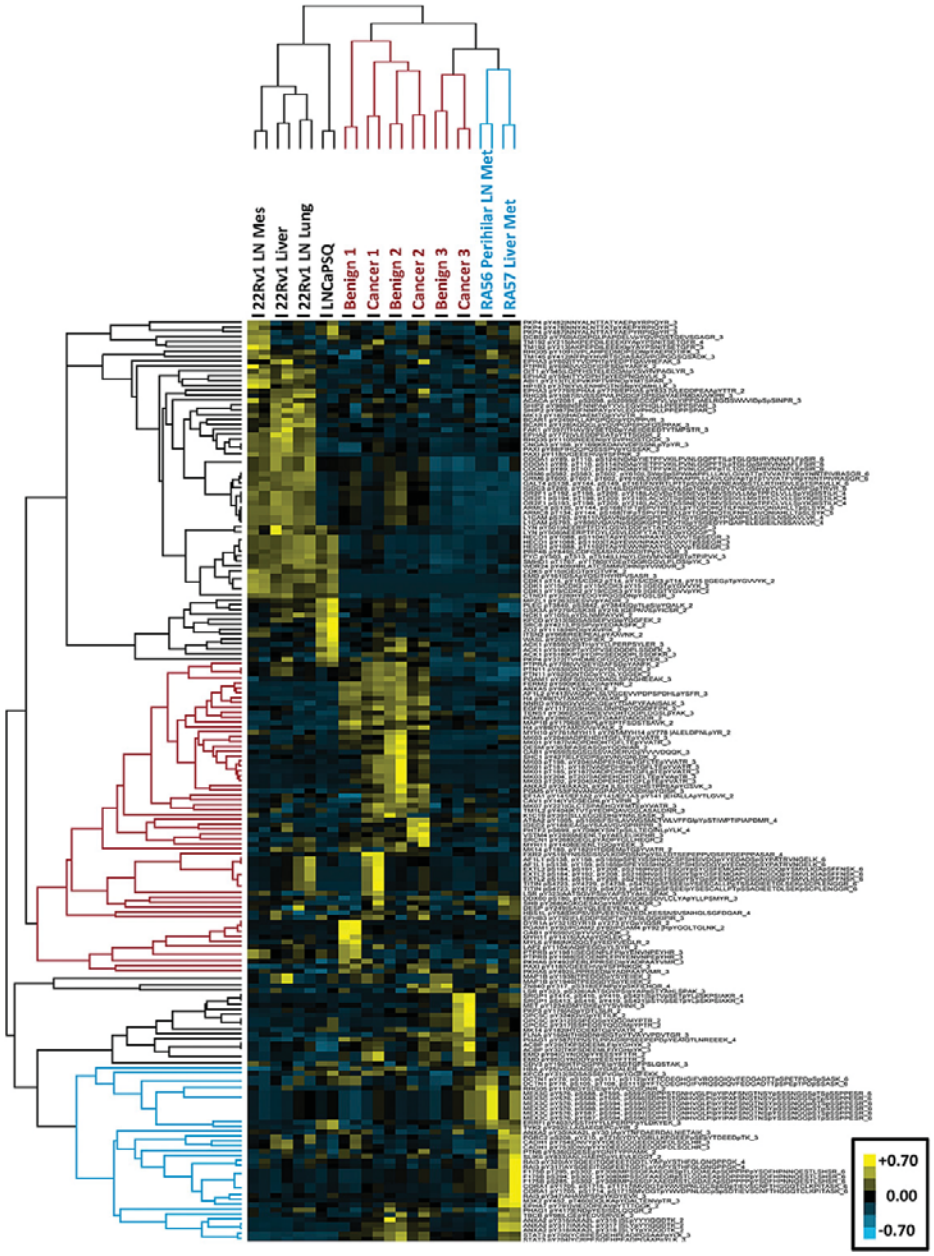

Fig. S1. Phosphoproteomic analysis exhibits distinct clusters of phosphorylation between the cell line-derived xenografts and primary prostate tissues. Unsupervised hierarchical clustering does not group cell line-derived metastatic xenograft tumors with either organ confined or metastatic castration-resistant prostate cancer (CRPC). In addition, treatment-naïve patient-matched benign and cancerous prostates display indistinguishable phosphopeptide signatures. The phosphoprofiling heatmap from Fig. 2*A* with the protein and residue identities of the phosphorylation events are listed. For all heatmaps, the labels are as follows: UniProt ID, phosphosite residue number, phosphopeptide (charge state of mass spectrometry ion). If the phosphopeptide has multiple identities, a slash separates each protein and phosphorylation residue number. The vertical line separates the proteins from the phospho-peptide. Yellow, hyperphosphorylation; blue, hypophosphorylation.

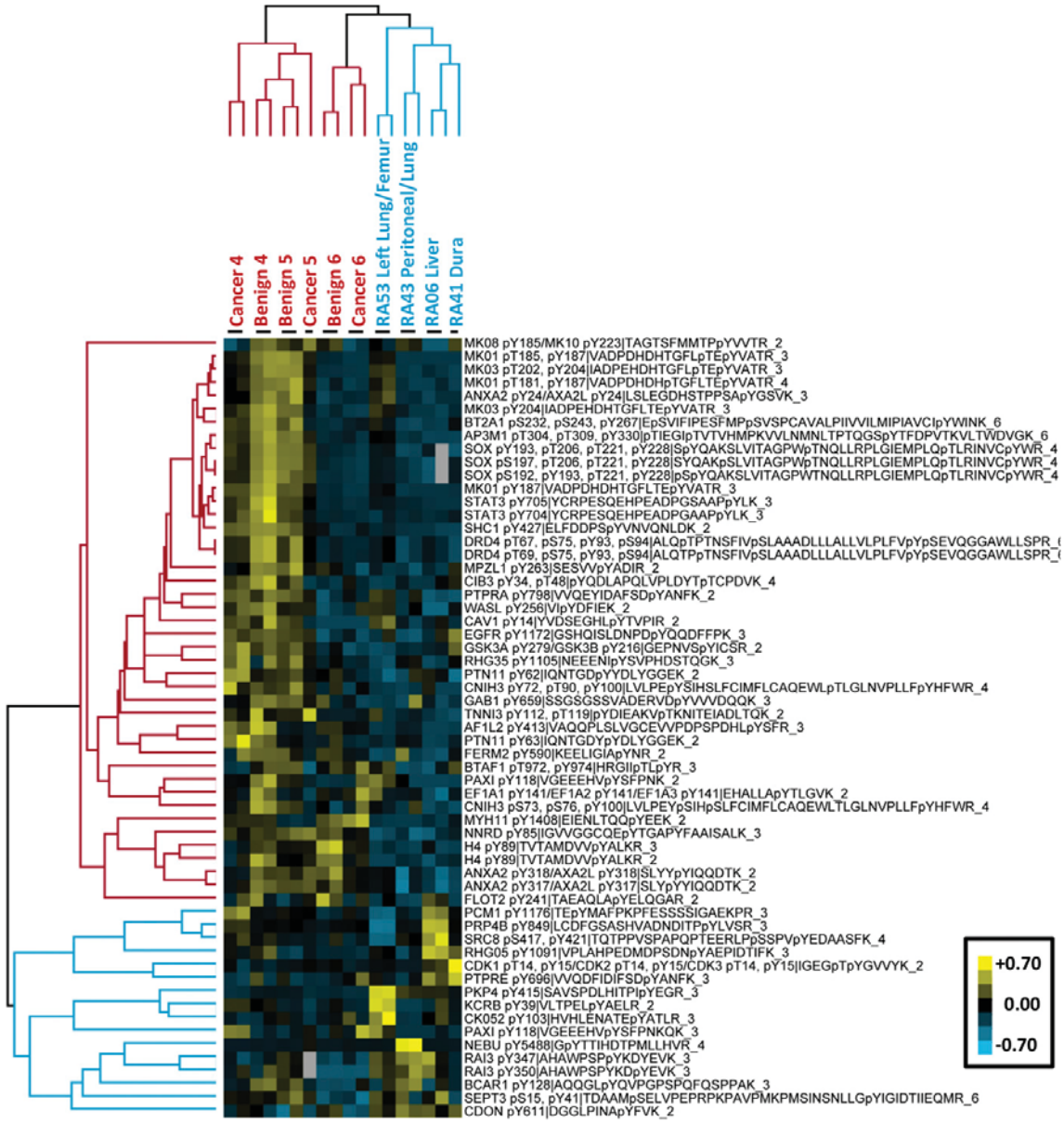

Fig. S2. Phosphoproteomic analysis exhibits distinct clusters of phosphorylation between treatment-naïve prostate cancer and metastatic CRPC. Unsupervised hierarchical clustering does not group organ-confined prostate benign or cancerous prostates with metastatic CRPC. Also, treatment-naïve patient-matched benign and cancerous prostates display indistinguishable phosphopeptide signatures. The phosphoprofiling heatmap from batch 2 with the protein and residue identities of the phosphorylation events are listed. For all heatmaps, the labels are as follows: UniProt ID, phosphosite residue number, phosphopeptide (charge state of mass spectrometry ion). If the phosphopeptide has multiple identities, a slash separates each protein and phosphorylation residue number. The vertical line separates the proteins from the phosphopeptide. Yellow, hyperphosphorylation; blue, hypophosphorylation.

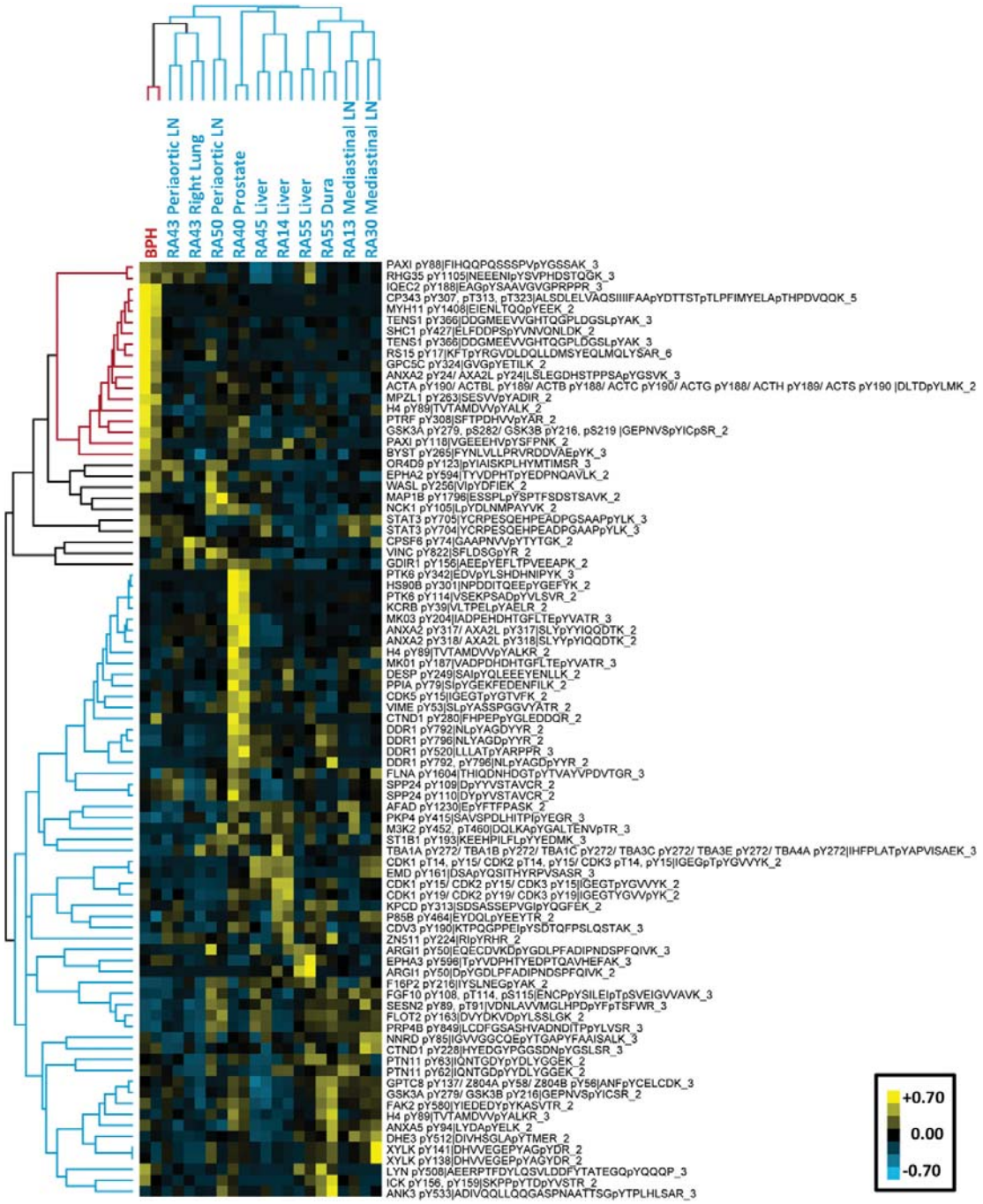

Fig. S3. Phosphoproteomic analysis exhibits both patient-specific and metastatic site-specific patterns of tyrosine kinase activation in metastatic CRPC. Unsupervised hierarchical clustering groups by organ site of metastases as well as by intrapatient metastatic lesions. Benign prostatic hyperplasia (BPH) was used as the treatment-naïve tissue for comparison. The phosphoprofiling heatmap from Fig. 2*B* with the protein and residue identities of the phosphorylation events is listed. For all heatmaps, the labels are as follows: UniProt ID, phosphosite residue number, phosphopeptide (charge state of mass spectrometry ion). If the phosphopeptide has multiple identities, a slash separates each protein and phosphorylation residue number. The vertical line separates the proteins from the phosphopeptide. Yellow, hyperphosphorylation; blue, hypophosphorylation.

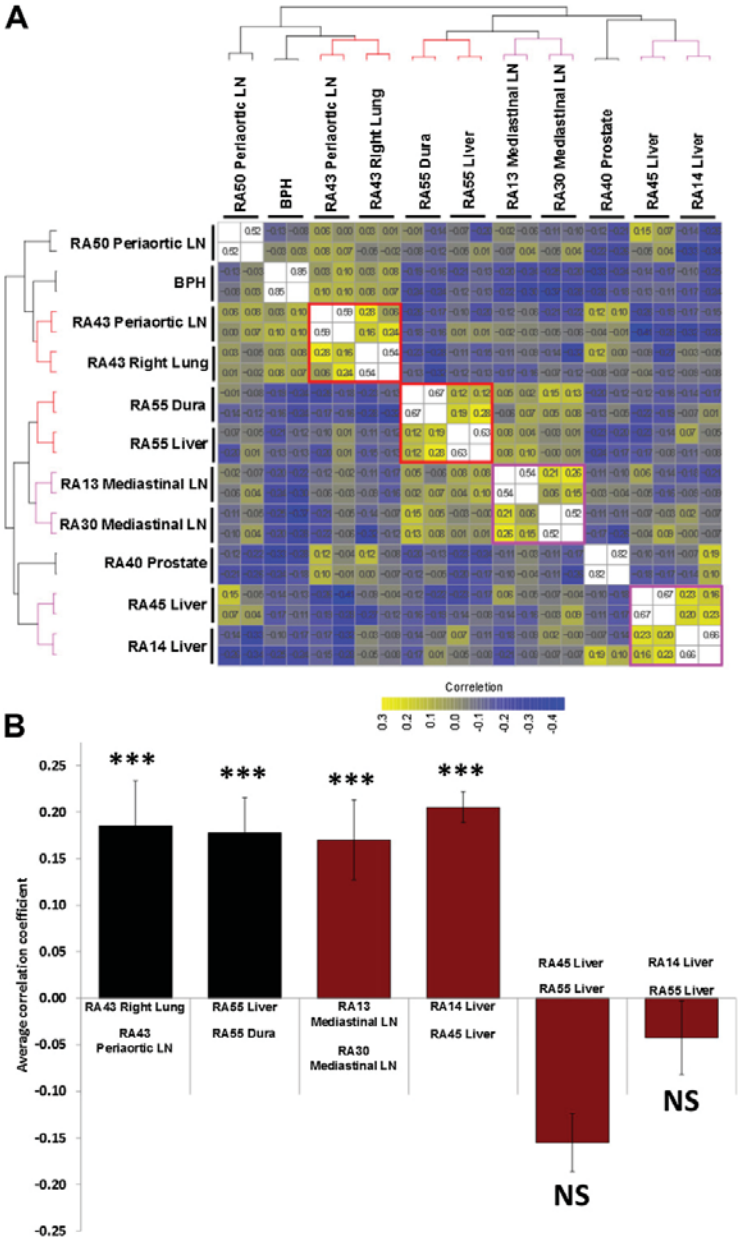

Fig. S4. Phosphoproteomic data reveal high levels of intrapatient similarity and occasional high levels of intraanatomical site similarity. (*A*) Pairwise Pearson correlation coefficients for each phosphotyrosine sample (including technical duplicates) were calculated and then clustered. The correlation coefficients are superimposed on each color-coded square. The correlation coefficients on the diagonal and the correlation coefficients for technical replicates were omitted from the color scale. (*B*) Pairwise correlation coefficients, excluding technical replicates, were averaged, and the statistical significance against the null hypothesis that the correlation was not greater than zero was calculated. Error bars are the SE. ***$P < 0.001$; NS, not significant.

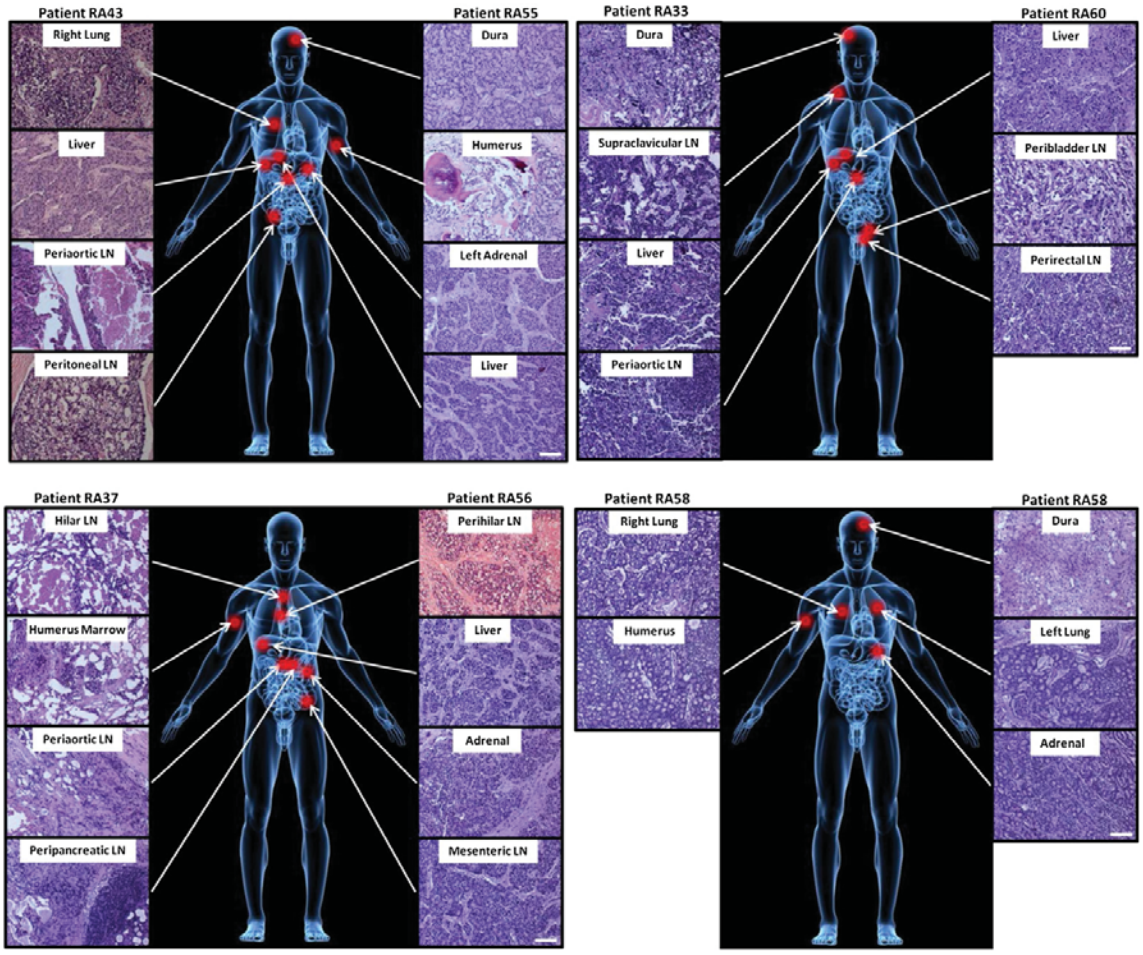

Fig. S5. Location and histological characterization of seven patients with anatomically distinct metastatic CRPC lesions. Seven separate patients' metastatic lesions are depicted with representative histology. These samples were used for western blot and phospho–receptor tyrosine kinase (RTK) and phosphokinase arrays. Red dots indicate the approximate location of the metastatic lesions analyzed. Tissues with greater than 50% tumor content were evaluated. (Scale bar, 50 μm.)

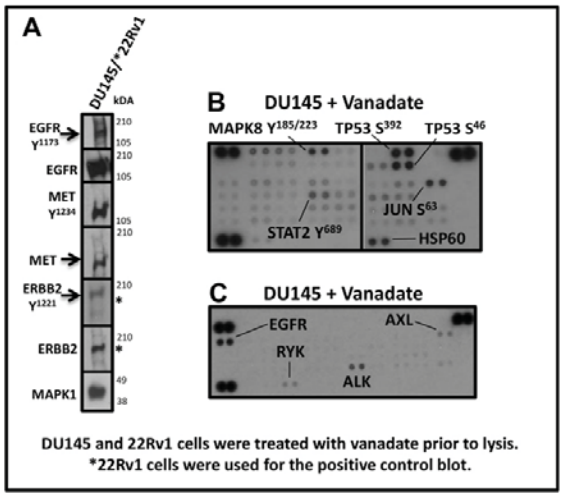

Fig. S6. Evaluation of RTK epidermal growth factor receptor (EGFR), erythroblastic leukemia viral oncogene homolog 2 (ERBB2 or HER2/neu), and hepatocyte growth factor receptor (HGFR or MET) and phospho-kinase and phospho-RTK arrays using positive control prostate cancer cell lines. Western blot analyses from DU145 or 22Rv1 cells treated with the phosphatase inhibitor, vanadate, were evaluated for the activated states of the RTKs EGFR, ERBB2, and MET (*A*); phosphokinase (*B*); or phospho-RTK arrays (*C*). DU145 or 22Rv1 (indicated by an asterisk next to the blot) cells were used as positive controls.

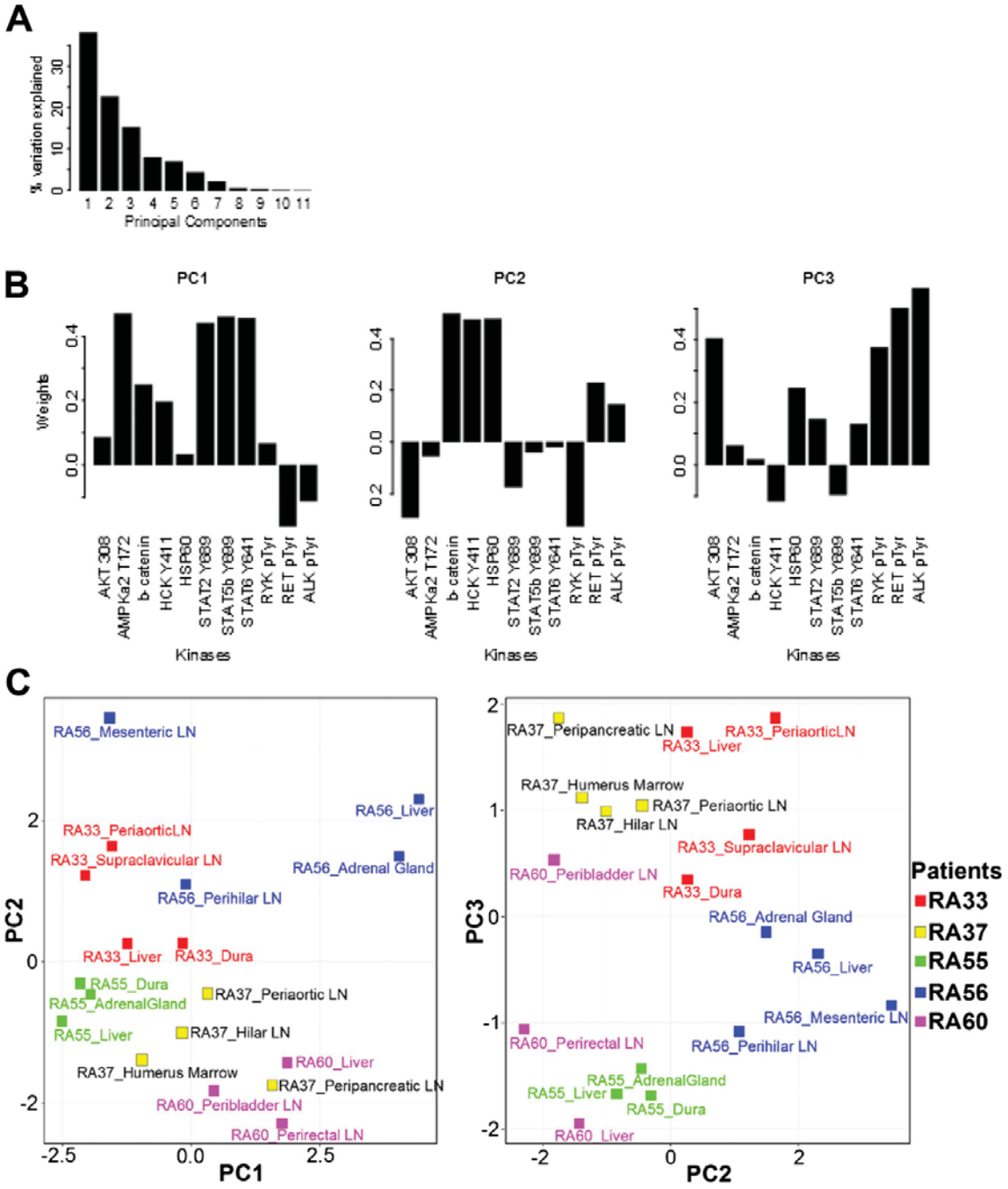

Fig. S7. Principal component (PC) analysis of phosphokinase arrays. Data from CRPC metastatic samples analyzed by phosphokinase arrays were subjected to PC analysis. After removal of antibodies with negligible signal, 11 kinases remained: AKT T^{308}, protein kinase, AMP-activated, alpha 1 catalytic subunit (PRKAA1 or AMPKa) T^{172}, β-catenin, hemopoietic cell kinase (HCK) Y^{411}, STAT2 Y^{689}, STAT5b Y^{699}, STAT6 Y^{641}, receptor-like tyrosine kinase (RYK) phosphotyrosine, rearranged during transfection (RET) phosphotyrosine, and anaplastic lymphoma kinase (ALK) phosphotyrosine. (*A*) Schematic of the loadings vectors for the first three PCs. (*B*) The percentages listed for each PC indicated the amount of variance explained by that PC. (*C*) Plots of the PC analysis for all five patients analyzed demonstrate intrapatient kinase expression similarity and individual differences.

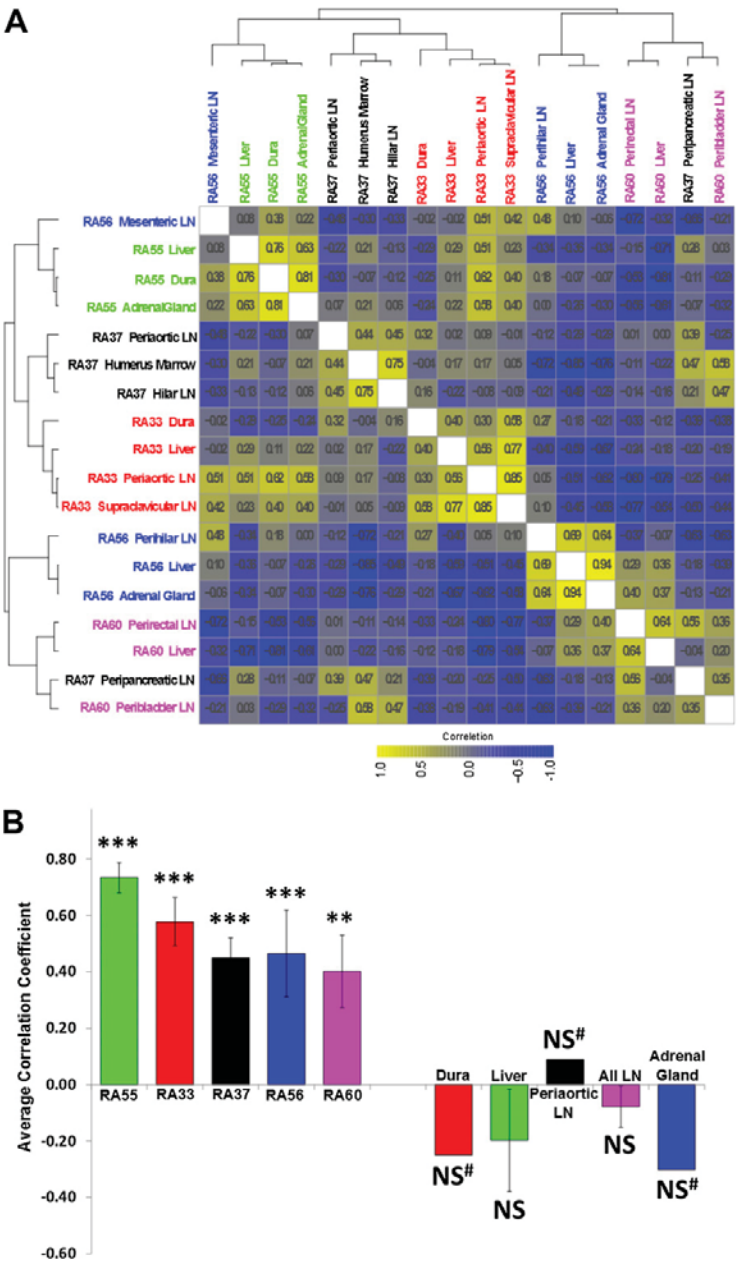

Fig. S8. Phosphokinase arrays demonstrate high levels of intrapatient but not interpatient similarity. (*A*) Pairwise Pearson correlation coefficients for each sample measured on the phosphokinase and phospho-RTK arrays were calculated and then clustered. The correlation coefficients are superimposed on each color-coded square. The correlation coefficients on the diagonal were omitted for readability. (*B*) Pairwise correlation coefficients were averaged, and the statistical significance against the null hypothesis that the correlation was not greater than zero was calculated. Error bars are the SE. Multiple *P* values were combined using Fisher's Method. ***$P < 0.001$, **$P < 0.01$; NS, not significant; #, single *P* value, not Fisher's combined.

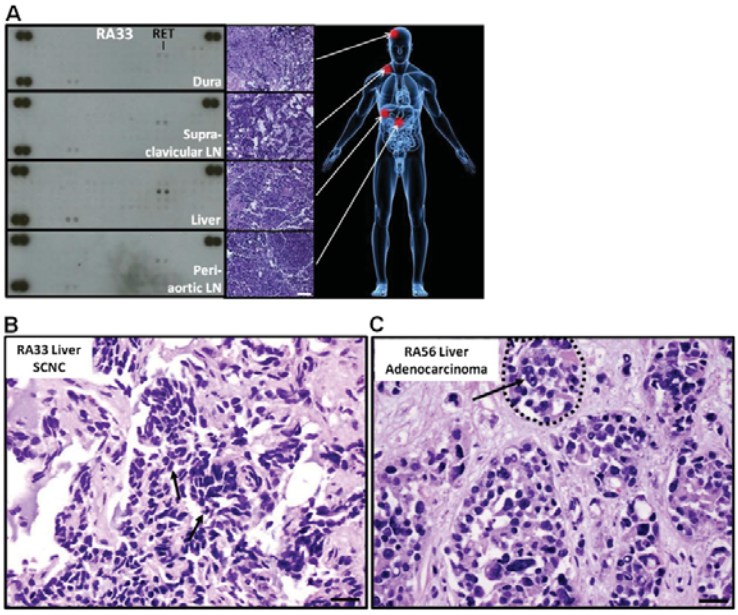

Fig. S9. Tyrosine phosphorylation of RTK RET in small cell neuroendocrine carcinoma (SCNC). (*A*) Analysis of patient RA33 using RTK arrays revealed the tyrosine phosphorylation of neuronal tyrosine kinase RET. (*B*) Metastatic tumor cells in this patient demonstrate typical nuclear morphology of SCNC including a darkly stained nucleus with a homogeneous chromatin pattern, high nuclear/cytoplasmice ratio, lack of nucleoli, and frequent mitotic figures (*B*, arrows). These characteristics are in sharp contrast to the nuclear morphology of adenocarcinoma tumor cells (*C*) that have open and vesicular chromatin patterns and prominent nuclei (*C*, arrow) and glandular formation (*C*, dashed circle). (Scale bar, 25 μm.)

Other Supporting Information Files

Dataset S1 (XLSX)
Dataset S2 (XLSX)
Dataset S3 (XLSX)
Dataset S4 (XLSX)
Dataset S5 (XLSX)

Chapter 3:

Functional screen identifies kinases driving prostate cancer visceral and bone metastasis

Functional screen identifies kinases driving prostate cancer visceral and bone metastasis

Claire M. Faltermeier[a], Justin M. Drake[b,1], Peter M. Clark[b], Bryan A. Smith[b], Yang Zong[c], Carmen Volpe[d], Colleen Mathis[b], Colm Morrissey[e], Brandon Castor[f], Jiaoti Huang[f,g,h,i,j], and Owen N. Witte[a,b,c,h,i,j,2]

[a]Molecular Biology Institute, University of California, Los Angeles, CA 90095; [b]Department of Microbiology, Immunology and Molecular Genetics, University of California, Los Angeles, CA 90095; [c]Howard Hughes Medical Institute, University of California, Los Angeles, CA 90095; [d]Division of Laboratory and Animal Medicine, University of California, Los Angeles, CA 90095; [e]Department of Urology, University of Washington, Seattle, WA 98195; [f]Department of Pathology and Laboratory Medicine, University of California, Los Angeles, CA 90095; [g]Department of Urology, University of California, Los Angeles, CA 90095; [h]Jonsson Comprehensive Cancer Center, University of California, Los Angeles, CA 90095; [i]David Geffen School of Medicine, University of California, Los Angeles, CA 90095; and [j]Eli and Edythe Broad Center of Regenerative Medicine and Stem Cell Research, University of California, Los Angeles, CA 90095

Contributed by Owen N. Witte, November 4, 2015 (sent for review September 17, 2015; reviewed by Theresa Guise and John T. Isaacs)

Mutationally activated kinases play an important role in the progression and metastasis of many cancers. Despite numerous oncogenic alterations implicated in metastatic prostate cancer, mutations of kinases are rare. Several lines of evidence suggest that nonmutated kinases and their pathways are involved in prostate cancer progression, but few kinases have been mechanistically linked to metastasis. Using a mass spectrometry-based phosphoproteomics dataset in concert with gene expression analysis, we selected over 100 kinases potentially implicated in human metastatic prostate cancer for functional evaluation. A primary in vivo screen based on overexpression of candidate kinases in murine prostate cells identified 20 wild-type kinases that promote metastasis. We queried these 20 kinases in a secondary in vivo screen using human prostate cells. Strikingly, all three RAF family members, MERTK, and NTRK2 drove the formation of bone and visceral metastasis confirmed by positron-emission tomography combined with computed tomography imaging and histology. Immunohistochemistry of tissue microarrays indicated that these kinases are highly expressed in human metastatic castration-resistant prostate cancer tissues. Our functional studies reveal the strong capability of select wild-type protein kinases to drive critical steps of the metastatic cascade, and implicate these kinases in possible therapeutic intervention.

kinases | metastasis | prostate cancer | bone metastasis

Metastatic prostate cancer is responsible for the deaths of ~30,000 men in the United States each year (1, 2). Ninety percent of patients develop bone metastases, and other major sites of metastases include lymph nodes, liver, adrenal glands, and lung (3). First-line treatments for metastatic disease are androgen deprivation therapies that block androgen synthesis or signaling through the androgen receptor (AR) (2). Inevitably, metastatic prostate cancer becomes resistant to androgen blockade. Second-line treatments such as chemotherapy (docetaxel, cabazitaxel) and radiation only extend survival 2–4 mo (4, 5).

Identifying new therapeutic targets for metastatic prostate cancer has proven difficult. Exome and whole-genome sequencing of human metastatic prostate cancer tissues have found frequent mutations and/or chromosomal aberrations in numerous genes, including *AR*, *TP53*, *PTEN*, *BRCA2*, and *MYC* (6–11). The precise functional contribution of these genes to prostate cancer metastasis remains unknown. Genomic and phosphoproteomic analyses have also revealed that metastatic prostate cancer is molecularly heterogeneous, which has complicated the search for common therapeutic targets (12). Few murine models of prostate cancer develop metastases. Mice having prostate-specific homozygous deletions in *SMAD4* and *PTEN* or expression of mutant *KRAS* develop metastases in visceral organs but rarely in bone (13–15).

Targeting genetically altered constitutively active protein kinases such as BCR-ABL in chronic myelogenous leukemia and $BRAF^{V600E}$ in melanoma has led to dramatic clinical responses (16). Although numerous oncogenic alterations have been identified in prostate cancer, DNA amplifications, translocations, or other mutations resulting in constitutive activity of kinases are rare (6, 9, 17). Genome sequencing of metastatic prostate cancer tissues from >150 patients found translocations involving the kinases BRAF and CRAF in <1% of patients (8, 18). Although uncommon, these genomic aberrations cause enhanced BRAF and CRAF kinase activity and suggest that kinase-driven pathways can be crucial in prostate cancer. Multiple lines of evidence indicate that nonmutated kinases may contribute to prostate cancer progression, castration resistance, and metastasis. SRC kinase synergizes with AR to drive the progression of early-stage prostatic intraepithelial neoplasia to advanced adenocarcinoma (19). SRC, BMX, and TNK2 kinases promote castration resistance by phosphorylating and stabilizing AR (20–22). Moreover, FGFR1, AKT1, and EGFR kinases activate pathways in prostate cancer cells to drive epithelial-to-mesenchymal transition and angiogenesis, both of which are key steps in metastasis (23–25). Despite the strong evidence implicating kinases in advanced prostate cancer, a systematic analysis of the functional role of kinases in prostate cancer metastasis has been lacking.

Metastasis of epithelial-derived cancers encompasses a complex cascade of steps, including (*i*) migration and invasion through

Significance

Therapies are urgently needed to treat metastatic prostate cancer. Mutationally activated and wild-type kinases such as BCR-ABL and BTK are effective therapeutic targets in multiple cancers. Genetically altered kinases are rare in prostate cancer. Wild-type kinases may be implicated in prostate cancer progression, but their therapeutic potential in metastatic prostate cancer remains unknown. Using phosphoproteomics and gene expression datasets, we selected 125 wild-type kinases implicated in human prostate cancer metastasis to screen for metastatic ability in vivo. The RAF family, MERTK, and NTRK2 drove prostate cancer bone and visceral metastasis and were highly expressed in human metastatic prostate cancer tissues. These studies reveal that wild-type kinases can drive metastasis and that the RAF family, MERTK, and NTRK2 may represent important therapeutic targets.

Author contributions: C.M.F. and O.N.W. designed research; C.M.F., J.M.D., P.M.C., B.A.S., Y.Z., C.V., and C. Mathis performed research; C. Morrissey and B.C. contributed new reagents/analytic tools; C.M.F., P.M.C., J.H., and O.N.W. analyzed data; and C.M.F. and O.N.W. wrote the paper.

Reviewers: T.G., Indiana University; and J.T.I., Johns Hopkins Oncology Center.

The authors declare no conflict of interest.

Freely available online through the PNAS open access option.

[1]Present address: Rutgers Cancer Institute of New Jersey and Department of Medicine, Rutgers-Robert Wood Johnson Medical School, New Brunswick, NJ 08901.

[2]To whom correspondence should be addressed. Email: owenwitte@mednet.ucla.edu.

This article contains supporting information online at www.pnas.org/lookup/suppl/doi:10.1073/pnas.1521674112/-/DCSupplemental.

surrounding stroma/basement membrane, (*ii*) intravasation and survival in circulation/lymphatics, (*iii*) extravasation through the vasculature, and (*iv*) survival and growth at a secondary site (26). With the exception of genetically engineered mouse models, no single experimental assay can model all steps of the metastatic cascade. As a result, most screens for genes involved in metastasis have focused on testing one step of the cascade. The migration/invasion step of metastasis is commonly interrogated in vitro by determining the ability of cells to invade through small pores in a membrane (27–29). Genes that function in other steps, or those dependent on the in vivo microenvironment to promote metastasis, are likely to be overlooked in these screens.

Multiple groups have performed in vivo screens for regulators of metastasis by manipulating cell lines in vitro with shRNA libraries or using genome editing techniques, and injecting cells either subcutaneously or into the tail vein of mice (30, 31). These methods are advantageous, because they interrogate multiple steps of the metastatic cascade (survival in circulation, extravasation, and colonization and growth at a secondary site) in a physiologically relevant environment. However, the majority of in vivo screens conducted so far have been based on loss-of-function genetics. These screens are limited to inhibiting the function of proteins expressed by a particular cell line. Using a gain-of-function in vivo screen, we sought to identify kinases that activate pathways leading to prostate cancer metastasis.

Results

Identifying Potential Metastasis-Promoting Kinases Using an Integrated Approach Combining Genomic/Transcriptomic, Phosphoproteomic, and Literature Data. The human kinome encodes over 500 kinases, many of which likely have a limited role in prostate cancer. We reasoned our results would have more relevance if we screened only kinases with evidence of enhanced expression and/or activity in human metastatic prostate cancer. Because no single analysis is both accurate and comprehensive in predicting relevant kinases, three different data sources were investigated. The database cBioPortal contains multiple genomic/transcriptomic datasets from patients with metastatic prostate cancer (6, 9, 32). Five hundred and five kinases were queried for increased RNA expression or genomic amplification in >10% of metastatic patient samples. From this analysis 54 kinases were identified (Table S1). However, high mRNA expression or genomic amplification of a kinase does not always correlate with kinase activity. Identification of phosphorylated kinases or their substrates by phosphoproteomics can better predict kinase activity. Analysis of our previously published phosphoproteomics dataset (33) identified 52 additional kinases with enriched activity in metastatic samples in comparison with benign or localized prostate cancer. Previously published functional studies also provide strong evidence of kinase activity. Searching PubMed using the terms "kinase," "prostate cancer," "metastasis," and "castration resistance" followed by prioritization of articles based on strength of functional data yielded an additional 19 kinases. Our selection method provided 125 kinases for further interrogation of their metastasis-promoting ability (Fig. 1 and Table S1).

Development of an in Vivo Lung Colonization Screen. We devised an in vivo lung colonization screen to test the metastasis-promoting ability of the 125 candidate kinases. A gain-of-function screening design was chosen given our interest in testing whether enhanced expression of a kinase is sufficient to drive metastasis. Additionally, it is unlikely that all 125 kinases are expressed in any single prostate cell line for loss-of-function studies.

Kinases were cloned into a lentiviral expression vector and stably overexpressed in Cap8 cells derived from PTEN null mice (34) (Fig. S1). Cap8 cells have minimal to no metastatic ability in vivo but metastasize when overexpressing a mutationally activated kinase, SRC^{Y529F} (Fig. S2). A luciferase reporter vector was also expressed in Cap8 cells to monitor their metastatic behavior in vivo by bioluminescence imaging (BLI).

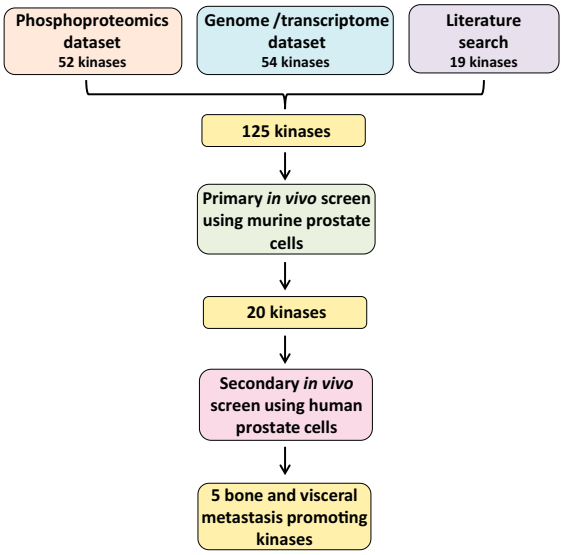

Fig. 1. Schematic summary of the screen for metastasis-promoting kinases. One hundred twenty-five candidate kinases were identified from a combination of genomic/transcriptomic, phosphoproteomic, and literature data. The primary screen entailed expressing all 125 kinases individually in a murine cell line followed by tail vein injection of cells into recipient mice. Twenty kinases strongly promoted lung colonization in vivo. The 20 kinases identified in the primary screen were subjected to a secondary in vivo screen using human prostate cells. Five kinases promoted bone and visceral metastasis in the human cell context.

Testing all 125 kinases as a "pool" in a single mouse would bias our screen toward kinases that are rapid inducers of metastatic colonization. Instead, we decided to test groups of five kinases per mouse to enable identification of kinases with varied metastatic potencies. Groups were selected by choosing five kinases with different molecular weights. Cap8 cells were stably transduced with individual kinases to make 125 different Cap8-kinase cell lines. Equal numbers of five different Cap8-kinase cell lines were pooled and injected into the tail vein of immunocompromised CB17 mice. Because all kinases were cloned with a V5 C-terminal tag (Fig. S1), the metastasis-promoting kinase in each group could be identified by Western blot analysis of the metastatic tissue with a V5 antibody (Fig. 2*A*).

In Vivo Colonization Screen Identifies 20 Kinases That Promote Metastasis in Murine Prostate Cancer Cells. From our screen of 125 kinases, we identified 20 kinases that promoted lung metastasis in vivo (Fig. 2 *B*–*D*). The most rapid detection of metastasis occurred 2 wk after injection, and was attributed to kinases NTRK2 and MAP3K8. Kinases MAP3K15, MERTK, and all members of the RAF family of kinases (ARAF, BRAF, and CRAF) drove the formation of significant lung metastasis within 3 wks. Kinases promoting metastasis but having a longer latency included FGFR1 (6 wk), SRC (6 wk), and BMX (7 wk) (Figs. 2*D* and 3*A*). Both FGFR1 and SRC have previously described roles in prostate cancer metastasis, which provides support for the validity of our screen (35, 36). Several small lung nodules were recovered at necropsy in 2/5 control mice after 10 wk (Fig. S3*B*). Albeit weak, the inherent metastatic ability of Cap8 cells in our model system implies that the 20 kinases identified are "enhancers of metastasis." It is still unclear whether they are actually "drivers" of de novo metastasis.

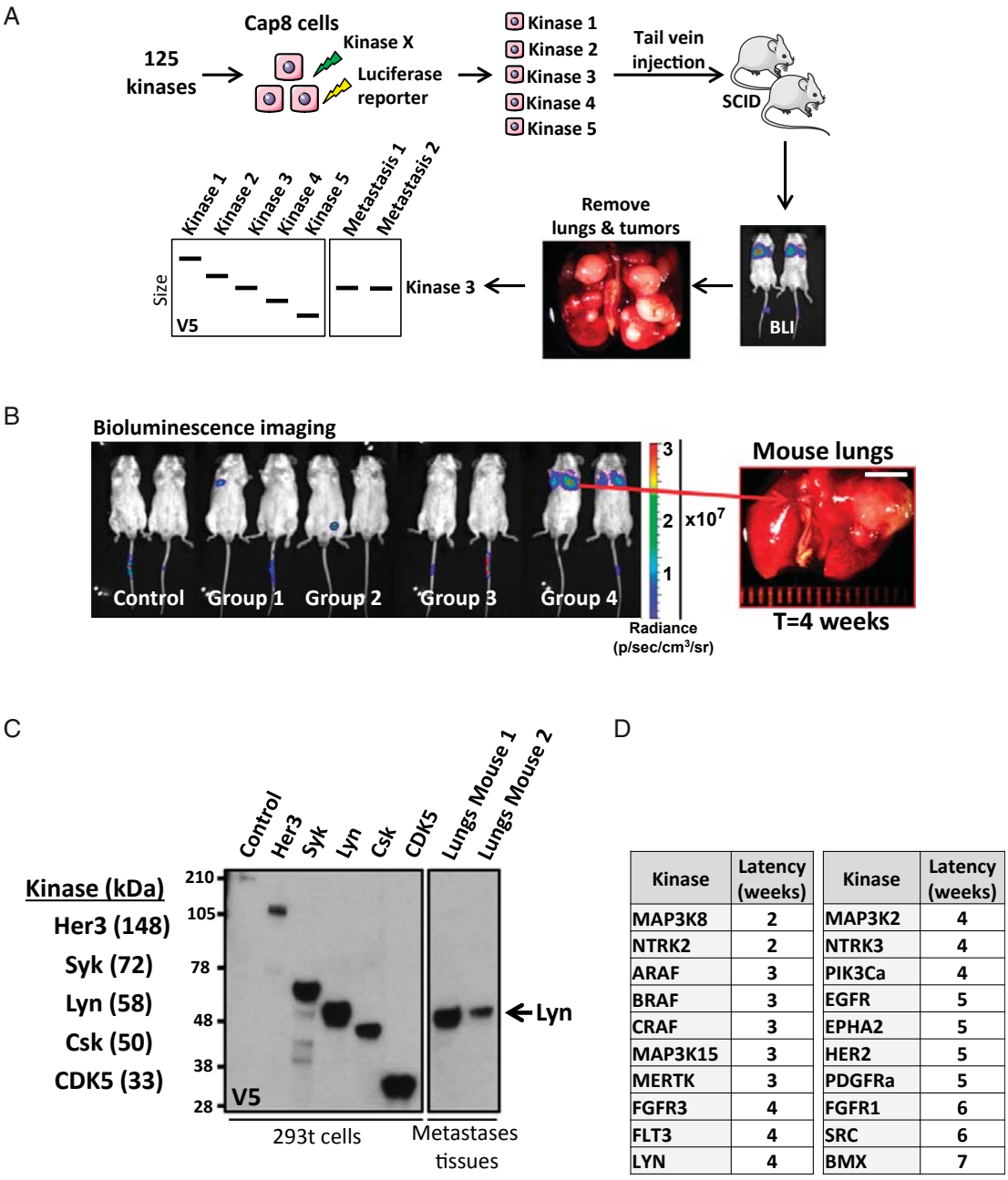

Kinase	Latency (weeks)	Kinase	Latency (weeks)
MAP3K8	2	MAP3K2	4
NTRK2	2	NTRK3	4
ARAF	3	PIK3Ca	4
BRAF	3	EGFR	5
CRAF	3	EPHA2	5
MAP3K15	3	HER2	5
MERTK	3	PDGFRa	5
FGFR3	4	FGFR1	6
FLT3	4	SRC	6
LYN	4	BMX	7

Fig. 2. In vivo screen of 125 candidate kinases identifies 20 kinases with metastasis-promoting ability when expressed in murine prostate cells. (*A*) Schematic diagram of the screen testing the metastatic ability of 125 kinases. Kinases were expressed individually in Cap8 cells, pooled into groups of five kinases (each with a different molecular weight), and injected into the tail vein of CB17 SCID mice. Bioluminescence imaging (BLI) was used to detect metastases that were subsequently removed for Western blot analysis. Because all kinases have a C-terminal V5 tag, the Western blot was probed with a V5 antibody to determine which size kinase was enriched in the metastasis tissues. (*B*) Composite BLI image of four different groups of mice. BLI images for each group were taken separately, but at the same time point. Each group was injected with a different set of five kinases. Corresponding bright field image of lungs removed from one of the group 4 mice is shown. sr noted in the units for radiance and refers to steradian. (Scale bar, 5 mm.) (*C*, *Left*) Names and molecular weights of five kinases in a representative group. Western blot analysis of 293t cells overexpressing kinases demonstrates that kinases can be differentiated by size using a V5 antibody. (*C*, *Right*) Western blot of lung tumors removed from mice injected with Cap8 cells overexpressing a group of kinases. By size alignment, the kinase enriched in the metastatic tissue from this particular group was identified as Lyn. (*D*) List of kinases identified in the primary lung colonization screen. Latency columns refer to the interval of time (in weeks) between time of injection and time at which metastatic burden detected by BLI and/or physical symptoms necessitated euthanasia.

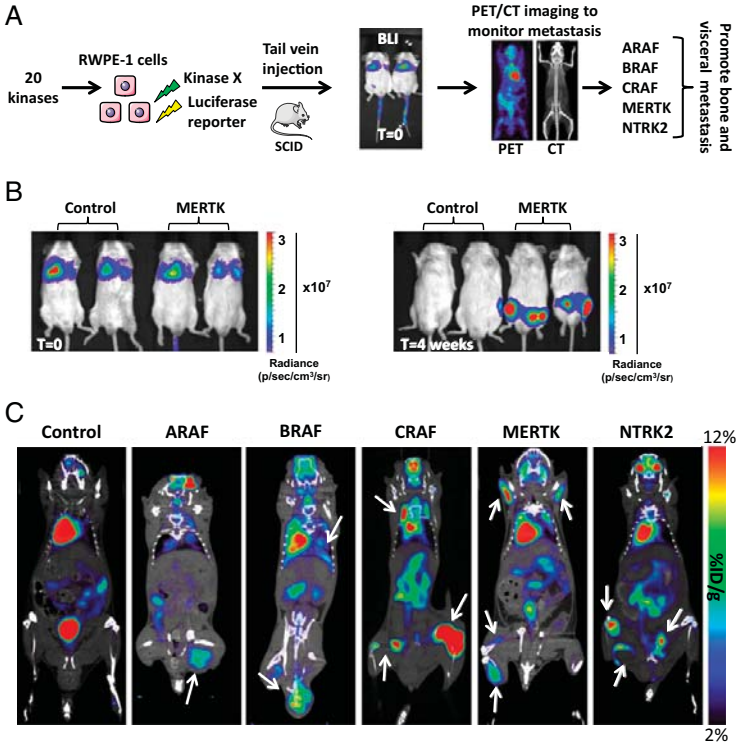

D

Kinase	Mice	Bone & visceral	Visceral only	No mets	Latency range (M)	Avg. latency (M)	Bone tumor burden
ARAF	8	7	1	0	2-6	4.3	Small
BRAF	4	2	1	1	4-5	4.5	Small
CRAF	6	4	1	1	1-4	2.5	Large
MERTK	6	5	0	1	2-5	3.0	Large
NTRK2	6	4	2	0	2-6	3.3	Large

Fig. 3. Screen of 20 kinases in human prostate cells identifies 5 kinases that drive bone and visceral metastasis. (*A*) Schema of the secondary screen. The 20 kinases identified in the primary screen were expressed in human prostate cells (RWPE-1 cells) and injected into the tail vein of mice. Immediately postinjection, mice were imaged by BLI to verify proper injection. Mice were monitored for metastasis by PET/CT imaging. (*B*) Representative BLI of mice injected with control or MERTK-expressing cells. At time (T) = 0, luciferase signal was detected in the lungs and, by T = 4 wk, luciferase signal was detected in the hind legs. (*C*) PET/CT images of mice injected with control cells or cells expressing the kinases ARAF, BRAF, CRAF, MERTK, and NTRK2. White arrows indicate anatomical sites of high glycolytic activity corresponding to sites of tumor growth. Scale bar on right corresponds to percent injected dose (ID) per gram (g) of tissue. (*D*) Table summarizing the outcomes of tail vein injections of RWPE-1 cells overexpressing ARAF, BRAF, CRAF, MERTK, and NTRK2. Listed are the number of mice tested per kinase, sites of metastatic colonization ("bone & visceral" or "visceral only"), latency (time point at which metastatic burden necessitated euthanasia), and tumor burden. The anatomical sites classified as visceral were lungs and lymph nodes. avg., average; M, month; mets, metastasis.

Screening in Human Prostate Cells Identifies Five Kinases That Drive Bone and Visceral Metastasis in Vivo. To identify which of the 20 candidate kinases drive rather than enhance metastasis in a human cell context, we next assayed their ability to promote metastasis when overexpressed in nonmalignant human prostate cells. The RWPE-1 cell line is derived from normal human prostate epithelium and immortalized with HPV-18 E6/E7 oncogenes (37). RWPE-1 cells do not form colonies in soft agar, nor are they tumorigenic in nude mice (37).

RWPE-1 cells expressing a luciferase reporter gene were separately infected with lentiviruses expressing each of the 20 kinases. Each kinase cell line was individually injected into the tail vein of NOD scid gamma (NSG) mice (Fig. 3*A*). Following tail vein injection, most cells are assumed to get lodged in the small capillaries of the lung rather than travel through the systemic circulation (38). This assumption is consistent with the BLI of mice conducted immediately after injection, showing tumor cells in the lungs but not in other anatomical sites (Fig. 3*B*).

Strikingly, mice injected with cells overexpressing the kinases MERTK, ARAF, BRAF, CRAF, and NTRK2 did not show symptoms of lung metastasis but rather developed hind leg weakness. Mice injected with CRAF-, MERTK-, and NTRK2-expressing RWPE-1 cells were the first to show symptoms 1–2 mo postinjection. A longer latency of up to 6 mo was observed in mice injected with cells expressing ARAF and BRAF. Using BLI, signal was detected in the hind legs (Fig. 3*B*). Although BLI is extremely sensitive, it lacks the precision to accurately predict the location of a metastasis, especially when signal is outside the lungs. Positron-emission tomography combined with computed tomography (PET/CT) is tissue depth-independent and enables precise identification of tumor localization based on cancer cell metabolic activity (39). PET/CT imaging of mice injected with cells expressing MERTK, ARAF, BRAF, CRAF, and NTRK2 showed high [^{18}F]FDG accumulation in the bones, lungs, and lymph nodes (Fig. 3*C*). Control mice were negative for [^{18}F]FDG accumulation in all corresponding anatomical sites (Fig. 3*C*). Further assessment of the CT scans suggested that the bone metastases in mice injected with cells expressing MERTK, ARAF, BRAF, CRAF, and NTRK2 are likely osteolytic.

Histological evaluation of tissues confirmed tumor cell colonization of the lungs, lymph nodes, and bone (femur, tibia, ilium, and vertebra) (Fig. 4 and Figs. S4 and S5). The RAF family members and NTRK2 drove the formation of lung and lymph node metastasis with a similar incidence, whereas MERTK-overexpressing cells did not colonize the lungs (Fig. 3*D*). Although not quantitative,

we observed by histology that metastases driven by CRAF, MERTK, and NTRK2 were extensive, with tumor cells often replacing large areas of bone marrow in the long bones, pelvis, and spine (Figs. 3*D* and 4). In contrast, small metastatic deposits were observed in the femur and spine of mice injected with cells expressing ARAF and BRAF (Fig. 4). To verify that each metastasis expressed the respective kinase and originated from human RWPE-1 cells, bone tissue sections underwent immunohistochemical (IHC) analysis for kinases (MERTK, ARAF, BRAF, CRAF, and NTRK2), HLA, prostate-specific antigen (PSA), and the epithelial cell marker E-cadherin. As shown in Fig. 4, strong IHC staining of each respective kinase, HLA, E-cadherin, and PSA was detected in all bone metastases.

After 8 mo, mice injected with RWPE-1 cells expressing PIK3Cα, MAP3K8, FGFR3, and NTRK3 developed lung, lymph node, and bone micrometastases. None of the mice injected with RWPE-1 cells expressing the other 12 kinases developed metastasis assessed by BLI and histology after 9 mo. Altogether, the functional data described indicate that RAF family members, NTRK2, and MERTK have strong metastasis-promoting ability in both human and mouse prostate cell lines and drive the formation of bone metastasis.

MERTK, NTRK2, and RAF Family Members Are Expressed in Human Prostate Cancer Bone and Visceral Metastasis Tissues. ARAF, BRAF, and CRAF were originally selected for the screen based on predicted activity from our human metastatic prostate cancer phosphoproteomics dataset. Due to the sequence similarity of the RAF kinases (40), some common phosphopeptide substrates could be shared by all three RAF family members. Which RAF family members are relevant to human metastatic prostate cancer remains unclear. MERTK and NTRK2 were added to the screen based on evidence of their role in lung (41), melanoma (42), and glioblastoma metastasis (43), but neither kinase has been previously implicated in prostate cancer metastasis.

To seek evidence of the relevance and therapeutic potential of candidate kinases, we evaluated their expression by immunohistochemistry in metastatic, localized, and benign human prostate cancer tissue samples. The University of Washington's Prostate Cancer Rapid Autopsy Program provided tissue microarrays (TMAs) containing 33 different patients' bone and visceral metastases for staining. We also obtained from the University of California, Los Angeles (UCLA), TMAs containing tissue from 115 patients with benign and medium- to high-grade localized prostate cancer (Gleason 7–9). Because an estimated 10% of patients with

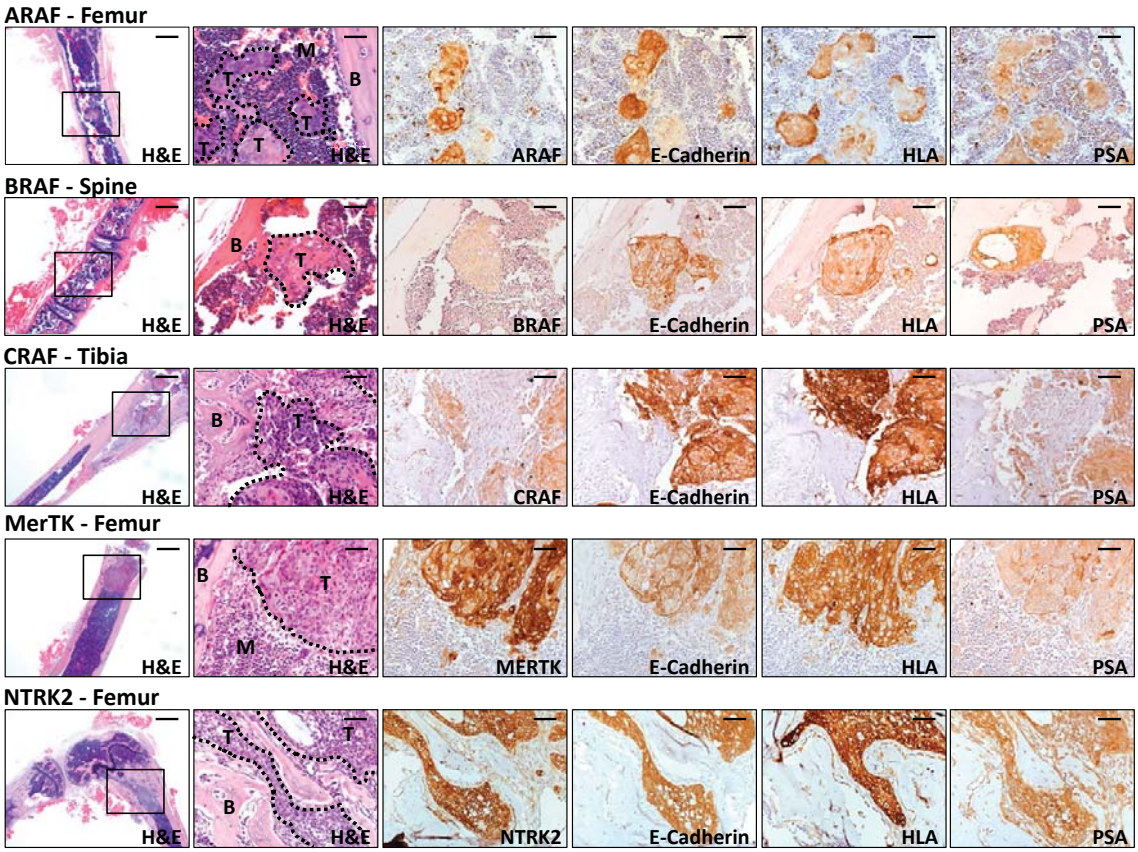

Fig. 4. Histological analysis of bones recovered from mice injected with cells expressing ARAF, BRAF, CRAF, MERTK, and NTRK2 confirms that metastases are of human prostate epithelial cell origin. (*Left* two columns) H&E stains of the affected bones removed from mice injected with RWPE-1 cells expressing the five metastasis-promoting kinases. Images in *Right* five columns are 20× magnification of the area outlined by a black box in the first column. Tumor areas are outlined by black dotted lines and indicated by "T." Bone and bone marrow are marked with "B" and "M," respectively. (*Right* four columns) IHC staining of bone metastasis for overexpressed kinase, E-cadherin, HLA class I, and PSA. [Scale bars, 320 μm (*Left*) and 40 μm (*Right* five columns).]

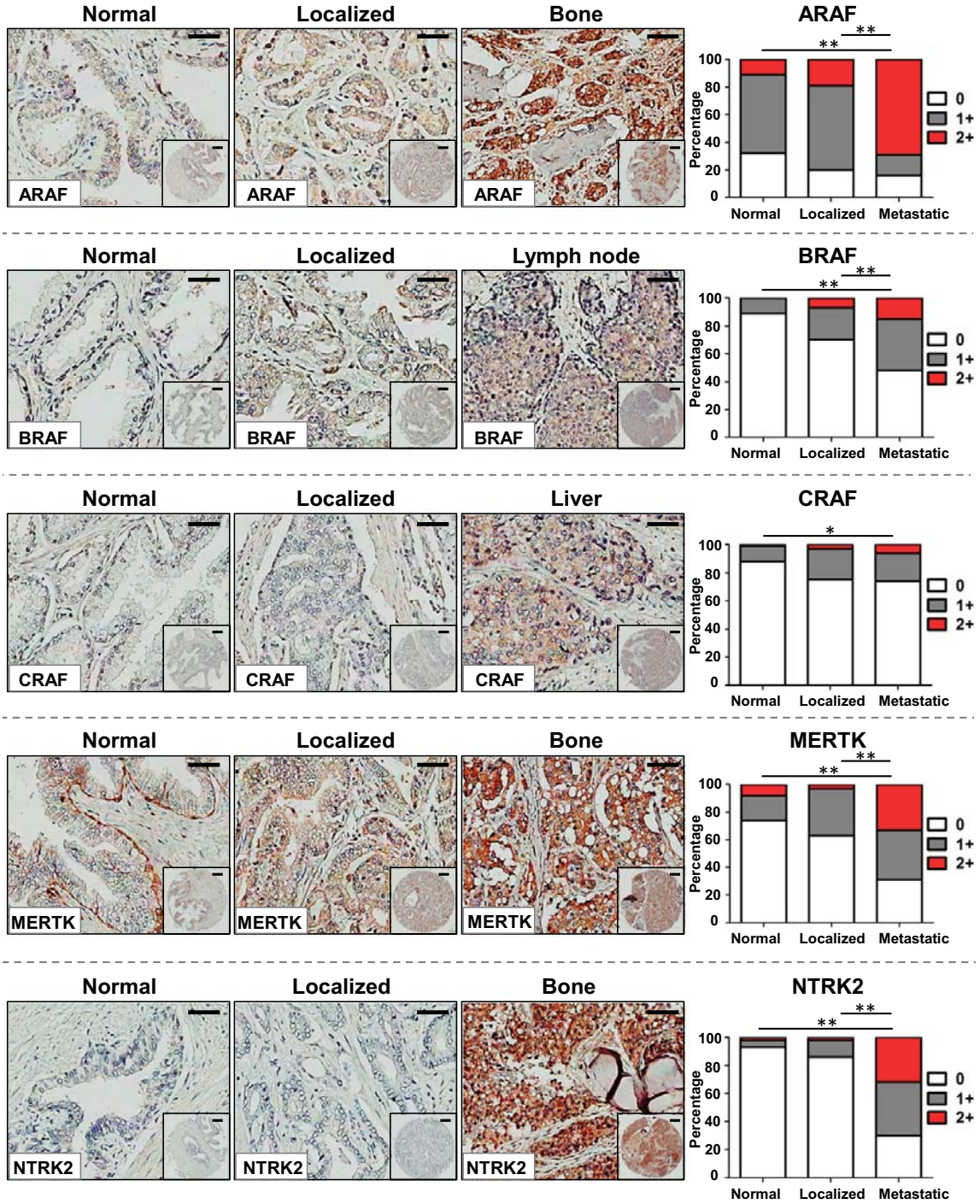

Fig. 5. High levels of the five metastasis-promoting kinases are detected in human prostate cancer metastasis tissues. (*Left*) IHC staining for ARAF, BRAF, CRAF, MERTK, and NTRK2 in representative samples from TMAs containing tissue sections from normal prostate tissue, localized prostate cancer (Gleason 7–9), and metastatic prostate cancer. [Scale bars, 50 μm (large images) and 100 μm (small images).] (*Right*) Quantification of kinase expression in TMAs based on staining intensity. No immunoreactivity was scored as 0, whereas positive immunoreactivity was scored as 1 or 2 based on intensity. The distributions of scores between normal + metastatic tissues and localized + metastatic tissues were subjected to χ^2 statistical analysis. Significance: $^*P \leq 0.05$, $^{**}P \leq 0.01$.

Gleason 7 prostate cancer develop metastasis (44), we hypothesized that the metastasis-promoting kinases would have low expression in the majority of benign and localized prostate cancer tissues in comparison with metastatic prostate cancer tissues.

Consistent with our hypothesis, we found ARAF, BRAF, MERTK, and NTRK2 to be highly expressed in metastatic tissues in comparison with benign or localized prostate cancer tissues (Fig. 5). Remarkably, 69% of metastatic tissues (68/99 samples) had strong ARAF staining (scored as 2+), whereas only 11% of normal (11/102 samples) and 19% of localized prostate cancer tissues (20/105 samples) had ARAF staining of similar intensity. Strong BRAF, MERTK, and NTRK2 staining was detected in 15% (15/100 samples), 33% (32/98 samples), and 32% (31/96 samples) of metastatic tissues, but less than ~10% of normal and localized prostate cancer tissues were scored 2+ for these three kinases. CRAF-positive staining was higher in metastases (26%, 26/99 samples) in comparison with normal prostate tissue (12%, 11/92 samples). However, no difference in CRAF staining was observed between localized (25%, 24/95 samples) and metastatic prostate cancer. We cannot exclude the possibility that the activation state of CRAF may be different between localized and metastatic prostate cancer samples. Overall, the IHC staining results provide evidence that MERTK, NTRK2, and the RAF family members are expressed and could be functionally relevant in human metastatic prostate cancer. Based on expression, ARAF, BRAF, MERTK, and NTRK2 are more likely to have a functional role in metastasis rather than in early-stage prostate cancer.

Discussion

The strong metastatic ability of RAF family members in our model is consistent with previous reports describing alterations of this pathway in human prostate cancer metastasis. Based on copy number alterations and transcriptome and mutational data, Taylor et al. found that RAS/RAF signaling is dysregulated in 43% of primary tumors and >90% of metastasis (9). Recently, two studies identified BRAF and CRAF fusion proteins with predicted constitutive kinase activity in a small subset (<0.05%) of advanced localized and metastatic prostate cancer tumors (8, 18). We found overexpression of CRAF in the human prostate cell line RWPE-1 to be a more potent driver of bone metastasis (with regard to metastatic burden and time point at which metastases necessitated euthanasia) than ARAF or BRAF. Despite its lower metastatic potency, ARAF expression in human metastatic prostate cancer tissues was much higher than BRAF or CRAF expression. It is possible that ARAF is the dominant RAF family member functioning in human prostate cancer metastasis.

The mechanism by which RAF family members drive metastasis and in particular bone colonization is unknown. Using Madin–Darby canine kidney (MDCK) cells, Lehmann et al. showed that dimerization of CRAF not only induces ERK/MAPK pathway activation but also leads to TGF-β secretion (45). Because the TGF-β signaling pathway is considered one of the key pathways driving prostate cancer bone metastasis (46), CRAF may contribute to metastasis by promoting autocrine TGF-β secretion. Much less is known about the role of ARAF in tumorigenesis, but a recent study showed that ARAF homodimerization or heterodimerization with BRAF enhanced the metastatic ability of lung cancer cells (47).

We also show that MERTK is a potent inducer of prostate cancer metastasis. As a member of the TAM family of tyrosine kinases, MERTK is best-known for its role in promoting phagocytosis of apoptotic cells and dampening the proinflammatory cytokine response (48). MERTK is overexpressed and/or has functional activity in multiple cancers but is rarely genetically amplified or mutated (48). We demonstrate that wild-type MERTK has functional activity in metastasis and is highly expressed in human prostate cancer metastasis tissues. Lending support to our findings are studies demonstrating that MERTK drives migration and invasion in glioblastoma and melanoma cells (42, 43). The downstream pathways activated by MERTK include the RAF/ERK/MAPK, AKT, Stat, and NF-κB pathways (48). Given the metastatic potency of the RAF pathway in our model, MERTK may be dependent on this pathway for its metastatic ability.

NTRK2 and NTRK3, belonging to the neurotrophin family of tyrosine kinases, were also identified in our screen as strong promoters of prostate cancer metastasis. Expression analyses have previously implicated these kinases in prostate cancer. NTRK2 and NTRK3 were undetectable in normal prostate epithelial cells but positive in bone metastasis tissues (49). The precise function of the neurotrophin tyrosine kinases in prostate cancer is unknown. In multiple cancer types, NTRK2 promotes resistance to anoikis (detachment-induced apoptosis), which is a key step in the metastatic cascade (28, 50). Preventing anoikis could be part of the mechanism by which NTRK2 contributes to prostate cancer metastasis.

One of the most interesting features of our metastatic model is the high frequency of metastasis to the lumbar spine, femur, pelvis, and tibia. This bone metastasis pattern is similar to sites of prostate cancer bone metastasis in humans, with the lumbar vertebrae being most common, followed by ribs, pelvis, and long bones (51). Greater than 80% of mice injected with cells overexpressing ARAF (7/8 mice) and MERTK (5/6 mice) developed bone metastasis, whereas BRAF, CRAF, and NTRK2 promoted bone metastasis in at least 50% of mice. In comparison, the few genetically engineered mouse models that develop prostate cancer metastasis have a lower penetrance (12.5–25%) of bone metastases (52–54). Intracardiac or direct bone injection of human prostate cancer cell lines results in a higher frequency of metastasis, but the incidence and location of bone metastasis vary widely between studies (55, 56). The similarities of our model to human prostate cancer and the high frequency of bone metastasis may increase the feasibility of studying the biological mechanisms of prostate cancer bone metastasis. Integrins and chemoattractants such as αVβ3 and SCF1 likely contribute to prostate cancer bone tropism, and our model could provide insights into how certain kinase pathways regulate these bone homing factors (57, 58).

Our results underscore the potential contribution of wild-type kinases to prostate cancer metastasis and provide rationale for therapeutically targeting MERTK, NTRK2, and RAF family members. Currently, there are no selective Food and Drug Administration (FDA)-approved inhibitors of MERTK or NTRK2. The multikinase inhibitor foretinib inhibits MERTK in addition to c-MET and VEGFR (59). Because c-MET inhibition is effective in some patients with metastatic prostate cancer, targeting both MERTK and c-Met with foretinib may be a promising therapeutic approach (60). Pan-NTRK family member inhibitors are excellent therapeutic candidates for prostate cancer, because they would block the bone metastasis-promoting functions of NTRK2 and NTRK3, and NTRK1-mediated bone pain (61). Sorafenib is an FDA-approved small-molecule inhibitor targeting RAF family members and other kinases such as VEGFR-2, VEGFR-3, and PDGF-β (62). Clinical studies involving a small number of patients have suggested that sorafenib may have therapeutic benefit in patients with castration-resistant prostate cancer (63, 64). Due to reports of paradoxical RAF inhibitor-mediated RAF activation, inhibiting the direct downstream targets of RAF, MEK1/MEK2, may be a better approach (65). Trametinib, an inhibitor of MEK1/MEK2, is currently in phase II clinical trials for patients with advanced prostate cancer (66). Future studies should focus on inhibition of MERTK, NTRK2, and RAF pathways in metastatic models to provide additional rationale for targeting these kinases in patients with metastatic prostate cancer.

Methods

Cell Culture and Reagents. Cap8 cells were obtained from the laboratory of Hong Wu, University of California, Los Angeles (UCLA), and propagated in DMEM supplemented with 10% (vol/vol) FBS (Gibco), 25 μg/mL bovine

pituitary extract (Lonza), 5 μg/mL human insulin (Gibco), 6 ng/mL recombinant human epidermal growth factor (PeproTech), glutamine (1 mM), penicillin (100 U/mL), and streptomycin (100 μg/mL) (34). RWPE-1 cells were purchased from ATCC and cultured in keratinocyte serum-free medium (K-SFM) (Gibco) supplemented with 0.05 mg/mL bovine pituitary extract (Gibco), 5 ng/mL EGF (Gibco), penicillin (100 U/mL), and streptomycin (100 μg/mL). 293t cells used for lentiviral production were cultured in DMEM supplemented with 10% (vol/vol) FBS, glutamine (1 mM), penicillin (100 U/mL), and streptomycin (100 μg/mL).

Cloning of Kinases. We obtained the Center for Cancer Systems Biology–Dana-Farber Cancer Institute–Broad Human Kinase ORF collection consisting of 559 kinases in pDONR-223 Gateway entry vectors. The plasmid kit (Addgene Kit 1000000014) was a gift from William Hahn and David Root, Broad Institute of Harvard and Massachusetts Institute of Technology, Boston. Using the pcDNA 6.2/V5-DEST (Invitrogen), we cloned the attR1-ccdB-CmR-attR2-V5-SV40-blasticidin cassette into the previously described third-generation lentiviral FUCGW vector (67). The FU-R1-R2-V5-SV40-Blasti-CGW vector (Fig. S1) is optimized for our screen based on the V5 tag enabling kinase detection with V5 antibody and selection of kinase-expressing cells using blasticidin. Kinases in pDONR-223 vectors were cloned into FU-R1-R2-V5-SV40-Blasti-CGW using LR Clonase II (Invitrogen) and sequenced to verify the wild-type sequence. Wild-type BRAF and RPS6KA4 were not included in the ORF kinase collection. We acquired these ORFs from the Harvard PlasmID Repository and subcloned them into the FUCGW vector.

Virus Production. Third-generation lentiviruses were prepared by calcium phosphate precipitation transfection of 293t cells with plasmids expressing kinases (FU-kinase-V5-SV40-Blasti-CGW) or luciferase (FU-ILYW). The lentiviruses were prepared as described (67).

Western Blot. Whole-cell lysates were prepared in RIPA lysis buffer (150 nM NaCl, 1% Nonidet P-40, 0.5% sodium deoxycholate, 0.1% SDS, 50 mM Tris, pH 8.0) with phosphatase inhibitor (cocktails 2 and 3; Sigma) and protease inhibitor cocktail (Roche). Equal amounts of protein were separated by 4–20% (mass/vol) Tris-Hepes SDS/PAGE (Thermo Fisher), followed by immunoblotting analysis with the indicated antibodies.

Kinase protein expression was detected using a V5 antibody (Invitrogen R960-25; 1:2,500). Because AXL and BRAF lacked a V5 tag, we verified their expression using an AXL antibody (Cell Signaling 4977; 1:1,000) and a BRAF antibody (Cell Signaling 55C6; 1:1,000).

Animal Studies. All animal experiments were performed according to the protocol approved by the Division of Laboratory Medicine at the University of California, Los Angeles. NOD.CB17-Prkdc^{scid}/J mice (for the primary screen) and NOD-scid gamma (for the secondary screen) were purchased from Jackson Laboratories. For all experiments, male mice between 6 and 8 wk of age were used.

Primary in Vivo Kinase Screen.

Infection of cells and tail vein injections. Cap8 cells were infected with lentivirus expressing luciferase and YFP (FU-ILYW) at a multiplicity of infection (MOI) of 10. Three days later, cells were sorted based on YFP expression using a BD FACSAria. Cap8-ILYW cells were expanded and frozen in aliquots so that all experiments would start at the same cell passage number. Upon starting an experiment, Cap8-ILYW cells were thawed and propagated for 5 d followed by infection with kinases individually at an MOI of 8 in media containing polybrene (8 μg/mL). Twenty-four hours after infection, media was removed and replaced with media containing 13 μg/mL blasticidin (InvivoGen). Cells underwent blasticidin selection for 5 d, followed by propagation for 48 h in complete media (without blasticidin). Instead of screening 125 kinases individually in vivo, we tested groups of 5 kinases in each mouse. Five kinases with different molecular weights were selected for each group. Each group was prepared by counting 2×10^5 cells of each of the five kinase cell lines and pooling the kinase cell lines together in 200 μL HBSS (Life Technologies). Using a 27-G needle, 200 μL (1×10^6 total cells) was injected into the lateral tail vein of CB17 mice in duplicate. D-luciferin substrate was injected i.p. into mice, followed by BLI to verify proper tail vein injection of kinase-expressing Cap8-ILYW cells (indicated by luciferase signal in the lungs). Mice were monitored for physical symptoms of metastasis (labored breathing, cachexia, difficulty moving) and by biweekly BLI. Upon detection of metastasis, mice were euthanized and lung tumors were dissected and stored at −80 °C.

Identification of metastasis-promoting kinase. Lung tumors were thawed, homogenized, and sonicated in RIPA lysis buffer. After a high-speed spin, protein concentration of the supernatant was measured in preparation for Western blotting. Because all kinases had a V5 C-terminal tag, the Western blot was probed with a V5 antibody to determine which size kinase was enriched in the metastasis tissues. To aid in identifying the enriched kinase, we included on our Western blot lysate from 293t cells expressing the five kinase cell lines individually. This Western blot was used as a reference of the individual kinase sizes. For the majority of the metastasis tissues analyzed by Western blot, only one out of the five kinases was enriched. If >1 kinase was identified in the metastasis tissues by Western blot, tail vein injections using cell lines expressing each of the kinases were repeated.

Secondary in Vivo Kinase Screen.

Infection of cells and tail vein injections. The same infection method described for the primary screen was used to transduce RWPE-1 cells with a lentivirus expressing luciferase followed by lentiviruses expressing the 20 kinases (identified in the primary screen). RWPE-1 cells expressing kinases were selected with 15 μg/mL blasticidin for 5 d and prepared for tail vein injection following the method described for the primary screen. However, instead of screening 5 kinases at a time, the 20 kinases were tested individually. Kinase-expressing RWPE-1 cells (1×10^6) were injected into the lateral tail vein of NSG mice in duplicate. D-luciferin substrate was injected i.p. into mice, followed by BLI to verify proper tail vein injection. Mice were monitored for physical symptoms of metastasis and by biweekly BLI. Upon symptom detection or positive BLI signal, mice underwent PET/CT imaging and were euthanized the following day. Macroscopic tumors and bones were removed and prepared for histology. Three biological replicates were performed for each of the five kinases (ARAF, BRAF, CRAF, NTRK2, and MERTK).

Imaging.

Bioluminescence imaging. BLI was conducted using an IVIS Lumina II (PerkinElmer). D-luciferin (150 mg/kg) was injected intraperitoneally. After 15 min, anesthetized mice [using 2.5% (vol/vol) isoflurane] were imaged. BLI analysis was performed using Living Image software, version 4.0 (PerkinElmer).

PET imaging. Mice were placed on a heated platform and anesthetized with 1.5% (vol/vol) isoflurane for the entirety of the experiment. Approximately 740 kBq of ^{18}F-labeled 2-fluoro-2-deoxyglucose ([^{18}F]FDG; obtained from the UCLA Department of Nuclear Medicine) was injected into the tail vein. After 1 h, the mice were imaged for 10 min on a Genisys 4 imager (Sofie Biosciences) followed by a high-resolution computed tomography scan on a CrumpCAT imager (UCLA).* PET and CT images were manually coregistered. Images were analyzed using AMIDE medical imaging software (68).

Immunohistochemistry. Metastatic tissues were removed from the mice and fixed in 10% (vol/vol) formalin overnight and paraffin-embedded. Bones were decalcified before paraffin embedding. Four-micrometer-thick sections were stained with hematoxylin and eosin for representative histology. For IHC analysis of TMAs, sections were heated at 65 °C for 1 h followed by deparaffinization in xylene and rehydration in 100%, 95%, and 70% (vol/vol) ethanol. Antigen retrieval was performed by heating samples at 95° for 20 min in 0.01 M citrate buffer (pH 6.0). Endogenous peroxidase activity was blocked with 3% (vol/vol) H_2O_2 for 10 min, followed by blocking for nonspecific binding with 2.5% (vol/vol) horse serum (Vector Laboratories) for 1 h. Primary antibodies (see below) were diluted in 2.5% (vol/vol) horse serum and incubated on slides overnight at 4 °C. Following three washes with 1× PBS, slides were incubated with anti-mouse HRP or anti-rabbit HRP secondary antibodies (Dako) for 1 h at 25 °C. Slides were developed using the liquid DAB+ Substrate Chromogen System (Dako), counterstained with hematoxylin, dehydrated, and mounted.

MERTK protocol. IHC staining for MERTK was conducted as described (69). Briefly, we followed the same primary antibody protocol as described above, but to increase the sensitivity of MERTK staining we used a biotinylated secondary antibody (goat anti-rabbit IgG; Boster Biotechnology), followed by peroxidase-conjugated streptavidin (SABC; SA1022; Boster Biotechnology). The slide development protocol was followed as described above.

Antibodies. The following primary antibodies and dilutions were used: E-cadherin (BD clone 36; 1:250), PSA (Dako; 1:2,000), HLA class I ABC (Abcam 70328; 1:350), ARAF (Abcam 200653; 1:700), BRAF (Cell Signaling 55C6; 1:100), CRAF (Cell Signaling 9422; 1:100), MERTK (Abcam 52968; 1:300), and NTRK2 (Cell Signaling 4607; 1:250). Dilutions were optimized on sections using metastatic tissues recovered from mice injected with RWPE-1 cells overexpressing each kinase. To ensure specificity and lack of cross-reactivity of RAF family member antibodies, we stained ARAF-overexpressing tissue with BRAF and CRAF antibodies, BRAF-overexpressing tissue with CRAF and ARAF antibodies, and CRAF-overexpressing tissue with ARAF and BRAF antibodies.

*Taschereau R, Vu NT, Chatziioannou AF, 2014 Institute of Electrical and Electronics Engineers Nuclear Science Symposium & Medical Imaging Conference, November 8–15 2014, Seattle, WA.

Clinical Prostate Tissue Microarrays.

Human metastatic prostate cancer tissue microarrays.

Tissue acquisition. Samples were obtained from patients who died of metastatic castration resistant prostate cancer (CRPC) and who signed written informed consent for a rapid autopsy performed within 6 h of death, under the aegis of the Prostate Cancer Donor Program at the University of Washington (70). The Institutional Review Board of the University of Washington approved this study. Visceral metastases were identified at the gross level, bone biopsies were obtained according to a template from 20 different sites, and metastases were identified at a histological level.

Tissue microarray construction. One hundred and three CRPC metastases (including 45 visceral metastases and 58 bone metastases) from 33 autopsy patients (up to four sites per patient) were fixed in buffered formalin [bone metastases were decalcified in 10% (vol/vol) formic acid] and embedded in paraffin. A TMA was made using duplicate 1-mm-diameter cores from these tissues.

Human benign prostate and localized prostate cancer tissue microarrays. Construction of TMAs was approved by UCLA's Institutional Review Board. Samples were obtained from prostatectomy specimens performed at UCLA between 2001 and 2010. A total of 115 cases of high-grade prostate adenocarcinoma (combined Gleason score 7–9) were selected. Three cores of tumor and three cores of corresponding benign prostate were obtained from each case and transferred to two recipient TMA blocks.

Scoring of TMAs. TMAs were scored 0, 1, and 2 based on intensity of staining, with 0 indicating no staining, 1 indicating weakly positive staining, and 2 indicating strongly positive staining. Two separate observers scored normal prostate, localized prostate cancer, and metastatic prostate cancer TMAs. TMAs and corresponding scores were reviewed by a board-certified pathologist. Because MERTK is expressed in normal human prostate basal cells and in macrophages, scores for MERTK were based on expression only in luminal cells. Representative images of TMAs were taken using a Zeiss Axio Imager A1 microscope. To optimize TMA images for print (Fig. 5), PowerPoint was used to equally adjust all images using the following parameters: sharpen (+25%), brightness (–33%), and contrast (+66%).

ACKNOWLEDGMENTS. We thank members of the O.N.W. laboratory for helpful comments and discussion. We are grateful to the patients and their families who were willing to participate in the University of Washington's Prostate Cancer Donor Program and the investigators Drs. Robert Vessella, Celestia Higano, Bruce Montgomery, Evan Yu, Peter Nelson, Paul Lange, Martine Roudier, and Lawrence True and the Rapid Autopsy team for their contributions to the University of Washington Medical Center Prostate Cancer Donor Rapid Autopsy Program. This research was supported by funding from the Pacific Northwest Prostate Cancer Specialized Program of Research Excellence (SPORE) (P50CA97186) and a P01 NIH grant (P01CA085859). We thank Dr. Daniel Margolis for radiological evaluation of PET/CT scans; UCLA Molecular Imaging Center and staff; H. Wu laboratory for cell lines; UCLA Translational Pathology Core Laboratory for assistance with tissue processing and H&E staining; and Donghui Cheng for help with FACS sorting. C.M.F. was supported by a California Institute of Regenerative Medicine Training Grant (TG2-01169) and USHHS Ruth L. Kirschstein Institutional National Research Service Award (T32 CA009056); J.M.D. was supported by the Department of Defense Prostate Cancer Research Program (W81XWH-14-1-0148); P.M.C. was supported by a California Institute of Regenerative Medicine Training Grant (TG2-01169), UCLA Scholars in Oncologic Molecular Imaging Program National Cancer Institute Grant (R25T CA098010), and UCLA in Vivo Cellular and Molecular Imaging Center Career Development Award (P50 CA086306); and B.A.S. was supported by a UCLA Tumor Immunology Training Grant (T32 CA00912). J.H. is supported by NIH Grants 5R01CA172603-02 [principal investigator (PI): J.H.], 2P30CA016042-39 (PI: Judith Gasson), 1R01CA181242-01A1 (PI: Chun Chao), and 1R01CA195505 (PI: Leonard Marks); Department of Defense Prostate Cancer Research Program W81XWH-12-1-0206 (PI: Lily Wu); UCLA SPORE in prostate cancer (PI: Robert Reiter); Prostate Cancer Foundation Honorable A. David Mazzone Special Challenge Award (PI: Robert Reiter); and UCLA Jonsson Comprehensive Cancer Center Impact Grant (PI: Sanaz Memarzadeh). O.N.W. is an Investigator of the Howard Hughes Medical Institute and is supported by a Prostate Cancer Foundation Challenge Award. J.H. and O.N.W. are supported by a Stand Up To Cancer–Prostate Cancer Foundation Prostate Dream Team Translational Research Grant (SU2C-AACR-DT0812). This research grant is made possible by the generous support of the Movember Foundation. Stand Up To Cancer is a program of the Entertainment Industry Foundation administered by the American Association for Cancer Research.

1. van Dodewaard-de Jong JM, et al. (2015) New treatment options for patients with metastatic prostate cancer: What is the optimal sequence? *Clin Genitourin Cancer* 13(4):271–279.
2. Nelson WG, De Marzo AM, Isaacs WB (2003) Prostate cancer. *N Engl J Med* 349(4): 366–381.
3. Bubendorf L, et al. (2000) Metastatic patterns of prostate cancer: An autopsy study of 1,589 patients. *Hum Pathol* 31(5):578–583.
4. de Bono JS, et al.; TROPIC Investigators (2010) Prednisone plus cabazitaxel or mitoxantrone for metastatic castration-resistant prostate cancer progressing after docetaxel treatment: A randomised open-label trial. *Lancet* 376(9747):1147–1154.
5. Parker C, et al.; ALSYMPCA Investigators (2013) Alpha emitter radium-223 and survival in metastatic prostate cancer. *N Engl J Med* 369(3):213–223.
6. Grasso CS, et al. (2012) The mutational landscape of lethal castration-resistant prostate cancer. *Nature* 487(7406):239–243.
7. Gundem G, et al.; ICGC Prostate UK Group (2015) The evolutionary history of lethal metastatic prostate cancer. *Nature* 520(7547):353–357.
8. Robinson D, et al. (2015) Integrative clinical genomics of advanced prostate cancer. *Cell* 161(5):1215–1228.
9. Taylor BS, et al. (2010) Integrative genomic profiling of human prostate cancer. *Cancer Cell* 18(1):11–22.
10. Hong MK, et al. (2015) Tracking the origins and drivers of subclonal metastatic expansion in prostate cancer. *Nat Commun* 6:6605.
11. Kumar A, et al. (2011) Exome sequencing identifies a spectrum of mutation frequencies in advanced and lethal prostate cancers. *Proc Natl Acad Sci USA* 108(41): 17087–17092.
12. Drake JM, et al. (2013) Metastatic castration-resistant prostate cancer reveals intrapatient similarity and interpatient heterogeneity of therapeutic kinase targets. *Proc Natl Acad Sci USA* 110(49):E4762–E4769.
13. Aytes A, et al. (2013) ETV4 promotes metastasis in response to activation of PI3-kinase and Ras signaling in a mouse model of advanced prostate cancer. *Proc Natl Acad Sci USA* 110(37):E3506–E3515.
14. Mulholland DJ, et al. (2012) Pten loss and RAS/MAPK activation cooperate to promote EMT and metastasis initiated from prostate cancer stem/progenitor cells. *Cancer Res* 72(7):1878–1889.
15. Ding Z, et al. (2011) SMAD4-dependent barrier constrains prostate cancer growth and metastatic progression. *Nature* 470(7333):269–273.
16. Zhang J, Yang PL, Gray NS (2009) Targeting cancer with small molecule kinase inhibitors. *Nat Rev Cancer* 9(1):28–39.
17. Drake JM, Lee JK, Witte ON (2014) Clinical targeting of mutated and wild-type protein tyrosine kinases in cancer. *Mol Cell Biol* 34(10):1722–1732.
18. Palanisamy N, et al. (2010) Rearrangements of the RAF kinase pathway in prostate cancer, gastric cancer and melanoma. *Nat Med* 16(7):793–798.
19. Cai H, Babic I, Wei X, Huang J, Witte ON (2011) Invasive prostate carcinoma driven by c-Src and androgen receptor synergy. *Cancer Res* 71(3):862–872.
20. Dai B, et al. (2010) Compensatory upregulation of tyrosine kinase Etk/BMX in response to androgen deprivation promotes castration-resistant growth of prostate cancer cells. *Cancer Res* 70(13):5587–5596.
21. Guo Z, et al. (2006) Regulation of androgen receptor activity by tyrosine phosphorylation. *Cancer Cell* 10(4):309–319.
22. Mahajan NP, et al. (2007) Activated Cdc42-associated kinase Ack1 promotes prostate cancer progression via androgen receptor tyrosine phosphorylation. *Proc Natl Acad Sci USA* 104(20):8438–8443.
23. Acevedo VD, et al. (2007) Inducible FGFR-1 activation leads to irreversible prostate adenocarcinoma and an epithelial-to-mesenchymal transition. *Cancer Cell* 12(6): 559–571.
24. Gan Y, et al. (2010) Differential roles of ERK and Akt pathways in regulation of EGFR-mediated signaling and motility in prostate cancer cells. *Oncogene* 29(35):4947–4958.
25. Conley-LaComb MK, et al. (2013) PTEN loss mediated Akt activation promotes prostate tumor growth and metastasis via CXCL12/CXCR4 signaling. *Mol Cancer* 12(1):85.
26. Nguyen DX, Bos PD, Massagué J (2009) Metastasis: From dissemination to organ-specific colonization. *Nat Rev Cancer* 9(4):274–284.
27. van Roosmalen W, et al. (2015) Tumor cell migration screen identifies SRPK1 as breast cancer metastasis determinant. *J Clin Invest* 125(4):1648–1664.
28. Douma S, et al. (2004) Suppression of anoikis and induction of metastasis by the neurotrophic receptor TrkB. *Nature* 430(7003):1034–1039.
29. Scott KL, et al. (2011) Proinvasion metastasis drivers in early-stage melanoma are oncogenes. *Cancer Cell* 20(1):92–103.
30. Chen S, et al. (2015) Genome-wide CRISPR screen in a mouse model of tumor growth and metastasis. *Cell* 160(6):1246–1260.
31. Duquet A, et al. (2014) A novel genome-wide in vivo screen for metastatic suppressors in human colon cancer identifies the positive WNT-TCF pathway modulators TMED3 and SOX12. *EMBO Mol Med* 6(7):882–901.
32. Cerami E, et al. (2012) The cBio Cancer Genomics Portal: An open platform for exploring multidimensional cancer genomics data. *Cancer Discov* 2(5):401–404.
33. Drake JM, et al. (2012) Oncogene-specific activation of tyrosine kinase networks during prostate cancer progression. *Proc Natl Acad Sci USA* 109(5):1643–1648.
34. Jiao J, et al. (2007) Murine cell lines derived from Pten null prostate cancer show the critical role of PTEN in hormone refractory prostate cancer development. *Cancer Res* 67(13):6083–6091.
35. Park SI, et al. (2008) Targeting SRC family kinases inhibits growth and lymph node metastases of prostate cancer in an orthotopic nude mouse model. *Cancer Res* 68(9): 3323–3333.
36. Yang F, et al. (2013) FGFR1 is essential for prostate cancer progression and metastasis. *Cancer Res* 73(12):3716–3724.
37. Bello D, Webber MM, Kleinman HK, Wartinger DD, Rhim JS (1997) Androgen responsive adult human prostatic epithelial cell lines immortalized by human papillomavirus 18. *Carcinogenesis* 18(6):1215–1223.

38. Fidler IJ (2003) The pathogenesis of cancer metastasis: The 'seed and soil' hypothesis revisited. *Nat Rev Cancer* 3(6):453–458.
39. Gambhir SS (2002) Molecular imaging of cancer with positron emission tomography. *Nat Rev Cancer* 2(9):683–693.
40. Leicht DT, et al. (2007) Raf kinases: Function, regulation and role in human cancer. *Biochim Biophys Acta* 1773(8):1196–1212.
41. Sinkevicius KW, et al. (2014) Neurotrophin receptor TrkB promotes lung adenocarcinoma metastasis. *Proc Natl Acad Sci USA* 111(28):10299–10304.
42. Schlegel J, et al. (2013) MERTK receptor tyrosine kinase is a therapeutic target in melanoma. *J Clin Invest* 123(5):2257–2267.
43. Wang Y, et al. (2013) Mer receptor tyrosine kinase promotes invasion and survival in glioblastoma multiforme. *Oncogene* 32(7):872–882.
44. Partin AW, et al. (1997) Combination of prostate-specific antigen, clinical stage, and Gleason score to predict pathological stage of localized prostate cancer. A multi-institutional update. *JAMA* 277(18):1445–1451.
45. Lehmann K, et al. (2000) Raf induces TGFbeta production while blocking its apoptotic but not invasive responses: A mechanism leading to increased malignancy in epithelial cells. *Genes Dev* 14(20):2610–2622.
46. Fournier PG, et al. (2015) The TGF-β signaling regulator PMEPA1 suppresses prostate cancer metastases to bone. *Cancer Cell* 27(6):809–821.
47. Mooz J, et al. (2014) Dimerization of the kinase ARAF promotes MAPK pathway activation and cell migration. *Sci Signal* 7(337):ra73.
48. Graham DK, DeRyckere D, Davies KD, Earp HS (2014) The TAM family: Phosphatidylserine sensing receptor tyrosine kinases gone awry in cancer. *Nat Rev Cancer* 14(12):769–785.
49. Dionne CA, et al. (1998) Cell cycle-independent death of prostate adenocarcinoma is induced by the trk tyrosine kinase inhibitor CEP-751 (KT6587). *Clin Cancer Res* 4(8): 1887–1898.
50. Geiger TR, Peeper DS (2007) Critical role for TrkB kinase function in anoikis suppression, tumorigenesis, and metastasis. *Cancer Res* 67(13):6221–6229.
51. Knudson G, et al. (1991) Bone scan as a stratification variable in advanced prostate cancer. *Cancer* 68(2):316–320.
52. Klezovitch O, et al. (2004) Hepsin promotes prostate cancer progression and metastasis. *Cancer Cell* 6(2):185–195.
53. Ding Z, et al. (2012) Telomerase reactivation following telomere dysfunction yields murine prostate tumors with bone metastases. *Cell* 148(5):896–907.
54. Grabowska MM, et al. (2014) Mouse models of prostate cancer: Picking the best model for the question. *Cancer Metastasis Rev* 33(2-3):377–397.
55. Jin JK, Dayyani F, Gallick GE (2011) Steps in prostate cancer progression that lead to bone metastasis. *Int J Cancer* 128(11):2545–2561.
56. Wu TT, et al. (1998) Establishing human prostate cancer cell xenografts in bone: Induction of osteoblastic reaction by prostate-specific antigen-producing tumors in athymic and SCID/bg mice using LNCaP and lineage-derived metastatic sublines. *Int J Cancer* 77(6):887–894.
57. McCabe NP, De S, Vasanji A, Brainard J, Byzova TV (2007) Prostate cancer specific integrin alphavbeta3 modulates bone metastatic growth and tissue remodeling. *Oncogene* 26(42):6238–6243.
58. Taichman RS, et al. (2002) Use of the stromal cell-derived factor-1/CXCR4 pathway in prostate cancer metastasis to bone. *Cancer Res* 62(6):1832–1837.
59. Knubel KH, et al. (2014) MerTK inhibition is a novel therapeutic approach for glioblastoma multiforme. *Oncotarget* 5(5):1338–1351.
60. Yakes FM, et al. (2011) Cabozantinib (XL184), a novel MET and VEGFR2 inhibitor, simultaneously suppresses metastasis, angiogenesis, and tumor growth. *Mol Cancer Ther* 10(12):2298–2308.
61. Ghilardi JR, et al. (2010) Administration of a tropomyosin receptor kinase inhibitor attenuates sarcoma-induced nerve sprouting, neuroma formation and bone cancer pain. *Mol Pain* 6:87.
62. Wilhelm SM, et al. (2008) Preclinical overview of sorafenib, a multikinase inhibitor that targets both Raf and VEGF and PDGF receptor tyrosine kinase signaling. *Mol Cancer Ther* 7(10):3129–3140.
63. Meyer A, et al. (2014) Role of sorafenib in overcoming resistance of chemotherapy-failure castration-resistant prostate cancer. *Clin Genitourin Cancer* 12(2):100–105.
64. Dahut WL, et al. (2008) A phase II clinical trial of sorafenib in androgen-independent prostate cancer. *Clin Cancer Res* 14(1):209–214.
65. Poulikakos PI, Zhang C, Bollag G, Shokat KM, Rosen N (2010) RAF inhibitors transactivate RAF dimers and ERK signalling in cells with wild-type BRAF. *Nature* 464(7287):427–430.
66. Zhao Y, Adjei AA (2014) The clinical development of MEK inhibitors. *Nat Rev Clin Oncol* 11(7):385–400.
67. Xin L, Ide H, Kim Y, Dubey P, Witte ON (2003) In vivo regeneration of murine prostate from dissociated cell populations of postnatal epithelia and urogenital sinus mesenchyme. *Proc Natl Acad Sci USA* 100(Suppl 1):11896–11903.
68. Loening AM, Gambhir SS (2003) AMIDE: A free software tool for multimodality medical image analysis. *Mol Imaging* 2(3):131–137.
69. Nguyen KQ, et al. (2014) Overexpression of MERTK receptor tyrosine kinase in epithelial cancer cells drives efferocytosis in a gain-of-function capacity. *J Biol Chem* 289(37):25737–25749.
70. Morrissey C, et al. (2013) Effects of androgen deprivation therapy and bisphosphonate treatment on bone in patients with metastatic castration-resistant prostate cancer: Results from the University of Washington Rapid Autopsy Series. *J Bone Miner Res* 28(2):333–340.

Supporting Information

Faltermeier et al. 10.1073/pnas.1521674112

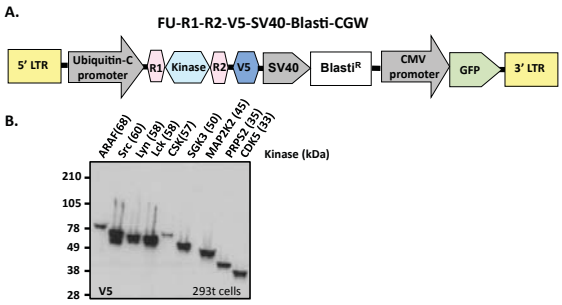

Fig. S1. Lentivirus-mediated overexpression of V5-tagged kinases. (*A*) Full-length kinases were cloned into the FU-R1-R2-V5-SV40-Blasti-CGW lentiviral vector shown. R1 and R2 represent recombination sites required for recombination-based Gateway cloning. LTR, Long-terminal repeat. (*B*) Western blot showing expression of selected kinases in 293t cells detected by a V5 antibody. The molecular mass of each kinase is indicated in parentheses.

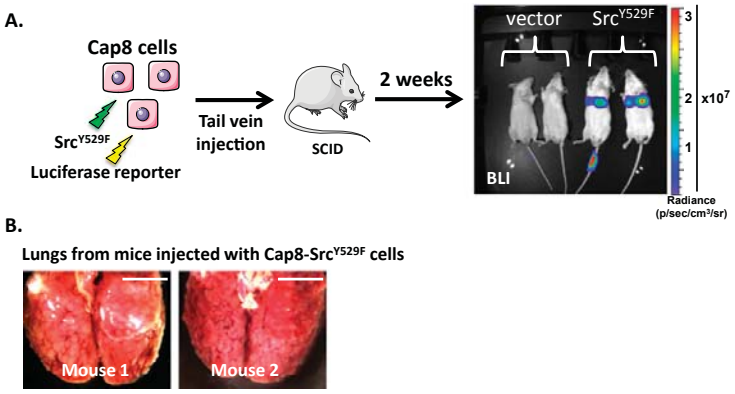

Fig. S2. Src^{Y529F} promotes lung colonization when overexpressed in murine prostate cells. (*A*) Experimental design to demonstrate that expression of mutationally activated kinase Src^{Y529F} in Cap8 cells promotes lung colonization. (*B*) Bright-field images of lungs removed from mice 3 wk after being injected with Cap8-Src^{Y529F} cells. (Scale bars, 5 mm.)

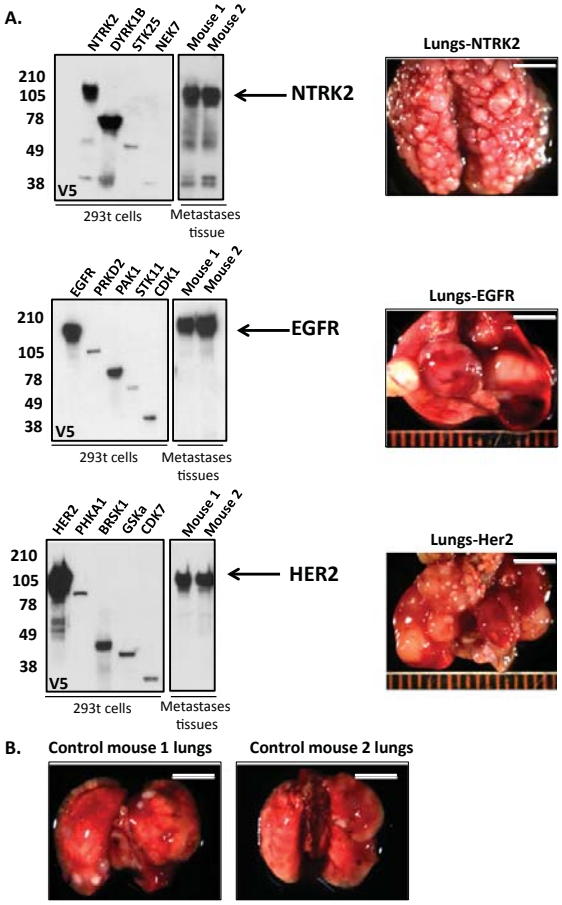

Fig. S3. Identification of kinases promoting lung colonization when expressed in murine prostate cells. (*A*, *Left*) Western blot analysis of lung tissues showing the specific kinase that was found to be enriched in lung metastasis. (*A*, *Right*) Representative bright-field images of tumor nodules in lungs from the corresponding mice. (Scale bars, 5 mm.) (*B*) Bright-field images of lungs removed from mice 10 wk after injection with control Cap8 cells. (Scale bars, 5 mm.)

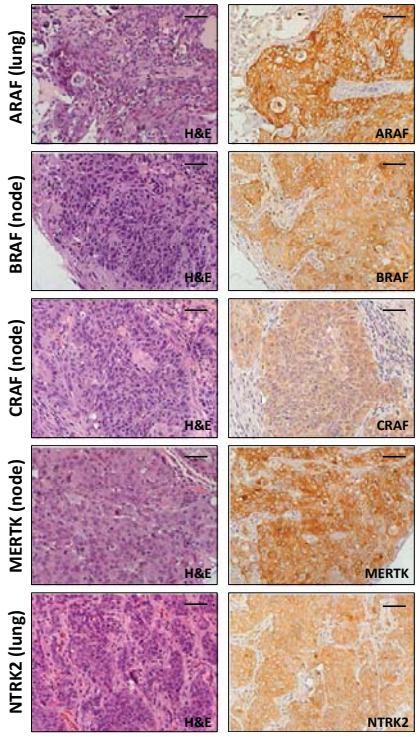

Fig. S4. Overexpression of kinases in RWPE-1 cells drives the formation of bone and visceral metastases. Representative histology of visceral (lung or lymph node) metastases removed from mice injected with RWPE-1 cells expressing RAF family members, MERTK, or NTRK2. (*Left*) H&E images. (*Right*) Corresponding kinase-specific staining. (Scale bars, 40 μm.) The histology of bone metastases removed from the same mice is shown in Fig. 4.

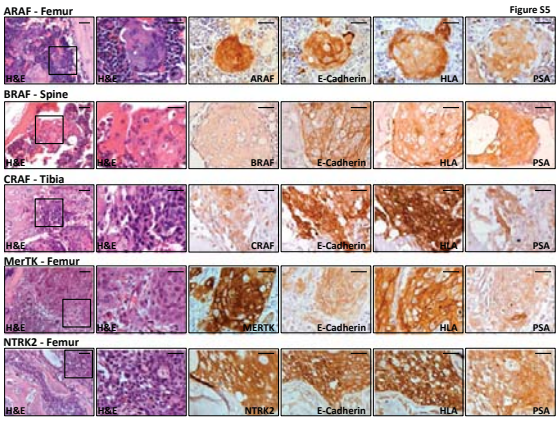

Fig. S5. Histological analysis of bones recovered from mice injected with cells expressing ARAF, BRAF, CRAF, MERTK, and NTRK2 confirms that metastases are of human prostate epithelial cell origin. (*Left* two columns) H&E stains of the affected bones removed from mice injected with RWPE-1 cells expressing the five metastasis-promoting kinases. Images in *Right* five columns are 20× magnification of the area outlined by a black box in the first column. (*Right* four columns) IHC staining of bone metastasis for overexpressed kinase, E-cadherin, HLA class I, and PSA. [Scale bars, 40 μm (*Left*) and 20 μm (*Right* five columns).]

Table S1. List and sources of the 125 kinases used in the screen

Kinase	pS, T, Y	cBioPortal	Literature
ABL	X		
ACVR2B		X	
ACVRL1		X	
ALK	X		
ARAF	X		
AXL	X		
BLK			X
BMP2K		X	
BMPR1A		X	
BMPR1B		X	
BMX	X		
BRAF	X		
BRSK1		X	
BTK		X	
CAMK2B		X	
CARD11		X	
CDC2 (CDK1)	X		
CDK10		X	
CDK2	X		
CDK3	X		
CDK4		X	
CDK5	X		
CDK6	X		
CDK9			X
CKB	X		
CSFR1	X		
Csk	X		
CSNK2A1	X		
DAPK1	X		
DDR1	X		
DGKB		X	
DYRK1b		X	
DYRK3		X	
EGFR	X		
EphA2		X	
EphA3	X		
EphA4	X		
EpHA6	X		
ERBB2	X		
ERBB3	X		
FASTK		X	
Fer			X
Fes	X		
FGFR1	X		
FGFR2			X
FGFR3			X
FLT1		X	
FLT3	X		
FLT4		X	
Fyn	X		
Gsk3A	X		
Hck	X		
INSRR			X
JAK1		X	
JAK3		X	
Lck	X		
LMTK2		X	
LYN	X		
MAP2K2	X		
MAP2K6		X	
MAP2K7	X		
MAP3K15		X	
MAP3K2	X		

Table S1. Cont.

Kinase	pS, T, Y	cBioPortal	Literature
MAP3K5	X		
MAP3K8			X
MAP4K3		X	
MAP4K4		X	
MAPK1	X		
MAPK12	X		
MAPK13	X		
MAPK14	X		
MAPK3	X		
MAPK8 (JNK1)	X		
MARK3		X	
MAST1		X	
MERTK			X
MET			X
MPP6		X	
MST1R		X	
Myt1	X		
NEK11		X	
NEK2		X	
NEK7		X	
NTRK2			X
NTRK3		X	
PAK1			X
PAK7			X
PCTK1		X	
PDGFRa	X		
PDGFRb	X		
PDK1	X		
PDK3			X
PHKA1		X	
PHKA2		X	
PIK3Ca		X	
PIK3CB		X	
PIM1			X
PRKD1			X
PRKD2			X
PRKX		X	
PRPF4B	X		
PRPS2		X	
PTK2		X	
PTK6	X		
RAF1	X		
RIPK2		X	
SGK2			X
SGK3		X	
SNX16		X	
Src	X		
SRPK1		X	
SRPK2		X	
SRPK3		X	
STK11			X
STK17B		X	
STK25		X	
STK3		X	
Syk	X		
TLK2		X	
TXK		X	
TYK2	X		
TYRO3		X	
ULK3			X
XYLB	X		

Listed are the 125 kinases evaluated in the in vivo screen, as well as the source from which they were identified: pS (serine), pY (tyrosine), pT (threonine): phosphoproteomics dataset; cBioPortal: genomic/RNA dataset; literature: PubMed.

Chapter 4:

Conclusion and Future Directions

Conclusion

Research described in this dissertation provides evidence that non-mutated protein kinases may play a critical role prostate cancer metastasis. In chapter 2, use of phosphoproteomics identified highly activated kinases in metastatic prostate cancer tissues. Additionally, the phosphotyrosine proteome of metastatic prostate cancer was found to be distinct from localized prostate cancer tissues. These data lead to the hypothesis that activation of wild-type kinases drives prostate cancer metastasis. In chapter 3, this hypothesis was addressed by screening the functional metastatic ability of over 100 kinases identified from previously published phosphoproteomic, transcriptomic, and genomic studies. Twenty kinases were capable of driving metastatic lung colonization when overexpressed in murine prostate cancer cells. Five of these kinases (ARAF, BRAF, CRAF, MERTK, and NTRK2) could promote benign human prostate cancer cells to colonize both skeletal and visceral sites. These studies suggest that non-mutated kinases are capable of driving metastatic colonization and should be considered as potential therapeutic targets for metastatic prostate cancer.

Future Directions

Our study discovered the strong metastatic ability of the RAF family members. This finding should prioritize future research to focus on elucidating the therapeutic potential of targeting RAF family members in metastatic prostate cancer. Additional important studies should investigate the signaling networks and mechanistic pathways contributing to the metastatic ability of RAF family members. Possible research approaches and preliminary data will be discussed in the following concluding sections.

I. Are RAF family members potential therapeutic targets for metastatic prostate cancer?

In chapter 3, evidence was provided that RAF family members may be therapeutic targets based on their ability to drive metastatic colonization and high protein expression in human prostate cancer tissues. The numerous FDA-approved small molecule inhibitors targeting RAF family members provide additional rationale for investigating their therapeutic potential(*1*). However, RAF family member inhibitors are usually selective for one or two family members. For instance, sorafenib preferentially inhibits CRAF over BRAF and does not inhibit ARAF(*2*). Hence it will be important to inhibit each RAF family member individually to propose future treatment approaches.

To address the therapeutic potential of blocking RAF family members in metastatic prostate cancer, questions to investigate are: 1) Does inhibition of ARAF, BRAF, or CRAF block metastatic colonization, and 2) Does inhibition of ARAF, BRAF or CRAF cause regression of established metastasis? Preliminary data addressing the first question has shown that shRNA inhibition of CRAF, but not ARAF or BRAF, in two different metastatic prostate cancer cell lines can block and/or reduce the development of lung metastasis *in vivo* (Figure 1). These data suggest that CRAF may be a therapeutic target for blocking metastatic colonization. The second question has clinical implications since it would help determine at which stage of disease progression a RAF inhibitor would be therapeutic. If the kinase is important for the initial steps of colonization, RAF inhibitors could be used in the adjuvant setting to prevent metastatic colonization. If the kinase is necessary for growth of established metastasis, RAF inhibitors could be used in the treatment of patients with metastatic disease.

II. Does the metastatic ability of RAF family members depend on activation of similar downstream signaling pathways?

The signaling pathways activated by RAF family members that contribute to their metastatic ability are unknown. The most well studied substrate of the RAF family members is MEK1/2, which in turn phosphorylates its only substrate ERK1/2(*3*). As a result, the most likely signaling pathway implicated in RAF-driven metastatic colonization is the MEK-ERK pathway. Yet, we observed in chapter 3 that the RAF family members had dramatic differences in metastatic potency. CRAF drove the formation of metastasis with a short latency and high metastatic burden, while micrometastasis established by ARAF or BRAF overexpression took much longer to develop. These differences suggest that RAF family members either have differential abilities in activating the MEK-ERK pathway, or ARAF, BRAF, and CRAF activate unique pathways in our model. Literature supports both hypotheses. ARAF and BRAF are considered to be the least potent MEK1/2 activators(*4*). ARAF, BRAF, and CRAF knockout mice have dramatically different phenotypes suggesting differences in signaling pathways(*5-7*).

To better understand the signaling pathways activated by these kinases in metastases, questions to investigate include: 1) Are the phosphoproteomic profiles activated in tumors driven by RAF family kinases similar or different, and 2) Is RAF mediated metastatic ability dependent on MEK-ERK pathway activation? A phosphoproteomics approach will enable identification of global differences in the serine, threonine, and tyrosine phosphoproteome between ARAF, BRAF and CRAF driven tumors. Integration of highly activated kinases with the types of proteins being phosphorylated in each tumor may help determine if the major signaling pathways activated by RAF family members are similar or different. While phosphoproteomics should help elucidate the activation state of MEK1/2 and ERK1/2 in ARAF, BRAF, and CRAF

overexpressing tumors, whether or not activation of the MEK-ERK pathway is required for metastatic colonization is unknown. Since there are highly specific MEK1/2 and ERK1/2 small molecule inhibitors(*1*), this question could by addressed through a pharmacological approach.

III. What is the mechanism by which RAF family members drive metastatic colonization?

Previous studies have implicated RAF family members in multiple steps of the metastatic cascade. Both ARAF and CRAF have been associated with promoting invasion and migration through kinase dependent and independent mechanisms(*8, 9*). BRAF confers resistance to anoikis by phosphorylating and decreasing the stability of pro-apoptotic proteins(*10*). However, the mechanism by which RAF family members drive metastatic colonization has not yet been elucidated.

Given the complexity of metastatic colonization, RAF family members probably enable colonization through multiple mechanisms. RAF family members may upregulate cell surface receptors, receptor-tyrosine kinases, or ligands that promote cancer cell survival upon interaction with the tumor microenvironment. To address this hypothesis, expression of cell surface proteins or the secretome of the prostate cancer cell lines used in chapter 3 could be evaluated. An alternative hypothesis is that RAF family members may activate pro-survival pathways or autocrine production of ligands enabling cells to survive at secondary sites in the absence of microenviromental influence. Support for this hypothesis would be if RAF family members could still promote metastasis when injected into an immunocompetent mouse model. Additionally, one could investigate if the metastatic colonization pattern of cells overexpressing RAF family members is dependent on the route of injection (intracardiac, orthotopic or

subcutaneous). If sites of metastasis vary based on injection sites, this would support that RAF family members promote metastatic colonization largely through cell autonomous mechanisms.

Concluding statement

We anticipate that the work described in this dissertation will contribute to the shifting paradigm that non-mutated kinases have significant functional activity in prostate cancer and should be considered as targets in the treatment of metastatic disease. Plans have been outlined to investigate the function of RAF family kinases in metastatic prostate cancer, but the additional kinases discovered in our phosphoproteomic analysis and *in vivo* functional studies should not be overlooked. Careful functional analyses of these kinases should help determine the appropriate context that upon targeting will yield the largest clinical benefit. We are also optimistic that this work will provide insight into long-standing questions related to metastasis. For instance, one hypothesis is that metastasis occurs late in tumor progression because cells must acquire numerous genetic lesions to be capable of metastasizing. However, our observation that overexpression of one wild-type kinase in benign human prostate cells can drive metastatic colonization may suggest that metastatic capability isn't a result of numerous genetic alterations. It is possible that metastatic ability depends on activation of key pathways. In closing, it is our sincere hope that this work and future studies will eventually contribute to changing the course of metastatic prostate cancer from a death-sentence to a manageable disease.

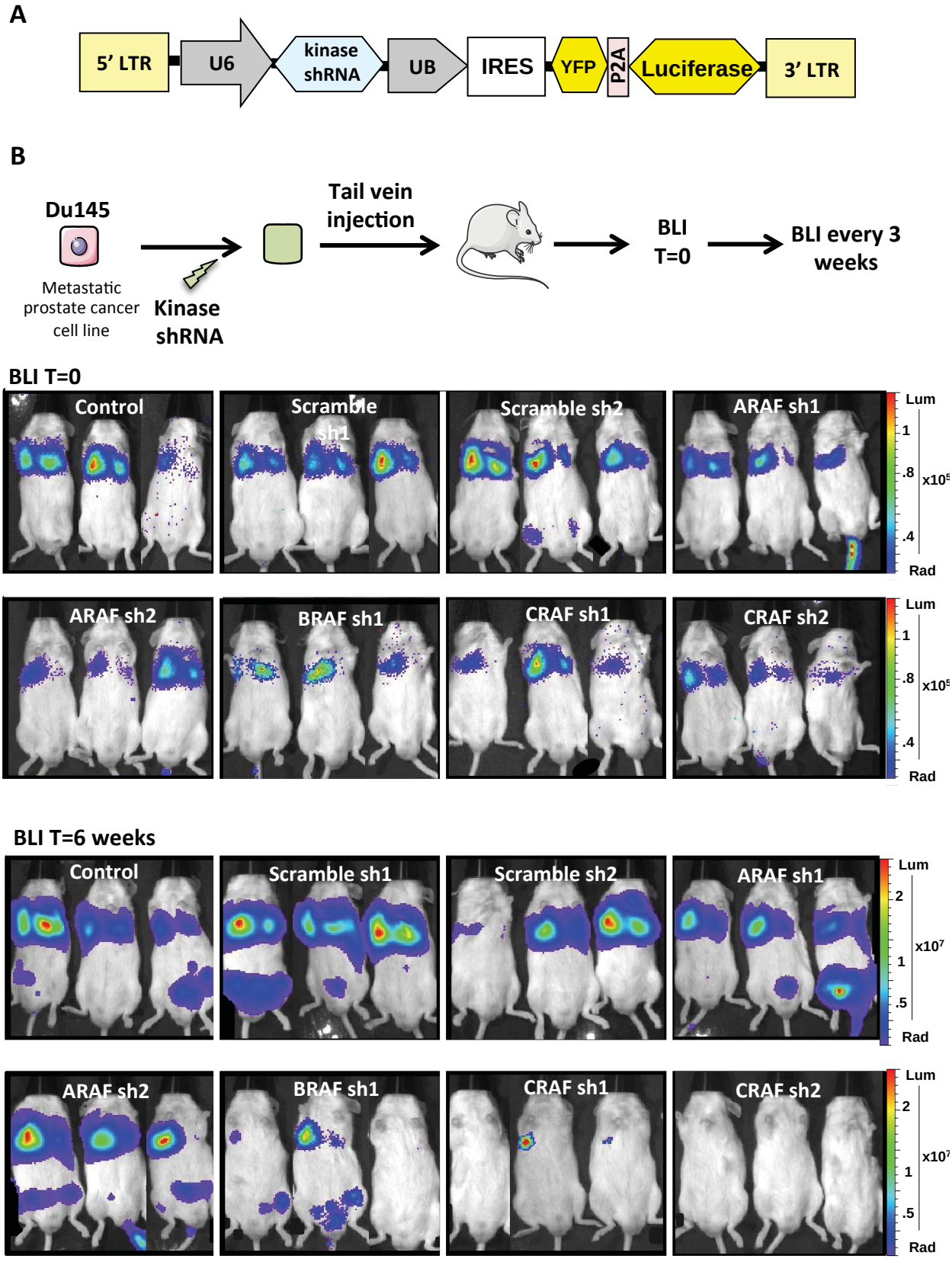
A
5' LTR
U6
kinase shRNA
UB
IRES
YFP
P2A
Luciferase
3' LTR
B
Du145
Metastatic prostate cancer cell line
Kinase shRNA
Tail vein injection
BLI T=0
BLI every 3 weeks
BLI T=0
Control
Scramble sh1
Scramble sh2
ARAF sh1
ARAF sh2
BRAF sh1
CRAF sh1
CRAF sh2
Lum
1
.8
x10⁵
.4
Rad
BLI T=6 weeks
Control
Scramble sh1
Scramble sh2
ARAF sh1
ARAF sh2
BRAF sh1
CRAF sh1
CRAF sh2
Lum
2
1
x10⁷
.5
Rad

Figure 1. Inhibition of CRAF with shRNA blocks metastasis in DU145 cells. A) Diagram of lentiviral vector expressing shRNA and luciferase used for *in vivo* experiments. B) Top: Schematic of in vivo experiment. Bottom: BLI images taken immediately post injection (T=0) and 6 weeks later. BLI, bioluminescence imaging; T, time; sh, small hairpin RNA; lum, luminescence; Rad, radiance (p/sec/cm^3/sr).

References

1. A. A. Samatar, P. I. Poulikakos, Targeting RAS-ERK signalling in cancer: promises and challenges. *Nature reviews. Drug discovery* **13**, 928-942 (2014).

2. S. M. Wilhelm *et al.*, BAY 43-9006 exhibits broad spectrum oral antitumor activity and targets the RAF/MEK/ERK pathway and receptor tyrosine kinases involved in tumor progression and angiogenesis. *Cancer Res* **64**, 7099-7109 (2004).

3. D. T. Leicht *et al.*, Raf kinases: function, regulation and role in human cancer. *Biochim Biophys Acta* **1773**, 1196-1212 (2007).

4. H. Lavoie, M. Therrien, Regulation of RAF protein kinases in ERK signalling. *Nat Rev Mol Cell Biol* **16**, 281-298 (2015).

5. L. Wojnowski *et al.*, Endothelial apoptosis in Braf-deficient mice. *Nat Genet* **16**, 293-297 (1997).

6. L. Wojnowski *et al.*, Craf-1 protein kinase is essential for mouse development. *Mechanisms of development* **76**, 141-149 (1998).

7. C. A. Pritchard, L. Bolin, R. Slattery, R. Murray, M. McMahon, Post-natal lethality and neurological and gastrointestinal defects in mice with targeted disruption of the A-Raf protein kinase gene. *Current biology : CB* **6**, 614-617 (1996).

8. J. Mooz *et al.*, Dimerization of the kinase ARAF promotes MAPK pathway activation and cell migration. *Sci Signal* **7**, ra73 (2014).

9. K. Ehrenreiter *et al.*, Raf-1 regulates Rho signaling and cell migration. *J Cell Biol* **168**, 955-964 (2005).

10. K. Boisvert-Adamo, A. E. Aplin, Mutant B-RAF mediates resistance to anoikis via Bad and Bim. *Oncogene* **27**, 3301-3312 (2008).